UNIVERSITY OF SANTIAGO DE COMPOSTELA

SCHOOL OF ENGINEERING

Department of Chemical Engineering

PHASE EQUILIBRIA FOR EXTRACTION PROCESSES WITH DESIGNER SOLVENTS

A thesis submitted by SARA LAGO GARCÍA DE DIOS for the degree of Doctor in Chemical and Environmental Engineering to the University of Santiago de Compostela

Santiago de Compostela, September 2013

Department of Chemical Engineering
School of Engineering

Rúa Lope Gómez de Marzoa s/n
15782 Santiago de Compostela
Tel: + 34 881816730

Authorization for submission by the thesis directors (in Galician)

Alberto Arce Arce e **Ana M. Soto Campos**, Catedráticos de Enxeñería Química,

INFORMAN:

Que a presente memoria, titulada *"Phase Equilibria for extraction processes with designer solvents"*, que para optar ó grao de Doutor en Enxeñería Química, Programa de Doutoramento de Enxeñería Química e Ambiental, presenta **Sara Lago García de Dios**, foi realizada baixo a nosa inmediata dirección no Departamento de Enxeñería Química da Universidade de Santiago de Compostela.

Considerando que constitúe traballo de Tese, autorizan a súa presentación ao Centro de Posgrao da Universidade de Santiago de Compostela.

E para que así conste, asinan o presente informe en Santiago de Compostela, a 01 de setembro de 2013.

Asdo.: Alberto Arce Asdo.: Ana Soto

Abstract

In recent years, there has been an increasing concern about the effects of toxic chemicals in the environment. In response to this concern, there is a growing impetus to develop chemical manufacturing processes which can reduce or eliminate the use or generation of hazardous substances. Within this aspect of green chemistry, in this Thesis, Ionic Liquids (ILs) and Deep Eutectic Solvents (DESs) have been tested as greener alternatives in different chemical processes.

In a first stage, the capability of using ILs as solvents for citrus essential oil deterpenation by liquid-liquid extraction was investigated. The liquid-liquid equilibria of ternary systems limonene + linalool + IL were determined. Results were analysed in terms of the solute distribution ratio and selectivity, allowing to draw conclusions about the influence of the structure of the ILs in these thermodynamic parameters. Experimental data were correlated by means of the NRTL and UNIQUAC equations.

To evaluate the capability of some ILs to act as surfactants in Enhanced Oil Recovery, two of these salts showing surfactant behaviour were tested. Liquid-liquid equilibria of ternary systems water + IL + n-dodecane were determined. Winsor Type III systems were found, and the interfacial tensions between phases were measured to prove the ability of these salts to reduce the water – oil interfacial tension. Physical and transport properties of the phases involved, such as density and viscosity, were also experimentally measured.

In a last stage, an introductory study on the processing of lignocellulosic biomass with DESs was carried out. Different renewable DESs were prepared from hydrogen bond donor and hydrogen bond acceptor starting materials. Solubility tests of pine wood and wheat straw in these solvents were carried out.

From the thermodynamic studies that were carried out in this Thesis, it turns out that designer solvents can be used to develop greener and/or more efficient chemical processes.

Acknowledgements

The last four years, I had the privilege of being part of the Group of Phase Equilibria and Separation Processes of the University of Santiago de Compostela working as a PhD student. The present thesis tries to summarise the experimental work carried out in this period. Now that the work is concluded and a new cycle is coming ahead, I would like to thank all the people who helped me one way or another.

I would like to thank Professors Alberto Arce and Ana Soto for giving me the great opportunity of being part of their group, teaching and giving me advise in every professional and personal aspect of my life, always making things easier. Also, for treating their PhD "children" as we all were members of a big family. I hope they can feel proud of the final result.

I would also like to thank all the people who were part of Laboratory 1.3 during more or less time for sharing such a great time together. Specially I would like to thank María Francisco who taught me all the knacks of the laboratory and was also a good friend. To Alicia and to Iago, for being not only great mates but also good friends and for making research so much fun. To Héctor for having always an answer for every question and for being such a patient and good teacher. I would like also to thank Eva for giving me advise and having very nice times at the coffee break. And last of all I would like to thank Borja, who besides of being the best working mate and friend, he is the best person in the world and I think I would had never reach this point without him.

My gratitude is extensive to all the members of Separation Technology Group of Eindhoven University of Technology where I spent three fabulous months learning and enjoying with them. It was my pleasure to work under the supervision of Professor M.C. Kroon, giving me the opportunity of spending this time at her laboratory and teaching me about the existence of Deep Eutectic Solvents. I would like to thank María Francisco again, who once more crossed in my life, this time as a postdoc, teaching me and spending a lot of time to take advantage of the research in such a short time. Thanks to this stay I was able of adding the chapter of biomass fractionation with DESs to this thesis work. I can not forget my lab colleagues. Adriaan who also helped me every day with the biomass processing and was a fantastic colleague, and of course Agustin, who was a great friend and I keep in mind really nice moments with him. Thanks to Somayeh and Lawien for sharing happy lunches.

And almost ending I would like to thank all my friends of Santiago de Compostela and A Coruña, for always being there and giving me support no matter what.

To Roge because you were always there unconditionally.

And finally, I would like to thank my family, Kira and Carlos and my parents as they believed in me from the very beginning and supported me unconditionally along the way.

I want to close these lines by expressing my gratitude to the University of Santiago de Compostela, and the "Ministerio de Educación y Ciencia" of the Spanish Government. We acknowledge the Ministry of Science and Innovation of the Spanish Government for financial support through project CTQ2009-10776.

Sara Lago

Santiago de Compostela, September 2013

CONTENTS

1 Objectives

1. OBJECTIVES

An industrial and chemical revolution started in the eighteenth century, gathering strength in the nineteenth, and has been running in full force in the last and present centuries. From the first soaps made from ashes or animal fat, and the obtaining of medicines from roots or plants, chemicals have been exponentially growing until becoming part of almost every aspect of human daily life. The vast array of products and systems produced by the chemical industry benefit and make more comfortable the new pace of life that modern times require. Food, paper, pharmaceuticals, garments, energy, fuels, plastics, paints, transport, glass, cosmetics, detergents, etc., are just a small, almost negligible, group of examples of all the facilities that the chemical industry can provide nowadays.

Some decades ago, few were aware of the potentially negative effects our modern lifestyle might have on the environment, and only the positive potential for creating new, useful materials and products was taken into account. Over the last years, the industry and wider public became aware of the damaging effects of some past practices and the need to protect the environment. Industrial processes in chemistry and petro-chemistry have demonstrated to play an important role in developing solutions to environmental problems such as climate change, waste management, recycling, energy efficiency, etc... Countless research is still being carried out in chemical industry. However, looking for new methods which ensure a better sustainability and a lower environmental impact has become one of its main objectives.

Common organic solvents used in chemical laboratories and industry constitute an important problem for the safety and health of humans and environmental pollution. The substitution of these solvents by new, greener alternatives has increasingly been acknowledged over the past decade. Designer solvents appear to be a main tool to reach this target, gathering properties which make them attractive as substitutes to conventional organic solvents.

The main objective of this thesis is the exploration of the capability of designer solvents, Ionic Liquids (ILs) and Deep Eutectic Solvents (DESs), to improve the efficiency and/or sustainability of chemical processes. More specifically, the suitability of using ILs as solvents for deterpenation of citrus essential oil by liquid-liquid extraction will be studied. Moreover, these solvents will also be investigated to improve chemical oil recovery processes, due to the amphiphilic properties that some of these salts present. And, finally, an introductory study on the suitability of using DESs for biomass deconstruction into its main

biopolymer constituents will also be carried out. The above mentioned specific objectives are presented ahead in detail.

– Citrus essential oil deterpenation

The objective of this section is to study the potential use of ILs as solvents to deterpenate citrus essential oil by liquid-liquid extraction. Thus, the use of a distillation process, which implies two stages and high energetic requirements, is avoided. Moreover, the degradation of the oil due to long time heating during the whole process usually happens, so the traditional method derives in a loss of product quality.

To carry out this investigation, citrus essential oil is simulated as a mixture of the terpene limonene (which represents 90-95% of the essential oil) and the oxyterpene linalool (representing 2-5%). Oxyterpenes are considered the most valuable components in the oil due to their organoleptic properties, and the deterpenation of the essential oil results in a more stable and valuable product. The choice of the solvent is carried out through a selection among several ILs, studying the properties that provide their anion and cation. The ILs 1-ethyl-3-methylimidazolium bis(trifluoromehylsulfonyl)imide, 1-hexyl-3-methylimidazolium bis(trifluoromehylsulfonyl)imide, 1-decyl-3-methylimidazolium bis(trifluoromehylsulfonyl)imide, 1-methylpyridinium methylsulfate, 1-ethylpyridinium ethylsulfate, 1-ethyl-3-methylimidazolium 2-(2-methoxyethoxy)ethylsulfate, 1-ethyl-3-methylimidazolium acetate and 1-butyl-3-methylimidazolium acetate are selected for this aim.

For all chosen solvents, the analysis of their suitability to deterpenate the citrus oil according to thermodynamic criteria will be carried out. With this objective in mind, the liquid-liquid equilibria of limonene + linalool + IL ternary systems will be determined. Obtained data will be correlated using NRTL and UNIQUAC models, in order to facilitate their use in process simulation and design.

– Enhanced oil recovery

With a decrease in world oil reserves and a higher demand for petroleum and its derived products, the effective exploitation of oil reservoirs has become increasingly important. Surfactant-assisted Enhanced Oil Recovery (EOR) has proven to be an effective method for recovering the oil from the reservoirs that have lost their drive after the application of the primary and secondary recovery methods. This has given rise to the importance of searching for more effective agents in chemical EOR processes, which traditionally use surfactants and polymers. Within the large family of ILs, some have been found to behave as surface active agents. The objective of this section is to study the potential use of several ILs to improve the surfactant flooding EOR methods.

To carry out this research, the interior of the reservoir is modeled as a ternary system of water/brine, oil (*n*-dodecane) and

surfactant (IL). The ILs trihexyl(tetradecyl)phosphonium chloride and trihexyl(tetradecyl)phosphonium bis(trifluoromehylsulfonyl)imide are selected for this aim, due to their surfactant character and them being room temperature liquids.

Both low interfacial tensions and a high degree of oil solubilisation are considered desirable for oil recovery. Thus, liquid-liquid equilibria of the water + *n*-dodecane + IL ternary systems will be determined in order to find a microemulsion capable of solubilizing high oil proportions. Moreover, the measurement of the interfacial tension between equilibrium phases will also be carried out to evaluate the IL ability to reduce the water-oil value of this property. Physical and transport properties of the involved phases, such as density and viscosity, will also be measured and reported. Viscosity is an important property in EOR to prevent the formation of digitations resulting from unfavourable mobility rates. The effect of working with brine instead of pure water and the temperature effect will also be studied.

– Biomass processing

Cellulose and lignin are, respectively, the first and second most abundant renewable organic polymers on earth and, combined with hemicellulose, they constitute the structural components of plants. In a biorefinery context, lignocellulosics could be used to provide sustainable sources of fuels and feedstock chemicals. However, separation of lignin from cellulose and hemicellulose is a critical step. As a last objective of this investigation, several DESs will be tested for lignocellulosic biomass processing.

The DESs will be prepared and used as solvents for wheat straw and pine wood biomass deconstruction. A solid-liquid extraction will be carried out under mild conditions with the aim of extracting the lignin. A raffinate enriched in cellulose and hemicellulose is expected.

2

Theoretical considerations

2. THEORETICAL CONSIDERATIONS

2.1. DESIGNER SOLVENTS

Green chemistry research based on new solvents is a topic of interest because many of the solvents commonly used in the chemical industry are considered as unsafe for reasons of environmental protection. They are often used in huge amounts and they are volatile liquids responsible of atmospheric contamination. Promising neoteric solvents are Ionic Liquids (ILs) and Deep Eutectic Solvents (DESs).

2.1.1. IONIC LIQUIDS

2.1.1.1. Definition

Even though numerous definitions can be found in literature for the term Ionic Liquid (IL), the most common is the one that defines them as salts with a melting point under 100 °C [1-3]. Within this family of salts we can find those which are liquid at room temperature, widely used due to their easier handling, these are the so-called Room-Temperature Ionic Liquids (RTILs).

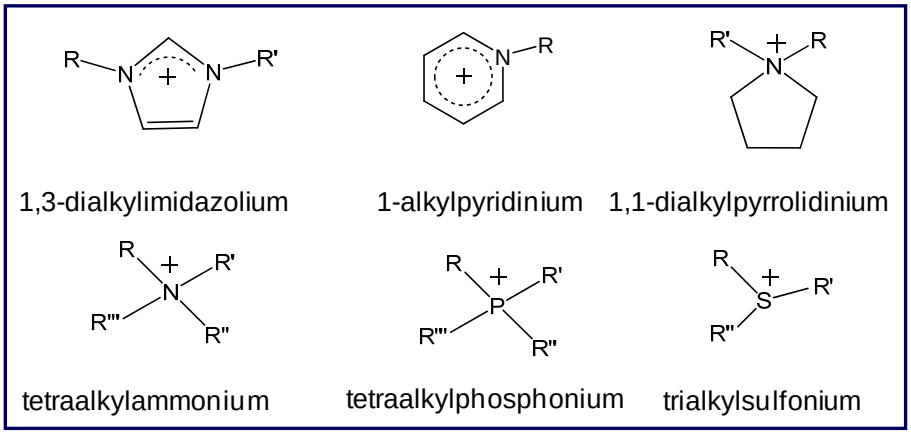

Figure 2.1. Schematic structures of some common cations in ILs. Alkyl substituent chains are represented by R, R', R" and R"'.

One of the very first uses of an IL can be dated in the latest 1880's by Gabriel and Weiner [4], who reported the use of the protic IL ethanol-ammonium nitrate. Even though, the year 1914, in which Walden's reported [5] the synthesis of ethylammonium nitrate, is nowadays considered the birth of ILs. Advances in research of these salts were slow and not numerous until 1990. That year, Wilkes and Zaworotko [6] arouse the interest on these salts with the report of

moisture stable ILs created by replacing the aluminum chloride with other anions, such as tetrafluoroborate or hexafluorophosphate. Since this date, the number of scientific publications on this topic has been exponentially increasing over the years.

ILs consist exclusively of ions. The low melting point of ILs is due to the poor coordination of the cations and anions which constitute them. ILs are formed by a weekly coordinating anion and a large asymmetrical organic cation. These characteristics of their constituting species tend to weaken the packing, thus reducing the lattice energy of the crystalline form of the salt and lowering this way the melting point of the IL [7]. Figures 2.1 and 2.2 show several cations and anions which constitute the most typical ILs found in bibliography.

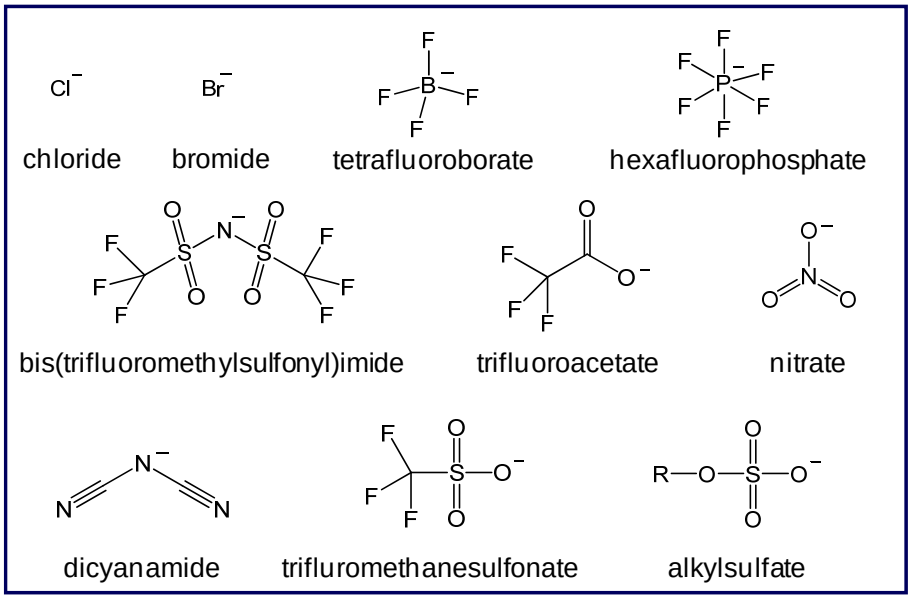

Figure 2.2. Schematic structures of some common anions in ILs. Alkyl substituent chains are represented by R.

Given the current emphasis on environmentally friendly chemistry and the sustainable use of resources, another area of growing interest is the obtaining of ILs that are based on low-toxicity natural products. Choline, for example, can be used as a cationic head-group, while the salts of fatty acids that have been modified by insertion of a few ethylene oxide groups between the alkyl chain and the carboxylate head-group can be liquid even at room temperature [8].

Regarding to the great variety of anions and cations present in nature, the freedom in designing the organic cation (by variation of the side chain length or by varying the substituents on the ring and/or on the chain), and the different possible combinations

between the cation and anion, there is the possibility of designing millions of different ILs [9]. Besides this, an almost limitless number of systems are theoretically possible by combination of two or more ILs.

2.1.1.2. Properties

The current technological revolution based on ILs is driven by their unique properties. Determination of these properties and their trends constitutes an essential point for "choosing" the right IL for a determinate application.

Their characteristic strong anion-cation interactions, gives them specific features which commonly used organic solvent or even high temperature molten salts do not show. Their negligible vapour pressure and the huge liquid range are two important consequences of these strong interactions. The consequence for green chemistry is that ILs represent the ultimate non-volatile solvents [10]. Thus, one of the primary driving forces behind research into ILs derived from the benefit of substituting traditional industrial solvents, most of which are volatile organic compounds (VOCs), with ILs which show a practically null vapour pressure [11]. This replacement would prevent the emission of a major source of environmental pollution.

The nature of the forces in different ILs may however differ from one to another and mainly control their physical properties. A key advantage derived from this characteristic of ILs over conventional solvents is their tuneability [2,7]. Specific properties for a determinate application can be obtained by subtly modifying the side chain length of the cation or by exchanging the anion. This tailoring allows obtaining ILs to dissolve a determined compound or making them miscible in aqueous or organic phases. Also their chemical and physical properties as viscosity, density, hydrophobicity, melting point, and reactivity, among others, can be modified by their specific design [7]. This feasibility in obtaining desired properties by changing as much the cation as the anion, has led to the introduction of the term "designer solvents" [12], which is an advantage for the development of task-specific ILs.

In conclusion, there are plenty of different properties which make ILs attractive compared with volatile solvents [12-14]. Furthermore, these properties can be changed by selecting a determinate cation or anion or changing the side length of the ions which constitute them. Some of these properties can be generalized for the big family of ILs, as their low melting points or negligible vapour pressure. For other properties, these generalizations can't be applied to all the ILs. For example, it has been established that some characteristics as thermal stability or miscibility depend basically on the anion structure, while viscosity, superficial tension or density are mainly affected by the side chain length of the cation or by its shape or symmetry. Some ILs are hydrophobic while others are hydrophilic. This change in a property can be seen in imidazolium halide ILs,

which show a high miscibility with water, but by just exchanging the halide anion for a bistriflamide, the IL becomes hydrophobic. Depending on the IL a wide range of inorganic, organic or polymeric materials can be dissolved. Some ILs are protic and other aprotic. Some are easily biodegradable and some aren´t. Some are toxic while others are non-toxic. Most of the ILs show high conductivity, thermal and electrochemical stability and they are normally non-flammable [15].

This long list of varied properties, their low vapour pressure, large liquid range and their attractive behaviour over common organic solvents, make these salts an outstanding field of study to find the right structure in a solvent to make it fit in a determinate application.

2.1.1.3. Applications

The increasingly interest in the study of ILs and the possibility of designing millions of different ILs by combining different anions and cations, multiplied by their numerous physical and chemical properties, make the number of laboratory and industrial applications of these solvents be practically countless. In this section just a brief overview of all these applications will be listed.

Due to the particular properties of ILs above cited, enthusiasm for these salts was initially focused on their use as an alternative to volatile organic solvents in synthesis and catalytic reactions [9,14]. ILs have been employed as reaction media for processes as Heck reaction, addition of thiols to unsaturated ketones, l-proline catalysed aldol reaction, Diels-Alder reactions, Friedel-Crafts alkylation and acylation reactions, hydroformylation reactions, Pd-mediated C-C bond formation, alkene polymerization and biotransformations… among many others. In general, it was found that reaction rates and selectivities are as good or better in ILs as in conventional organic solvents. Nevertheless, in the last years, ILs have opened new technological possibilities for a constantly increasing range of application fields [16,17], due to their wide range of physical and chemical properties enhanced by their promise for environmentally friendly applications.

ILs in general, present attractive properties to be considered as alternative to common organic solvents in separation processes. These applications are mainly due to their high capacity of solubilisation and selectivity for some compounds instead of others. In this line, ILs are investigated as solvents for liquid-liquid extractions [18] and gas separations (specially CO_2 capture) [19]. The long-term stability of a liquid membrane configuration is mainly dependent on the volatility of the liquid membrane, thus these salts are of great interest because they offer improved liquid membrane stability with high permeability and selectivity [20,21].

Electrochemical processes have been another important application area for ILs since their early development. As ILs present

a wide electrochemical window, high conductivity, and vanishingly low vapour pressure, they have been explored for being used in various electronic applications [22], including substituent of organic volatile electrolytes for Li-ion batteries and solar cells [22,23], capacitors and charge storage devices [24], as well as electrodeposition of metals [22,25], among many others.

ILs provide amazing functional properties such as dissolution of bio-related materials that are hardly dissolved in common solvents. The dissolution of biopolymers as cellulose or lignin is one of such examples [26,27]. Chloride based ILs dissolve cellulose better than other solvents because of the hydrogen bonding between chloride anions with the hydroxyl groups of the cellulose. The use of ILs allows a simple system for the processing of cellulose and has potential environmental and cost advantages over current processing methodologies.

Another interesting feature of ILs is their application as reaction media for different organic and inorganic nanomaterials [28,29]. The theories of the formation and solubility of nanoparticles in ILs have different foundations, for example the salting out effects or cation exchange processes, among others. In addition, ILs can be used for the characterization of nanomaterials. The fact that they can be easily solubilized in ILs facilitates the analysis.

Petroleum industry has also put attention in the use of ILs because of their properties and versatility of potential application in this field [30]. ILs may be used to inhibit the aggregation of asphaltenes and paraffins which deposition into the rock reservoir. Clogging pumps, valves and pipes represent a very serious and constant problem (with an enormous economic impact) in oil production and transport [31,32]. Furthermore, the self-organization, micelle formation and surface properties of ILs as well as their use to dehydrate and desalt crude oil have been reported [33,34]. Another interest field of ILs application in the oil industry is the petroleum refining. These solvents have been reported as extraction solvents for desulfurization and denitrogenation of diesel and gasoline fuels by mere liquid-liquid extraction or liquid-liquid extraction coupled with catalytic oxidation [35].

There is a huge amount of research done on ILs. Their potential application in many and diverse fields of research as: gas chromatography stationary phases, lubricants, heat-transfer fluids, additives, absorbents in absorption refrigeration, liquids for thermometers, etc… has been carried out [10].

In spite of this big research effort, the number of processes working at an industrial level is still very reduced [16]. Among them, the BASIL (Biphasic Acid Scavenging using ILs) can be highlighted. This process produces an alkoxy-phenyl-phosphine and generates an IL *in situ* that facilitates the removal of the waste HCl formed in the reaction. BASF realized therefore the first commercial application of ILs in industry. Eastman Chemical Company has been running a

process for the isomerization of 3,4-epoxybut-1-ene to 2,5-dihydrofuran since 1996. The plant is now idle, because the market for the product has declined. The IFP (Institute Français du Pétrole) has modified the Dimersol process (dimerization of alkenes) using chloroaluminate (III) ILs as solvents for these nickel-catalysed dimerization reactions. The Dimersol-Difasol process become much more efficient. QUILL (Queen's University Ionic Liquid Laboratories) has developed a new technology in partnership with Petronas for scrubbing toxic and corrosive mercury from natural gas streams [36]. The system, HycaPure Hg, has been installed in a full-scale commercial on-shore gas terminal in Malaysia successfully producing sales-quality natural gas for over a year. Many other companies, such as BP, Degussa, Air products, ExxonMobil, IoLiTec, etc. do also have projects involving ILs at advanced stage of development.

The main limitation of the use of ILs, even with all of the synthetic advances, is still their cost. Common ILs remain quite expensive, particularly when compared to conventional organic solvents. As a result, a very important area of study in the design of equally stable anions much less expensive, and also less toxic and more biodegradable, is being carried out.

2.1.2. DEEP EUTECTICS SOLVENTS

2.1.2.1. Definition

Green solvents are characterised for their low toxicity, higher low solubility in water (low miscibility), easily biodegradability under environmental conditions, high boiling point (not very volatile, low odour, less health problems to workers), and easily to recycle after use [37]. In this line of green chemistry we can find some relatively new solvents which have gained increasing attention over the last years, the so called Deep Eutectic Solvents (DESs). These are ionic fluids generally composed by a hydrogen bond donor and a hydrogen bond acceptor in solid state, self-associated by hydrogen bond interactions, deriving in a eutectic mixture with lower melting point than that of each individual component. These starting materials are usually easily biodegradable, cheap and non-toxic compounds. DESs are generally liquid at temperatures lower than 150 ºC. Although the term DES is standardized and its use generalized in bibliography, Francisco *et al.* [38] introduced an alternative term: Low Transition Temperature Mixtures (LTTMs). They choose this term for mixtures that do not show eutectic melting points but glass transitions instead.

Abbott *et al.* [39], presented these new solvents based on new renewable sources in 2003, with the mixture of choline chloride and urea, with melting points of 302 ºC and 133 ºC respectively, in a ratio 1:2. The resulting liquid mixture has a melting point of 12 ºC. Nevertheless, the term DESs does not appear until 2004, when the

same author proposes these solvents as an alternative to ILs due to their "greener" characteristics [40].

One of the most interesting advantages of these solvents is their easy and cheap fabrication by simply mixing two or three compounds, avoiding additional volatile organic solvents as synthesis medium. Even more, these precursors are normally cheap, easily available, biodegradable and non-toxic compounds as quaternary ammonium salts (usually choline chloride) combined with different hydrogen bond acceptors as natural amino acids (i.e. alanine or glycine) or carboxylic acids present in fruits and vegetables [38, 41]. Figure 2.3 shows typical structures of halide salts and hydrogen bond donors used for DESs syntheses.

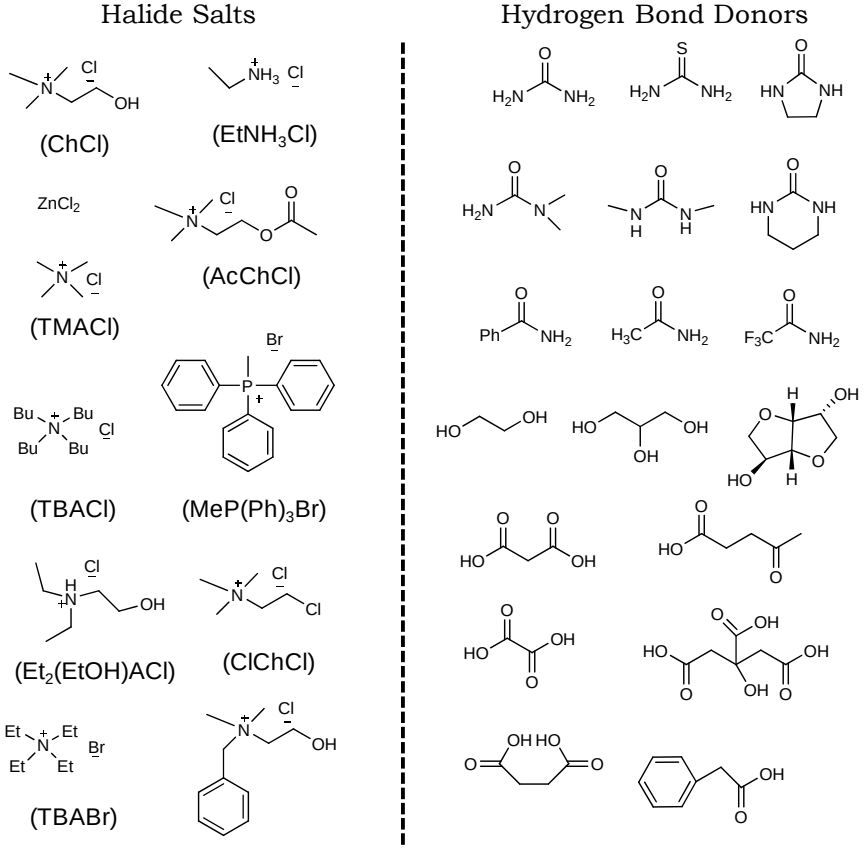

Figure 2.3. Typical structures of halide salts and hydrogen bond donors used for DES preparation.

2.1.2.2. Properties

DESs show a wide range of properties which make them an attractive new family of solvents for different applications. Due to the similar characteristics of DESs compared to ILs, it is hard to find

bibliography on DESs where ILs are not mentioned and compared with these solvents [41, 42].

As in ILs, physico-chemical properties of DESs can be tuned by changing the nature of the hydrogen-bond acceptor and the hydrogen-bond donor, making possible the preparation of task-specific DESs for a specific application.

One of the most attractive characteristic of DESs is their renewability, alluding with this term to their biodegradability and availability of precursors. The grade of renewability of a DES depends mainly on its starting materials. In most of the cases found in literature, precursors used in preparation of DESs are abundant natural compounds. Other implicit property derived from the nature of these precursors is their low toxicity [42].

DESs are usually denser than water and they show different freezing points depending on the starting materials and also on the molar ratio of these precursors. Nevertheless, the number of DESs which are liquid at room temperature is still limited. They are considered as non-volatile solvents and non-flammable, and they are usually water-miscible. As ILs, DESs generally show relatively high viscosities at room temperature. Derived from these high values of viscosity, DESs usually show low ionic conductivities [42].

2.1.2.3. Applications

Ionic nature of DESs drove to the use of these compounds in electrochemical processes as one of their first applications. Several publications can be found in the use of DESs as electrolytes for electrodeposition of metals and alloys, as solvents for electrochemistry reactions, preparation of electrolytes and for electropolishing (metal dissolution), among others [42].

Due their attractive characteristics as low volatility, non-toxicity or water miscibility, DESs are interesting substituents of common volatile organic solvents in organic synthesis. Some examples of these applications were the use of DESs has derived into high yields are Diels-Alder, Suzuki, Heck and Sonogashira reactions and the Huisgen 1,3-dipolar cycloaddition. Also several references can be found in the field of investigation of DESs as solvents for biotransformations [41].

A few works can be found in the study of DES for the preparation of inorganic materials. These compounds may play different roles such as solvent, structure-directing agent, water inhibitor, reactant for structure crystallization, etc. Synthesis of inorganic materials is usually carried out in an aqueous or organic media, with a posterior crystallization step at high pressures. Due to low volatility of DES, the process for the formation of crystals is simplified and risks of working at high pressures (due to the volatility of common organic solvents) are avoided. Namely, synthesis of nanomaterials, preparation of porous carbon materials, zeolite-type

materials, metal–organic frameworks (MOFs) and metal oxides, among others, are some examples of this application of DESs [42].

Suitability of DESs as possible solvents for separation processes has also being investigated. Some publications can be found in the use of these solvents in solid-liquid, liquid-liquid and vapour-liquid extractions, biomass processing and CO_2 capture [43]. A few examples of these separation processes reported in the literature are purification of biodiesel, drug solubilisation, dissolution of metal oxides [42] and deconstruction of lignocellulosic biomass [38].

Due to the interesting properties of DES, primarily their low ecological foot print and their attractive price, research on these solvents has been exponentially growing in the last years. As a result, their emergence in new laboratory and industrial applications (not existing at the moment) will be enhanced in a near future.

2.2. SOLVENT EXTRACTION PROCESSES

2.2.1. CITRUS ESSENTIAL OIL DETERPENATION

2.2.1.1. Essential oils: definition and composition

Essential oils are volatile, aromatic and oily liquids obtained from different parts of the plants (leaves, seeds, shoots, roots, bark, fruits, etc.). They give the plant its characteristic smell and flavour (organoleptic properties). They are used as colorants and scents in different foods and drinks, as well as to give a better taste to bitter medicaments. They are also used in perfumes, cosmetics, soaps and other products of personal hygiene, in pharmaceutical and parapharmaceutical products and aromatherapy [44].

Essential oils are mixtures of dozens of components constituted by carbon, hydrogen, and oxygen atoms, and with a relatively low molecular weight (300-350 g/mol approximately). Generally, the essential oil is formed of 90-95 wt% terpenes, 2-5 wt% oxygenated compounds (also called terpenoids or oxyterpenes) and less than 1 wt% of non-volatile compounds as waxes and pigments [45].

Therefore, most of the chemical substances within the essential oil correspond to family of terpenes, which are constituted of isoprenes unities with an orientation head-tail (Figure 2.4).Terpenes can be aliphatic, alicyclic or polycyclic, with different saturation grades. The simplest ones are the monoterpenes, which are constituted of ten carbon atoms (corresponding to two isoprene unities). Oxyterpenes can also be estructurated in isoprene unities, regarding to its carbonated framework.

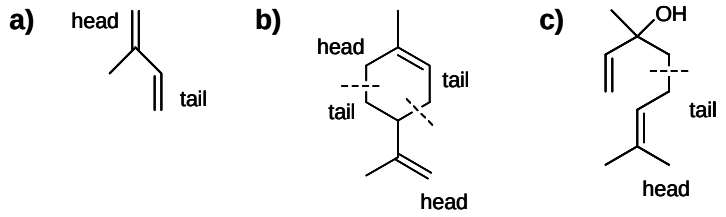

Figure 2.4. Structure of a terpene and a terpenoid from isoprene unities: a) isoprene unity, b) terpene limonene, c) terpenoid linalool.

When referred to the generous *Citrus* plants, most of the essential oil is contained in the skin of the fruit inside small glandules, and it is composed of more than one hundred components (terpenes, alcohols, aldehides, and esters, among others) which determine the different properties of the oil. Chemical composition and quality of an essential oil depends on different factors: land quality, climatic factors, ripeness of the fruit when it is harvested,

handling of the harvest (washing, drying, storing...), etc. Another important factor is the method by which it is extracted from the plant and any subsequent technique to which the oil can be subjected to improve its organoleptic properties.

2.2.1.2. Citrus essential oil: extraction processes

As mentioned above, citrus essential oil is retained in numerous glands or sacs irregularly distributed in the coloured layer of the peel, called the flavedo, which comprises the exocarp and several layers of subepidermal tissue [46]. Thus, the extraction of the essential oil needs to be carried out by separating the peel from the rest of the fruit without processing it all together. This treating results in a higher quality of the extracted essential oil.

Cold pressing is the basic extraction process for obtaining high-quality citrus essential oil. Among this method, several variants can be found. One of them is the manual sponge process, which is the oldest method employed for this aim. The flesh is separated from the peel, and the last is soaked in water during some hours, to be finally pressed between two sponges which absorb: the essential oil contained in the peel, aqueous components, peel cells, and other substances. The sponges are then wringed out to release the liquid retained, and essential oil is separated from the aqueous phase by decantation. The principles of this traditional process have been applied to semi-industrial citrus essential oil extraction methods. In the equipment developed for the sponge process (s*fumatrici*), the peel is compressed and afterwards rotated against fixed elements. The pressed oil is removed by fine jets of water. This semi-industrial process results in higher yields of oil recovery than the manual method. Despite this, the operation has to be carried out carefully to avoid high pressures which could result in the contamination of the desired oil by other fruit components.

Another traditional method for citrus essential oil extraction is the *ecuelle* process. The fruit is rolled under pressure inside a bowl covered with blunt teeth, which has a central exit connected to a tube for collecting the mixture. The *pellatrici*-type machines (*ecuelle* process) have the target of grating the whole fruit by means of toothed rolls. The mixture of oil and grated peel is washed away and filtered. Finally, the separation of the oil from the filtrate is carried out by centrifugation. This method is generally less effective than the sponge method. The operation time for these methods should be as short as possible to avoid fruit components degradation, to which multiple factors, as contact with air or water, can contribute [46].

The distillation processes for the extraction of the essential oil from the fruit, usually results in lower quality products. Even though distillation is carried out under vacuum, the working temperature can deteriorate some constituents of the oil. This method is therefore used as a complementary step to extract the oil which can remain in the residues after cold pressing.

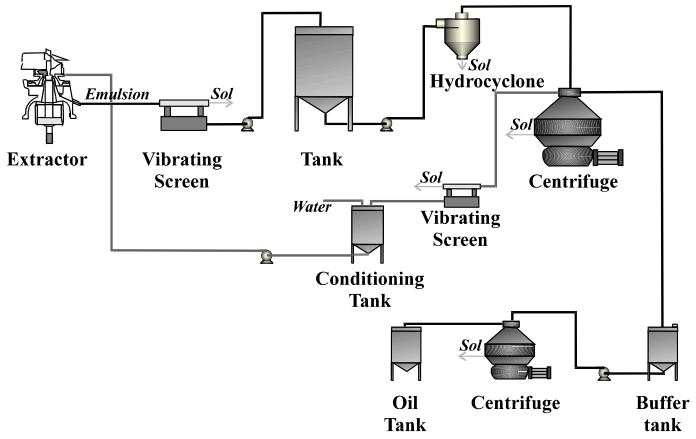

Figure 2.5. Citrus essential oil production [46]

On an industrial scale (Figure 2.5), fruits are thoroughly selected, washed and disinfected before the extraction process. In this case, the essential oil is obtained as a by-product of fruit juice production. The extraction of the oil can be previous to the juice extraction in *pellatrici* style, as in Brown International Corp.'s oil extractors or the *pellatrici Indelicato* and *Speciale*. It also can take place simultaneously with the juice extraction, as in the whole juice extractor of Food Machinery Corp. (FMC) (now called John Bean Technologies Food Tech). Or finally, the essential oil can be extracted in *sfumatrici* style after juice extraction, by, for example, Brown citrus juice extractors. After the cold pressing process the product obtained consists on a mixture of water, oil and other components which need to be separated to ensure a good quality of the oil. The first step is the removal of gross solids through a screen. The outflow is then centrifuged to obtain an aqueous phase, a sludge mostly constituted of solids, and an emulsion with 70-80 % oil content. Finally, a second step centrifugation is carried out to remove the remaining water and solids. A less commonly used purification method is steam distillation. The outflow from the extractor is put in contact with steam, and the resulting vapour is condensed until water and oil separates. This method has the risk of degradation of the oil due to the operation temperatures. Waxes which constitute the essential oil are also removed by storage of the oil during weeks at temperatures between -25 and -5 ºC.

2.2.1.3. Deterpenation: definition and methods

Terpenes are the main class of compounds present in an essential oil, however they have a poor contribution to its flavour or aroma [46]. In the case of citrus essential oils, the most representative terpene is limonene. These compounds are easily oxidized by air or free oxygen. Furthermore, they suffer hydrolysis reactions under heat and light conditions, and they are degraded generating

undesirable compounds. Furthermore, oxygenated terpenes (or oxyterpenes) are present in a smaller percentage, but they are the compounds mainly responsible for most of the odour and flavour characteristic of the oil. They mostly consist of alcohols, aldehydes and esters [47]. In the case of citrus essential oils, the most representative oxyterpenes are linalool (alcohol), citral (aldehyde) and linalil acetate [48]. Selective elimination of terpenes is called deterpenation. Thus, the deterpenation of the essential oil results in a more stable and valuable product.

Desired oxyterpenes usually have a boiling point between that of the monoterpenes and that of the heavier compounds. Currently, vacuum distillation is one the most used processes to deterpenate essential oils [46,49]. One main drawback of this method is the impossibility of removing all the non-desired monoterpenes without also removing some of the oxyterpenes, thus, driving to a second distillation stage. Moreover, the degradation of the oil due to long time heating during the whole process can happen, deriving in a loss of quality of the product.

Liquid-liquid extraction at ambient temperature appears as a more suitable operation for deterpenation of essential oils. The choice of solvent is the most critical aspect in the design of liquid-liquid extraction processes. The selection of a better solvent will result in an improved, more efficient process. Some factors to take into account are its solubility and selectivity, physical properties, toxicity, recoverability or its cost. Currently, some works can be found in the literature about the use of conventional solvents as extractants for citrus essential oils [50-57]. Water diluted ethanol seems to be the best option for this aim [54], but still, results need to be improved to obtain a solvent which better dissolves, and more selectively, the solute.

In the other hand, new possibilities are also being developed in this emerging industry, such as membrane technologies [46,58,59] or supercritical extraction [46,60-62]. These technologies avoid the distillation stage to recover the solvent, which can cause degradation of the product due to the temperature. In membrane separations the refined stream is removed by ultrafiltration or also by reverse osmosis. This process is carried out at room temperature. Its main drawback is the membranes clogging and, derived from this, its high maintenance costs. Supercritical fluid extraction is also carried out at room temperature avoiding thermal degradation of some compounds of the oil. The most popular supercritical fluid used for this aim is CO_2 which is non-toxic, non-flammable, has a low cost and a critical temperature of only 31 ºC. Nonetheless, high pressures needed in supercritical processes imply high operational costs and safety problems.

ILs in essential oil deterpenation

Interesting properties and advantages that ILs present in liquid-liquid extraction over conventional solvents [17,18] have drove to the exploration of the use of these innovative solvents in extraction processes for the separation of different valuable compounds of essential oils. Among other applications in liquid-liquid extraction, the suitability of using ILs as solvents for the deterpenation of essential oils has been already proposed for the Group of Separation Processes of the University of Santiago de Compostela [55,63]. In these works, the essential oil was simulated as a mixture of two compounds: the terpene limonene and the oxyterpene linalool. Two ILs based on an imidazolium cation were investigated for the deterpenation of the model of the citrus essential oil: 1-ethyl-3-methylimidazolium methanesulfonate ([C_2mim][OMs]) and 1-ethyl-3-methylimidazolium ethylsulfate ([C_2mim][$EtSO_4$]). In the first work [55], the extraction capability of the IL [C_2mim][OMs] was compared to that of other conventional organic solvents, obtaining good results for the extraction with the IL over them. Also, the suitability of the IL [C_2mim][$EtSO_4$] for the extraction of linalool was studied, obtaining high selectivity values for the solute [63]. Nevertheless, low solubilities of linalool have been found in both cases, meaning large quantities of IL needed for an efficient separation. Therefore, their use on an industrial scale could not be competitive even though the recovery of IL could be practically quantitative.

In conclusion, results obtained from the studies done in this field to date invite to be optimistic to the use of ILs as solvents for an efficient citrus essential oil deterpenation by means of liquid-liquid extraction. Nevertheless, an IL showing high solubilities and selectivities is needed to ensure the efficacy of the process.

2.2.2. ENHANCED OIL RECOVERY

Energy availability is strongly linked to health and to the level of welfare of the human being. While improving the exploiting efficiency of other sources of energy (renewable, hydrogen, nuclear…), dependence on fossil fuels remains enormous, and their greater exploitation is needed. Petrochemical industry is, moreover, the platform for global growth and development. It supplies to more than 30 derived industrial activities with raw materials. This demand of oil has driven to the search of new methods to recover a bigger part of the oil retained in the wells. With the increase in oil price, new technologies developed for this task have become more interesting over the years and lots of investigations are being carried out in this field.

2.2.2.1. General methods for oil recovery

The extraction of natural gas and oil from deep underground reserves consists on a hard task which can be affected by numerous factors of the subterranean environment, i.e. the porosity of the rock

and the viscosity of the deposit. These conditions can impede the free flow of product into the well. Some decades ago, the maximum recovery of oil did not go up to 10% of the total oil contained in the reservoir, leaving the rest underground because the technology did not exist to bring the rest to the surface. Today, advanced technology allows production of about 60% of the available resources from a formation. The overall recovery of oil can be divided in three categories: primary, secondary and tertiary or Enhanced Oil Recovery [64].

Primary recovery occurs because of natural energy, inherent in the oil reservoir, which pushes fluids into the well bore and lifts them to surface. The main source of this energy is the liberation and expansion of dissolved gas, the expansion of the gas cap of an active aquifer, gravity drainage, or a combination of these effects. The primary recovery stage reaches its limit either when the reservoir pressure is so low that the production rates are too low, or when the proportions of gas or water in the production stream are too high. Before this point is achieved, there is a need of an extra-energy source to drive the oil towards the production well. During primary recovery, only a small percentage of the initial hydrocarbons in place is recovered, typically around 10-15 % of oil reservoir [65].

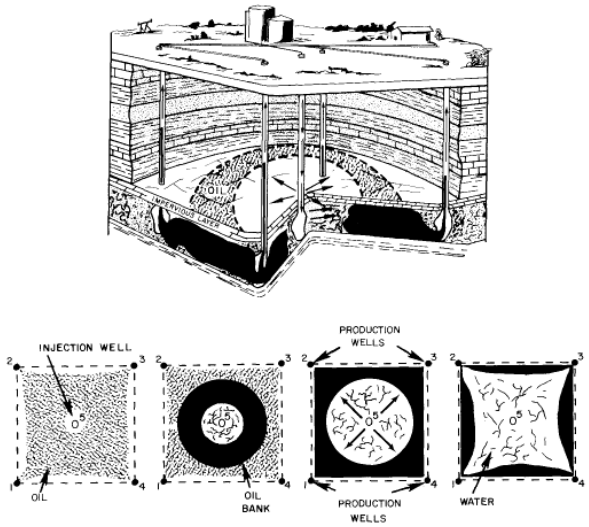

Figure 2.6. Displacement of oil through the reservoir rocks by water-flooding (five-spot pattern) [64].

Secondary recovery methods rely on the supply of external energy into the reservoir in the form of injecting fluids to increase reservoir pressure, hence replacing or increasing the natural reservoir drive with an artificial alternative. Sometimes pumps are used to bring the oil to the surface. Other secondary recovery techniques increase the reservoir's pressure by water

injection, natural gas reinjection and gas lift, which injects air, carbon dioxide or some other gas into the bottom of an active well, reducing the overall density of fluid in the wellbore. The most commonly used technique, water-flooding, drags out oil mobilised by viscous forces. Ultimately secondary recovery techniques reach a state where the oil production is too low to maintain profitability. Typical recovery factor from water-flooding operations is about 25-30 %, with variations depending on the properties of oil and the characteristics of the reservoir rock [65]. Figure 2.6 shows an example of the mechanism and functioning of a water-flooding process within the reservoir [64].

Primary and secondary oil extraction methods typically recover one third of the original oil in place. This is due to their limitations regarding to two factors [65]:

– At a pore scale, crude oil is trapped by capillary forces inside the pores as discontinuous globules.

– At a reservoir scale, there are zones where the injected fluid while secondary extraction does not penetrate because of low permeability of the reservoir, preferential paths, or the non favourable geometry of the wells.

Tertiary oil recovery (also known as Enhanced Oil Recovery, hereinafter EOR) consists on the extraction of the residual oil which remains in the reservoir after primary and secondary recovery methods. EOR occurs when media of increasing fluid mobility within the reservoir are introduced in addition to secondary techniques. A deeper study of these EOR methods will be carried out in the following section.

2.2.2.2. Tertiary oil recovery

The worldwide diminution of easy-to-access oil, along with an increase in the demand for oil and its high price, has rendered full exploitation of reservoirs (including the recovery of the hard-to-access oil) necessary. EOR methods have been proven to be effective in recovering the remaining oil from reservoirs that have lost drive during the application of primary and secondary recovery methods [66]. Remaining oil left after primary and secondary recovery operations is usually distributed in pores in the reservoir, where the oil is trapped, mainly due to capillary and viscous forces. Tertiary recovery begins when secondary oil recovery isn't enough to continue adequate extraction, but only when the oil can still be extracted profitably. This depends on the cost of the extraction method and the current price of crude oil. When prices are high, previously unprofitable wells are brought back into use and when they are low, extraction is curtailed.

The three major EOR methods currently used can be classified in three categories [66]:

– Chemical flooding, which can be divided into three main categories: surfactant flooding, polymer flooding and alkaline flooding.

– Miscible flooding: Carbon dioxide, nitrogen and hydrocarbons are commonly used.

– Thermal recovery. The thermal processes include: steam drive, cyclic steam injection and in situ combustion.

All these techniques employ one or more of the following mechanisms for improving the extraction of oil:

a) Increasing the mobility of the displacement medium by increasing the viscosity if the water, decreasing the viscosity of the oil, or both.

b) Extraction of the oil with a solvent.

c) Decrease of the oil/water interfacial tension.

Thermal recovery is normally applied in reservoirs which contain heavy oil. It mainly consists on the injection of steam into a petroleum reservoir or propagation of a combustion zone through a reservoir by air or oxygen-enriched air injection. The principles of functioning of this process are illustrated in Figure 2.7. This high increase of temperature reduces oil viscosity within the reservoir facilitating its drive towards the production wells.

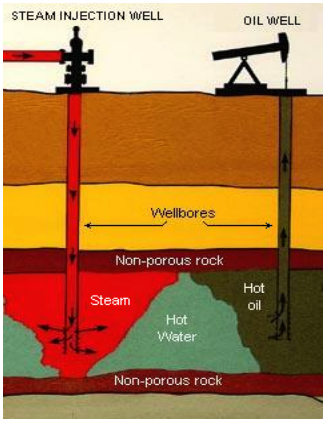

Figure 2.7. Thermal recovery by steam injection into the reservoir.

The fastest growing EOR process is miscible flooding. It consists on the injection into a petroleum reservoir of a material that is miscible, or can become miscible, with the oil in the reservoir. This miscibility enhances the mobility of the oil trapped in the porous rocks. Miscible flooding with CO_2 is one of the most widely used EOR processes. CO_2 is highly soluble in oil, swelling the oil and reducing the viscosity. This process is illustrated in Figure 2.8. The main problem with miscible gas flooding is the adverse mobility ratio caused by the low viscosity of the typical injecting gas compared to oil, which can be as high as one or two orders of magnitude. This can derive in the formation and propagation of viscous fingers thorough the displaced fluid, reducing the contact with some oil zones [67].

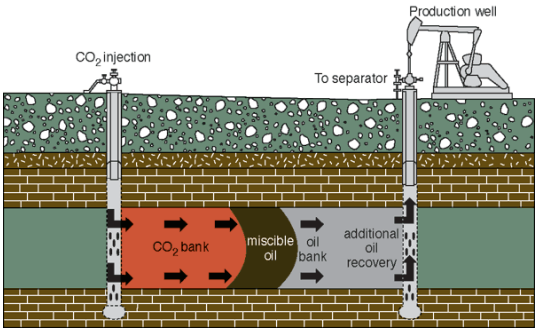

Figure 2.8. Miscible flooding using CO_2 as miscible gas.

An alternative method that does not suffer from the shortcomings of the miscible flooding is chemical EOR. The development of EOR processes based on operations which involve chemicals is greatly promising. The principles of chemical flooding operation are schematized in Figure 2.9.

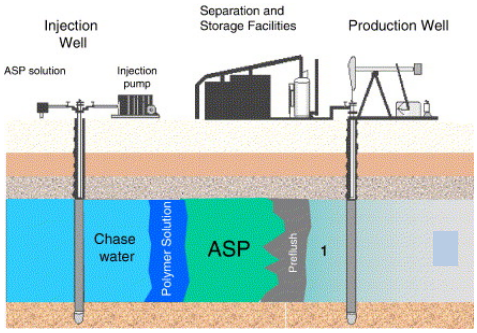

Figure 2.9. Principles of chemical flooding. ASP stands for Alkali-Surfactant-Polymer.

Chemical flooding consists on the injection of water together with other chemicals (surfactants, alkalis…) into the reservoir. The lowering of the interfacial tension between water and oil is the main driving force that enables the use of such methods. Change in fluid viscosity upon addition of chemicals like polymer mixtures are also observed and present some advantages. In general, there are three types of chemical EOR: surfactant flooding, polymer flooding and alkaline flooding.

2.2.2.3. Surfactant flooding

Surfactant flooding (also known as microemulsion flooding) is based on injecting an aqueous solution of surfactant and co-surfactants into the reservoir creating advantageous conditions in order to mobilize the trapped oil. The injection of surfactant reduces the water/oil interfacial tension, enhancing the mobility of the oil

trapped inside the pores of the rocks, letting it be flushed away by the flowing water.

Correctly designed surfactant systems together with the crude oil can create microemulsions at the interface between crude oil and water, thus reducing the interfacial tension to ultra low values, which consequently will mobilize the residual oil and results in improved oil recovery. Figure 2.10 illustrates the principles of surfactant flooding.

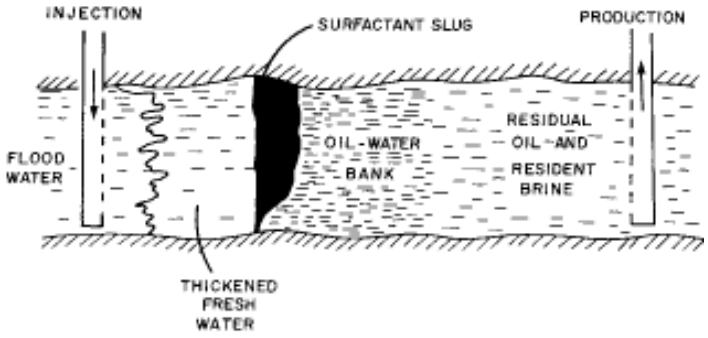

Figure 2.10. Principles of surfactant flooding [64].

There are two possible ways of application of this process. In the first, a relatively low concentration of surfactant (2-4 %) is injected in the bigger pores to reduce the interfacial tension between water and crude oil, enhancing the recovery. If phase formulation is the adequate, interfacial tension between aqueous and oil phases can achieve a minimum. The conditions of obtaining such tension have to do with the optimum formulation. This optimum formulation is associated to the presence of a triphasic system where a microemulsion, an oil excess phase and a water excess phase are coexisting. In the second case, bigger quantities of surfactant (8-12 %) are injected in smaller pores. The micelles solubilize the trapped oil and water into which is called a mobile microemulsion [66]. Mobility control is important in order to obtain an effective process. Surfactant viscosity should be high enough to decrease the water/oil mobility ratio, but not as much to create pumping problems**.** To avoid phase degradation an aqueous polymer phase is usually introduced into the reservoir after injection of the surfactant slug. The aim of the polymer is increasing the water viscosity, increasing this way the sweep efficiency. This method is called surfactant-polymer flooding.

Although surfactant flooding techniques are very promising, its application to date has been limited due to several factors as the high cost of the surfactant and the difficulty in its recovery, as a result of its adsorption onto the bearing forming rocks. Furthermore, the surfactants must remain active at reservoir conditions such as high temperatures, pressures and salinities. For these reasons, there is growing interest in finding new surfactants which properties that

best fit the surfactant EOR requirements, and which optimise the process.

Phase behaviour

During surfactant-assisted EOR, once within the reservoir, the fluid system can be considered as a pseudo-ternary system of water/brine, oil and surfactant. To analyse the effectiveness of a proposed surfactant flooding method, it is critical to have knowledge of the phase behaviour of the ternary system water + surfactant + oil, as well as the physical and transport properties of each phase. The behaviour of these components and their different concentrations in equilibrium can be represented in ternary diagrams. Winsor [68,69] studied the behaviour of these components defining three different types of ternary phase diagrams at a fixed temperature and pressure. These representations are showed in Figure 2.11 and explained below.

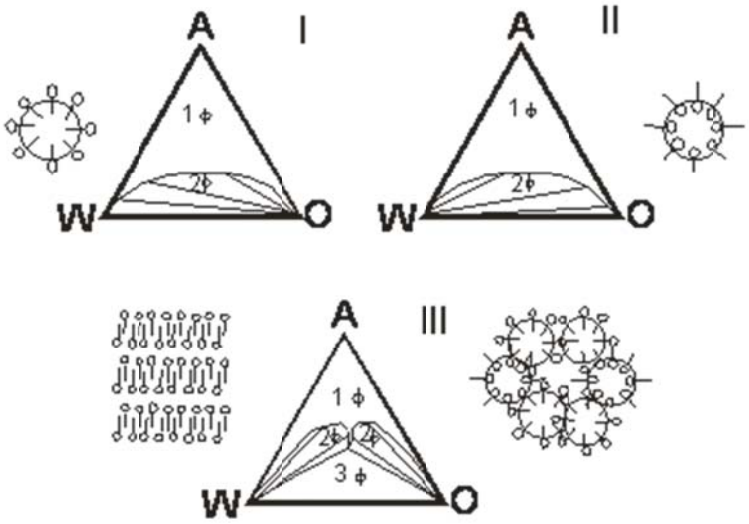

Figure 2.11. Winsor ternary diagram types. A: Surfactant, W: Water, O: Oil.

Winsor type I and type II diagrams have one biphasic region (2ϕ) and a monophasic region (1ϕ), while type III diagrams are constituted by one triphasic region (3ϕ) surrounded by three biphasic regions and one monophasic region [70]. Concerning to type III diagrams, it was demonstrated that the inferior biphasic region is generally very reduced and negligible for this type of systems. This tie-line is generally horizontal and corresponds to a surfactant concentration on the critical micelle concentration order [71].

In the type I diagram, any mixture within the immiscibility region separates into a lower aqueous microemulsion in equilibrium with an upper oil excess phase when the concentration of surfactant is low. The affinity of the surfactant towards the aqueous phase is

bigger than that of the oil. In the monophasic region the surfactant concentration ensures a complete miscibility between oil and water.

Type II diagram shows a similar situation to the type I. Nevertheless, oil and water behaviour are "inverted". The surfactant affinity for the oily phase predominates. Any composition within the binary region separates into an upper oily microemulsion phase in equilibrium with a water excess phase.

For the type III diagram, any system with global composition within the biphasic regions separates equally to previous explained systems. For systems with global composition within the triphasic region, the separation results into three phases in equilibrium: a lower water phase and an upper oil phase, which are mainly constituted of water and oil, respectively, and a microemulsion medium phase. In this diagram interactions are equilibrated and the surfactant is in which is called the optimum formulation. This physicochemical situation corresponds to the obtaining of an extremely low interfacial tension, and consequently the practically total elimination of the capillary forces which trap the crude oil in the porous medium.

Although real systems are multicomponent and diagrams are more complex, the optimum formulation concept maintains its original definition. Besides this, the number of phases can be visually analysed and compositions can be determined by adequate analytical methods.

Ionic liquids in surfactant flooding

Within the large family of ILs, some have been found to be surface active agents. Pino *et al.* [72] have described several dozens of ILs that exhibit characteristics of cationic surfactants (long carbon chain substituents appended to a charged cationic headgroup) and summarize their important applications in analytical chemistry and separation science. The amphiphilicity responsible for a remarkable interfacial and aggregation capability of IL surfactants may be associated with the cation, with the anion, or with both [73]. Properties such as the critical micelle concentration or the aggregation number can be controlled by changing the length and shape of the hydrocarbon tail, the type of polar head group, and/or the nature and size of the counter-ion [74-77].

In the patent by Collins *et al.* [73] a great variety of ILs which show surfactant characteristics are listed. These ILs show important properties for the formation of stable emulsions and microemulsions. At some point of this patent, authors cite the use of the water-in-oil microemulsions obtained for deploying water soluble or water dispersible oil field or gas field production chemicals as described in EOR. Other researchers have investigated the use of ILs to demulsify water-in-crude oil emulsions to obtain water free oil [33,34,78]. Shang et al. [79] use ILs as co-surfactants complementing the action of classical surfactants in EOR.

Several Winsor type III diagrams have been found in the literature for water + IL + oil systems [80-82] although they are not focused in EOR. The first direct proposal of using ILs as surface active agents in EOR was done by the Group of Separation Processes of the University of Santiago de Compostela, as consequence of this PhD work [83]. We advanced that ILs have the potential to constitute an attractive alternative to the surfactants commonly used in EOR processes, with important advantages over the traditional surfactant or polymer flooding methods, as for example:

– ILs are often liquid (and essentially non-volatile) over a wide range of temperatures.

– It is possible, in principle, to "design" an optimum IL for specific reservoir conditions (considering different fluid and rock properties).

– ILs have a relatively high viscosity, which is important to avoid the formation of digitations (phase degradation) resulting from unfavourable mobility ratios.

– The use of co-surfactants (usually long chain alcohols, which are volatile compounds and pose an environmental risk) may be avoided. This is a result of the strong cohesive forces in ILs, which enable them to form stable micelles without the need of additional chemicals.

Moreover, Murillo-Hernández and Aburto [30] summarized several applications of ILs in the petroleum industry. One of these is the capacity of ILs to solubilize heavy compounds in oil as asphaltenes or paraffins. Several works on this topic show that the viscosity of crude oil decreases considerably after being treated for removal of asphaltenes and similar substances [78,84,85]. Thus, the ability of some ILs to solubilize those heavy compounds may also be advantageous if ILs are used in EOR, where such solubilisation into a distinct phase would contribute to levelling the viscosity of the aqueous and organic phases.

After our work, first presented about ILs in EOR, only another recent publication was found on this application [86]. In that work, no phase diagrams are studied, systematic core flooding experiments are carried out and 1-dodecyl-3-methylimidazolium chloride is proposed as possible surfactant in EOR.

Limited investigation on this field of application of ILs makes the study of the use of these salts in chemical flooding an interesting and challenging aim. Attractive surface properties of ILs and advantages that these solvents present over commonly used surfactants rend optimistic to obtaining promising results in EOR processes.

2.2.3. BIOMASS PROCESSING

Since the last century, coal, natural gas, and petroleum are our main sources of energy and chemicals. It is estimated that they provide

approximately the 86% of world energy and the 96% of organic chemicals [87]. The dependence on fossil fuels remains enormous, and research for their greater exploitation is needed. Nevertheless, the depletion of this source of energy in a near future, associated to an increase of global energy demand, remains as a major concern. Hence, there is an urgent need to look for alternative renewable and greener energy sources. The answer lies in biomass, which possesses huge amounts of stored chemical energy. An efficient access to natural biopolymers, and subsequent enabling of fuels and materials platform, is a major step towards sustainability and a worldwide goal. Other than being renewable and abundant, biomass is a cost effective feedstock.

2.2.3.1. Biomass composition

Biomass is one of the most valuable products from living beings where simple molecules such as H_2O, CO_2, N_2 are transformed into complex substances activated or catalysed by biochemical processes (*e.g.* photosynthesis). Trees trap approximately 1% of solar energy and transform it into biomass. This energy is stored in the form of complex molecules such as lignin, carbohydrates, proteins, glycerides and others. Lignocellulose is mainly composed of cellulose, lignin, hemicellulose, and extractives, which represent an abundant carbon-neutral renewable resource [88]. The relative proportions of the three depend on the material source. The structure of these polymers is represented in Figure 2.12 [89].

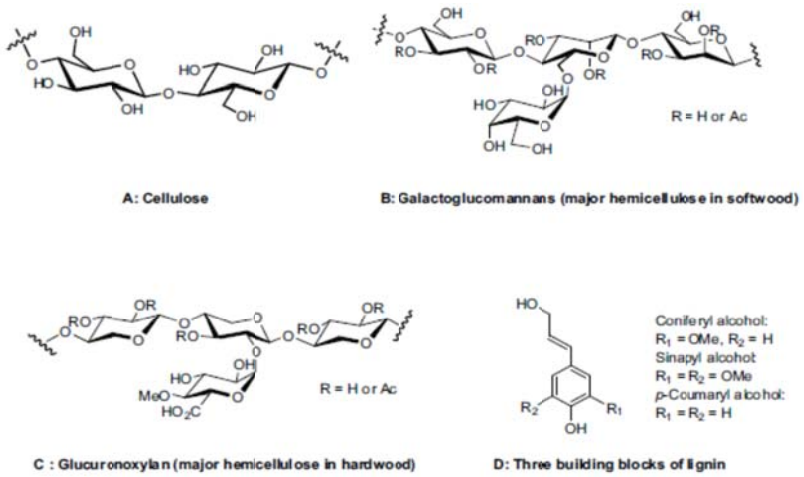

Figure 2.12. Structure of the three major biopolymers of the plant cell walls [89].

Cellulose consists on a semi-crystalline polymeric structure of glucose molecules connected primarily by glycosidic bonds. It is the most abundant biopolymer on Earth and can readily be enzymatically fermented to yield ethanol and catalytically

depolymerized to form 5-hydroxymethylfurfural [90]. Other major constituent of lignocellulosic biomass is lignin, which consists of a three-dimensional polymeric structure of phenylpropanoid units. Lignin is considered the cellular glue. It provides the plant tissue and the individual fibres with compressive strength, and the cell wall with stiffness. Hemicellulose consists on different 5 and 6 carbons monosaccharide units which connect cellulose fibres into micro fibrils and cross-links with lignin. This results in a complex network of bonds providing structural strength [91]. Figure 2.13 schematizes the location of these polymers in the plant cell.

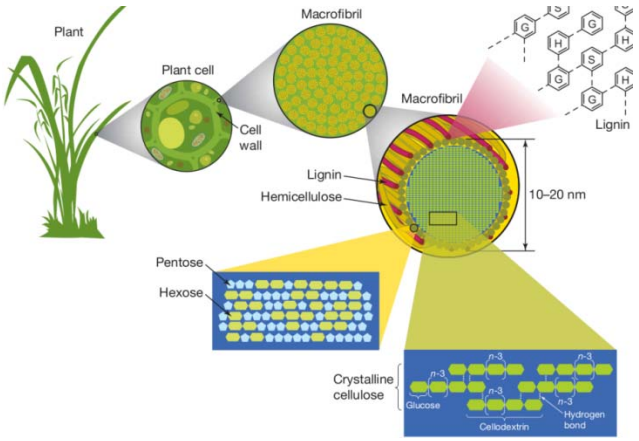

Figure 2.13. Schematic representation of the location and structure of lignin and lignocellulosic biomass in general [91].

Two important aspects have to be considered in the biomass processing. The combination of the heterogeneous and linear biopolymers leads to the formation of a strong and recalcitrant network. The biopolymer composition of lignocellulosic biomass changes for every type of biomass.

2.2.3.2. Biomass fractionation

If the biopolymers could be cleanly and easily separated from any lignocellulosic biomass source (forestry waste, agricultural residues, energy crops…), they could serve as ready feedstock for not only polymeric composite materials, but also for base chemicals and fuels (Figure 2.14). The true biorefinery would not be based on production of only a fuel, but a rich, near limitless variety of chemicals [92].

However, intrinsic recalcitrance of biomass, known as resistance of the plant cell walls to break down due to its complicated structure, has limited economic transformation of lignocellulosic biomass. Lignin is widely recognized as the major factor of biomass recalcitrance problem. The lignin seal of the cellulose must be broken and then the crystalline structure of cellulose can be disrupted.

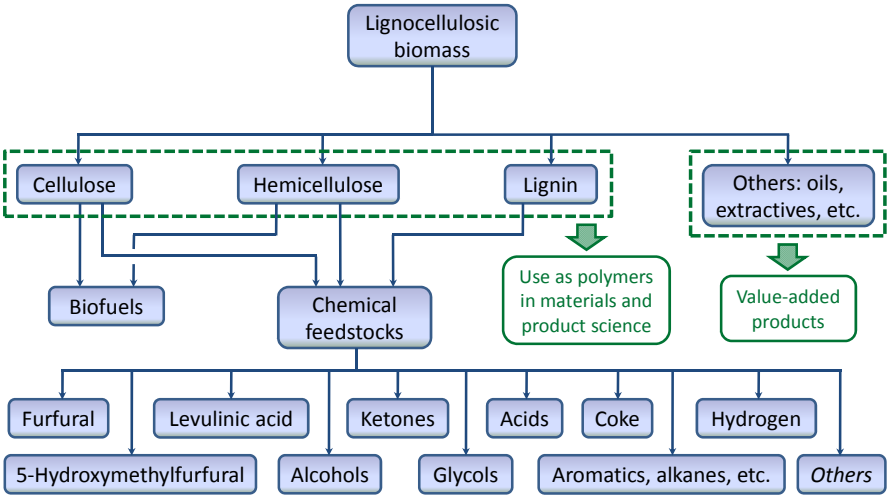

Figure 2.14. Possible applications of the three major components from lignocellulosic biomass [92].

Applied pretreatment methods for biomass fractionation can be mainly classified in chemical or physical [93]. Combination of pretreatment techniques from the same or different categories is also common. Physical pretreatment does not use chemical agents, and typically includes un-catalysed steam explosion, liquid hot water pretreatment, mechanical comminution (mechanical reduction in a particular biomass size), and high energy radiation. Chemical is the most studied pretreatment technique among the two categories. Solvents such as acids and bases, alkaline peroxide, ozone, organosolv, glycerol, dioxane, and phenol are known to disrupt the cellulose structure and promote hydrolysis.

To separate cellulose from lignocellulosic biomass, the most prevalent process is chemical pulping. It includes the Kraft, sulfite, soda and organosolv processes, among which the first accounts for 80% of chemical pulping [94]. In kraft pulping, aqueous solutions of caustic sodium hydroxide and sodium sulphide are used to extract lignin from the wood. The odour from sulphur compounds, high environmental impact, delignification, energy demand, and processing costs, are some examples of the challenges that need to be overcome for a cheap and environment friendly lignocellulosic biomass pretreating.

Ionic Liquids in biomass fractionation

Among a considerably large list of desired features, a lignocellulosic biomass solvent must primarily exhibit: the capability of dissolving cellulose at low temperatures, non volatility, non toxicity and chemical stability, no decompose cellulose, an easy regeneration, recyclability, effective cost, easy processing, and non-toxicity to enzymatic and microbial fermentation [95]. Designer solvents appear

as a suitable and potential alternative to organic solvents used in biomass pretreatment by chemical methods.

In 2002, Rogers *et al.* [26] published by first time that cellulose can be directly dissolved in specific ILs without pretreatment and be easily regenerated by precipitation upon addition of water or other common solvents without severe degradation of the cellulose. From this point, a big amount of research has been carried out focused on the use of ILs for biomass dissolution. Several good reviews can be found on bibliography about this subject [90, 96-103].

Most papers focus on dissolution of cellulose in ILs. It has been observed that the IL anion plays an important role in determining the salt's ability to dissolve cellulose [103]. Suitable ILs contain anions that can form strong hydrogen bonds with hydroxyl groups: chloride, carboxylates, dialkyl phosphates, dialkyl and trialkylphosphonates, amino acid anions... The choice of the cation also plays a role, however there are not clear trends and more studies are needed. ILs can be also used in lignin solubilisation. As with cellulose, the solubility seems to be strongly affected by the choice of the anion, although hydrogen-bond basicity does not need to be as high as for cellulose. Anions as triflate, methyl sulphate, chloride, bromide, acetate... exhibit high lignin solubility.

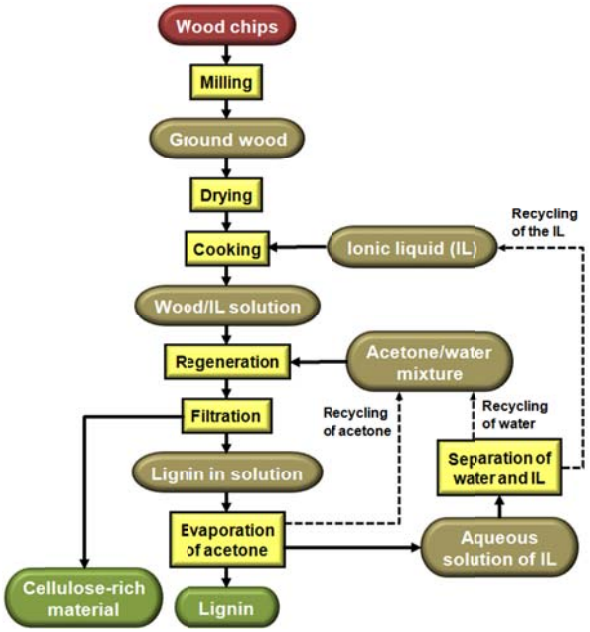

Figure 2.15. Flowchart for the process of dissolution and regeneration of wood in the IL [C_2mim][OAc] [92].

ILs have also been used to simultaneously dissolve all three major biomass components facilitating their separation and even to dissolve the whole lignocellulosic biomass [92]. Two of the most commonly encountered ILs associated with biomass dissolution are 1-ethyl-3- methylimidazolium acetate ([C_2mim][OAc]) and 1-butyl-3-methylimidazolium chloride ([C_4mim]Cl). These ILs can extensively disrupt the hydrogen-bonding interactions present in the three-dimensional network of lignocellulosics, leading to either dissolution of the whole biomass or selected individual components depending on the nature of the anion. Selective precipitation of individual biomass components can be achieved by the addition of an antisolvent as water or acetone. Figure 2.15 shows the flowchart for the process of dissolution and regeneration of wood in the IL [C_2mim][OAc] [92]. This *Dissolution Process* decrystallise the cellulose portion of lignocellulosic biomass and simultaneously disrupt the lignin and hemicellulose network. Some changes in cristallinity of cellulose can be found but they could have a positive impact, for example, in a posterior step of saccharification [103].

Despite the excellent chemical and physical properties of task-specific ILs which make them effective for biomass fractionation, still much research needs to be carried out in order to find less toxic and more economic ILs. For example, Liu *et al.* [104] synthetized a series of RTILs in which cholinium acts as the cation and amino acids as the anions. Most of these ILs dissolved lignin efficiently and selectively while cellulose was scarcely soluble.

Deep Eutectic Solvents in biomass fractionation

In this line of work of environmentally-friendly designer solvents for biomass fractionation, DESs are an interesting alternative to explode. They share the promising characteristics of ILs (low volatility, wide liquid range, designer solvents…) but their starting materials are usually easily biodegradable, cheap and non-toxic compounds, overcoming the high price and toxicity of ILs [41,42]. Practically no publications can be found in this interesting research about DESs in biomass processing.

Only one recent publication, which is the origin of the research work presented in this thesis, has been recently published in this subject. In that work [38], Francisco *et al.* synthetize several DESs (which they call LTTMs) and some of them are screened as solvents for lignin, cellulose and starch. Most of the tested solvents showed high lignin solubility and very poor or negligible cellulose solubility, being therefore promising for biomass fractionation.

The use of these more environmentally–friendly solvents for biomass pretreatment is of great interest but it is still in the early stage of the research.

3

Research protocol

3. RESEARCH PROTOCOL

For a better understanding of the research protocol, it will be divided in the main subsections of this thesis work: citrus essential oil deterpenation, EOR, and biomass processing.

3.1. CITRUS ESSENTIAL OIL DETERPENATION

3.1.1. CHEMICALS

Citrus essential oil was simulated as a mixture of its two main compounds, the terpene limonene and the oxyterpene linalool.(*R*)-(+)-limonene was supplied by Sigma-Aldrich with a nominal purity of 97 wt% , and (±)-linalool was purchased from SAFC and its purity is ≥97 wt%. Both chemicals were used as received, without further purification.

The IL 1-ethyl-3-methylimidazolium acetate ([C_2mim][OAc]) was purchased from Iolitec with a nominal purity of >95wt% and 1-buthyl-3-methylimidazolium acetate ([C_4mim][OAc]) with a nominal purity of ≥95 wt% was purchased from Fluka. Both ILs were purified by stirring and heating at 70 ºC for 48 h under high vacuum (< 0.1 mbar) to remove any residual volatile compound present. The improved purity of the ILs was verified by proton and carbon nuclear magnetic resonance spectroscopy (^{1}H NMR and ^{13}C NMR, respectively).

The rest of the ILs used as solvents for the deterpenation of citrus essential oil were synthesized in the laboratory as it is explained below.

- ***Synthesis of 1-ethyl-3-methylimidazolium bis(trifluoromehylsulfonyl)imide ([C_2mim][NTf_2]):***

This reaction was carried out in two stages: first an alkylation of 1-methylimidazolium with bromoethane, and a metathesis second stage with lithium bis(trifluoromethylsulfonyl)imide (Li[NTf_2]) [105].

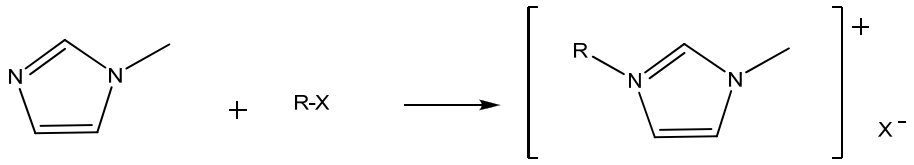

Figure 3.1. Alkylation reaction of 1-methylimidazolium with the haloalkane (R = akyl-group; X = halide) for the obtaining of 1-alkyl-3-methylimidazolium halide.

1-methylimidazole (Aldrich, 99 wt%) was placed in a round-botton flask with a reflux condenser attached. A 5 wt% molar excess of bromoethane (Aldrich, 99 wt%) was added dropwise under inert atmosphere at 40°C during 48 h (Figure 3.1). A few milliliters of acetonitrile (Panreac, >99.9 wt%) were added to the reaction product, 1-ethyl-3-methylimidazolium bromide ([C_2mim]Br), to avoid its solidification. Sample was then washed several times with ethylacetate (Aldrich, ≥99.5 wt%). The remaining molecular compounds were removed first with a rotary evaporator and, to complete the purification, high vacuum was used (<0.1 mbar) at 70 °C at least 48 h. The purity of the intermediate product was checked with ^{1}H NMR and ^{13}C NMR.

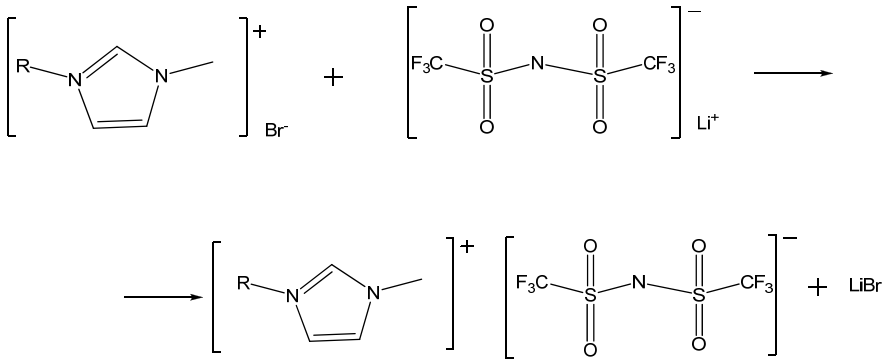

Figure 3.2. Methathesis reaction to synthesize 1-alkyl-3-methylimidazolium bis(trifluoromethylsulfonyl)imide (R = alkyl-group).

Once the purity of the [C_2mim]Br was checked, the second stage of the reaction was carried out (Figure 3.2). The IL was dissolved in water and mixed with a 5wt% molar excess of a Li[NTf_2] (Solvionic, >99 wt%) water solution. The solution was left reacting during 4 hours with vigorous stirring. The aqueous phase was separated in a decantation funnel and the reaction product (water immiscible) was dissolved in dichloromethane (Fluka, >99.9 wt%). Following, several washing steps were carried out with distillated water until there was no observance of a precipitate by adding silver nitrate to the residual aqueous phase, thus indicating the absence of halide in significant levels. Part of this water and dichloromethane were removed in a rotatory evaporator. Finally, a more exhaustive purification was done by putting the product in high vacuum (<0.1 mbar) during at least 48 h and 70 °C. A slightly yellow liquid was obtained. The IL purity was verified with ^{1}H NMR and ^{13}C NMR.

- ***Synthesis of 1-hexyl-3-methylimidazolium bis(trifluoromehylsulfonyl)imide ([C_6mim][NTf_2]):***

The synthesis was carried out following the method above explained (Figures 3.1 and 3.2). Alkylation of the 1-methylimidazolium was done with 1-chlorohexane (Aldrich, 99 wt%) and higher temperature (70 °C). The reaction product was the IL

[C_6mim]Cl. The following steps of metathesis and washing were similar to that of [C_2mim][NTf_2].

- ***Synthesis of 1-decyl-3-methylimidazolium bis(trifluoromehylsulfonyl)imide ([C_{10}mim][NTf_2]):***

The synthesis was analogous to that of the [C_6mim][NTf_2] (Figures 3.1 and 3.2), but using 1-chlorodecane (Aldrich, 99 wt%) as the initial haloalkane. The final product had a yellow coloration.

- ***Synthesis of 1-ethyl-3-methylimidazolium 2-(2-methoxyethoxy)ethylsulfate ([C_2mim][$Me(OEt)_2SO_4$]):***

The IL 1-ethyl-3-methylimidazolium 2-(2-methoxyethoxy)ethylsulfate, [C_2mim][$Me(OEt)_2SO_4$], was synthesized in the laboratory following the procedure proposed by Himmler *et al.* [106]. This method consists of two reaction steps: a quaternization of 1-ethylimidazolium with diethylsulfate followed by a transesterification.

In the first step, a determinate quantity of 1-methylimidazolium (Sigma-Aldrich, 99 wt%) was placed in a round bottom flask with an excess amount of toluene (Sigma-Aldrich, 99.5 wt%) as solvent. Diethylsulfate (Fluka, ≥99 wt%) in an equimolar proportion was added dropwise under inert atmosphere. The reaction was carried out in an ice bath due to its exothermicity. As showed in Figure 3.3, the formed IL is the 1-ethyl-3-methylimidazolium ethylsulfate ([C_2mim][$EtSO_4$]). Temperature was kept under 10 ºC. After 2h, toluene and the reactants in excess were separated by decantation in a funnel. [C_2mim][$EtSO_4$] was washed with fresh toluene several times. The process was completed with removal of remaining starting materials, first in a rotary evaporator and later under high vacuum (<0.1 mbar) during 48 h at 70 ºC. The product purity was verified by ^{1}H NMR and ^{13}C NMR.

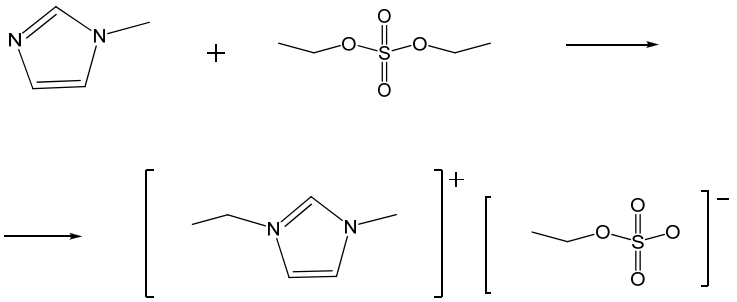

Figure 3.3. Synthesis of 1-ethyl-3-methylimidazolium ethylsulfate ([C_2mim][$EtSO_4$]).

A 1:2 molar relation of [C_2mim][$EtSO_4$] and di(ethylenglycol) methylether (Aldrich, ≥99.0 wt%) was mixed with a small quantity of methane sulfonic acid (Merck, ≥99.0 wt%), in a molar rate of 1:0.1. The reaction, Figure 3.4, was carried out at 70ºC, argon atmosphere

and constant stirring during 5 hours. Afterwards, the ethanol formed as co-product was removed introducing the flask first in a rotatory evaporator from 1 to 2 hours at 70ºC, and later under high vacuum at 70ºC and 12 h. Afterwards, a 1:1 molar quantity of di(ethylenglycol) methylether (in relation to the starting quantity of $[C_2mim][EtSO_4]$) was added and left reacting during 30 minutes in the above mentioned conditions. The formed ethanol was removed as explained for the previous stage. The IL was washed 5 times with a twofold excess of diethyl ether (Sigma-Aldrich, 99 wt%, ACS reagent). To remove the residual volatile compounds left in the IL, the flask was introduced first in a rotatory evaporator and later under high vacuum (<0.1 mbar) at 70 °C. ^1H and ^{13}C NMR spectra were obtained to check the purity of the product $[C_2mim][Me(OEt)_2SO_4]$.

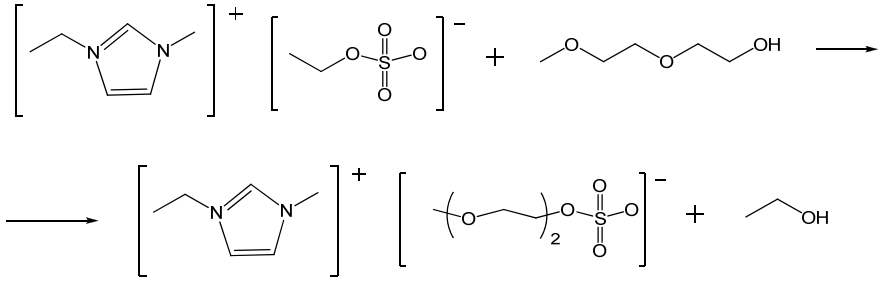

Figure 3.4. Synthesis of 1-ethyl-3-methylimidazolium 2-(2-methoxyethoxy)ethylsulfate ($[C_2mim][Me(OEt)_2SO_4]$).

- ***Synthesis of 1-methylpyridinium methylsulfate ($[C_1py][MeSO_4]$):***

The IL $[C_1py][MeSO_4]$ was synthesized by alkylation of pyridine (Riedel-de Haën, ≥99.5 wt%) with dimethylsulfate (Aldrich, ≥99 wt%) [107]. Careful dropwise addition of dimethylsulfate to mildly stirred pyridine, in a round-bottomed flask with reflux condenser attached, under argon atmosphere, was carried out in an ice bath to keep the temperature low due to the exothermic character of the reaction. After melting of the ice and natural warming of the water to room temperature, the flask was placed in an oil bath and heated up to 100 ºC for 8 h. The resulting mixture, with an IL appearance, was placed in a rotary evaporator for removal of unreacted materials or other volatile impurities. This removal of volatiles was completed by heating of the mixture at 70 ºC, with stirring, for 48 h under high vacuum (<0.1 mbar). The chemical identity and the purity of the desired products were assessed by ^1H NMR and ^{13}C NMR spectroscopy.

Table 3.1. CAS number, water content (ω_{H2O}), and experimental and literature values for density (ρ) and refractive index (n_D) of the pure components at 25 °C and atmospheric pressure.

		ω_{H2O} (ppm)	ρ (g cm^{-3})		n_D	
Compound	CAS number	Exp.	Exp.	Lit.	Exp.	Lit.
Limonene	5989-27-5	152	0.83868	0.8383[109]	1.47081	1.4701[109]
Linalool	78-70-6	204	0.85683	0.85760[110]	1.45961	1.4601[111]
[C_2mim][OAc]	143314-17-4	1200	1.09902	1.0993[112]	1.50069	1.50091[112]
[C_4mim][OAc]	284049-75-8	2087	1.05270	1.0532[113]	1.49372	1.49381[113]
[C_2mim][Me(OEt)$_2$SO$_4$]	790663-77-3	289	1.23861	1.2367[114]	1.48113	------
[C_2mim][NTf$_2$]	174899-82-2	298	1.51891	1.51845[115]	1.42298	1.4230[115]*
[C_6mim][NTf$_2$]	382150-50-7	87	1.37209	1.37213[116]	1.42879	1.42958[116]
[C_{10}mim][NTf$_2$]	433337-23-6	76	1.27840	1.2780[117]	1.43584	1.4356[117]
[C_1py][MeSO$_4$]	37943-43-4	149	1.34812	1.34483[118]	1.51353	1.51296[118]
[C_2py][EtSO$_4$]	2073-48-5	124	1.25283	1.2520[119]	1.50527	1.50525[119]

* Interpolated value.

- ***Synthesis of 1-ethylpyridinium ethylsulfate ([C_2py][$EtSO_4$]):***

The same method used for the synthesis of [C_1py][$MeSO_4$] was applied. In this case the alkylation of the pyridine was done with diethylsulfate (Fluka, ≥99 wt%). The final product was a colourless liquid.

3.1.1.1. Physical properties of pure compounds

Some representative physical properties, as density or refractive index, were determined for the used chemicals as a proof of their purity. It is well known that the behaviour of ILs is notably sensible to their water content [108], for this reason their water content was also measured by using the Karl-Fischer titration method. The ILs were stored in desiccators, in order to avoid moisture uptake.

The CAS number and water content of the pure compounds used in this work are reported in Table 3.1. Their experimental densities and refractive indices at 25 ºC are also shown and were found to be in good agreement with values previously reported in literature [109-119], thus confirming the purity of the commercial and synthesized chemicals.

3.1.1.2. Recoverability of ILs

The ILs used all along the experimental section were recovered in the laboratory. Due to their negligible vapour pressure they can be recovered, to obtain a required purity, by evaporation of the volatile compounds in the sample. For this purpose, a rotatory evaporator was used in a first place, followed by a high vacuum line (<0.1 mbar) at 70 ºC until the obtaining of the desired purity, which was checked by ^{1}H and ^{13}C NMR. The water content as well as their physical properties of the recovered ILs were also verified before their use.

3.1.2. EQUIPMENT

Densities were measured in an Anton Paar DMA 5000 densimeter with viscosity correction and with self-control of temperature to ±0.01 K using the Peltier effect. The measurement was repeated at least three times for each sample. The uncertainty in the density measurement is 10^{-5} g·cm^{-3}. Refractive indices were measured in an ATAGO RX-5000 refractometer. The temperature was controlled with an uncertainty of ±0.02 K by means of a HetoTherm thermostat. The measurement was repeated at least three times for each sample. The uncertainty in the refractive index measurement is $\pm 4 \times 10^{-5}$.

Water content of the chemicals used in this work was determined by Karl-Fischer titration with a MetrOhm 737 KF coulometer. The measurement was repeated at least three times for each sample. The uncertainty in the measurements is 5 µg when water content is lower than 10^3 µg and 0.5 wt% for higher mass of

water. The product used for these titrations is Hydranal® (Riedel-de Haën).

Specially designed jacketed glass cells were used for the determination of tie-lines of the Liquid-Liquid Equilibrium (LLE). These cells were connected to a Selecta (UltraTerm 6000383 model) thermostatic bath which allows the control of the temperature with an uncertainty of ±0.05 °C. The special design allows vigorously stirring the content of the cell, settling, and taking sample of each layer in which an immiscible liquid mixture splits, while keeping it at a constant temperature. Figure 3.5 shows the experimental setup for measurement of the LLE.

Figure 3.5. Experimental setup for determination of the LLE data.

Two analytical techniques were used to determine the compositions of equilibrium phases: gas chromatography and ^{1}H NMR spectroscopy. For calibration of both methods, all the weighing was carried out in a Mettler Toledo AE 240 analytic balance with a precision of 10^{-4} g.

Column chromatography quantitative analysis is based on the existing rate between the height or the analytic area of the peaks of the studied substances in the chromatogram and the concentration of these substances in the sample (in most of the cases, only when the chromatograph conditions are well-controlled). When using the height of the peaks, a high precision can only be obtained if the variations in the operational conditions of the column barely affect the width of the peak during the run time needed to obtain the chromatograms. This is only possible if there is an exhaustive control of several variables such as oven temperature, effluent flux speed and sample injection speed. Even more, a possible overloading of the column should be taken into account. The analysis of compositions by means of areas under the peaks is independent of the effect on

the peak shape produced by the previously cited variables. From this point of view, areas are analytic variables more adequate than height of peaks to carry out a quantitative analysis. For this reason, in this work, the compositions of the different compounds in the sample were determined by the areas under the peaks.

The equipment used was a HP 6890 Series gas chromatograph (Figure 3.6) using a thermal conductivity detector, an injector, a HP-5 capillary column of 30 m × 0.32 mm × 0.25 μm (film thickness), and an empty pre-column (without stationary phase) to avoid the ILs, not retained in the liner, reach the column. Table 3.2 summarises the chromatograph operation conditions for this experimental work. These conditions are the results of an optimisation process to achieve the best analytical precision.

Figure 3.6. HP 6890 Series gas chromatograph.

Table 3.2. Gas chromatograph operation conditions for the analysis of the ternary systems limonene + linalool + IL.

Column	Type:	HP-5
	Flux:	Constant flux of 1 mL/min
Detector	Type:	TCD
	Temperature:	240 °C
Carrier gas		He
Injector	Temperature:	250 °C
	Split rate:	20/1
	Injection volume:	1μL
Oven	Temperature program:	70 °C (3.70 min) → 60 °C/min until 250 °C (3.10 min)

As alternative to gas chromatography, the ^{1}H NMR spectroscopy combines simplicity and sufficient accuracy for practical purposes. Several satisfactory examples of the use of this analysis method in studying LLE of systems involving ILs can be found in literature [120-122].

Figure 3.7. Mercury 300 with robot sampler spectrometer.

In a ^{1}H NMR spectrum, a series of peaks over a baseline are recorded. These peaks are related to the hydrogen atoms of the chemical structures present in the sample, the hydrogens with equivalent 'chemical vicinity' accounting for the same peak. Thus, every chemical species in a mixture, with hydrogen atoms in its structure, will generate a series of peaks in the spectrum. In principle, the areas under these peaks are proportional to the number of hydrogens they are representing. This proportionality opens a door to the use of ^{1}H NMR spectroscopy as a quantitative technique for the determination of compositions of mixtures. In the case of ternary systems, it is very important to select a peak not overlapped for each component, to make quantitative this analysis method.

The NMR runs were performed at 25 ºC with a relaxation time of 20-30 s in a Varian Mercury 300, with robot sampler, of 7.04 T (300 MHz resonance for ^{1}H). This equipment is shown in Figure 3.7.

3.1.3. PROCEDURE

The experimental procedure for the development of this work can be divided in two sections: solubility tests and equilibrium determinations.

3.1.3.1. Solubility tests

For a first overview of the suitability of using ILs as linalool extracting agents, solubility test were performed to pre-select the apparently most promising ILs within their big family. The main goal of this first approach was selecting the ILs with the lowest limonene solubility and highest linalool solubility.

This test was carried out by means of the turbidity test. Samples of each of the studied components with different concentrations of IL were prepared in 2 mL vials. Following, each vial was vigorously stirred with a vortex mixer and a possible formation of "cloud" or turbidity, indicating the separation of the simple in two phases, was observed.

3.1.3.2. Equilibrium

In a first place, the shape of the solubility curve formed by the system limonene + linalool + IL was determined using the cloud point method. This is a visual method, so approximated, but gives a clue of where the immiscibility border of the system is.

A certain amount of limonene or IL was introduced in a thermostated solubility cell (Figure 3.8) depending on the part of the solubility curve wanted to be determined. The IL (when the liquid contained in the cell was limonene) or limonene (when the cell contained the IL) was added drop wise with a burette into the cell until turbidity. The mixture was vigorously stirred until the turbidity was permanent. This way, the first point corresponding to the mutual solubility between limonene and IL was obtained. With another burette, linalool was added also drop wise until the turbidity disappeared, afterwards, the IL (or limonene) was added until new apparition of the immiscibility, and this procedure was followed until obtaining the complete shape of the solubility curve.

Afterwards, different mixtures of the three components (or two when determining the tie-lines corresponding to the binary systems), with global composition within the immiscibility region, were prepared for each ternary system. Special care was put in choosing global compositions in order to get well-distributed tie-lines fully covering the immiscibility region. Also, the relative volume of the two phases generated has to be taken into account to make the extraction of the sample easier. The so prepared mixtures were placed in the equilibrium glass cells (Figure 3.8) and sealed to avoid losses by evaporation or pickup of moisture.

Figure 3.8. Solubility (left) and equilibrium (right) cells.

Temperature inside the cells was kept constant with a thermostat and their content was vigorously stirred until achieving the equilibrium. The time needed to achieve this equilibrium between phases was determined by performing several tests with different agitation times and proving that the composition of each phase was the same after each agitation period. This time was established to be 2 h. After this time, the samples were allowed to settle during 5 h to ensure a complete separation of the phases. Preliminary tests also showed that this time was enough to guarantee that the thermodynamic equilibrium was achieved. The exceptions were the systems involving $[C_npy][RSO_4]$ and $[C_nmim][OAc]$ ILs, which needed a longer settling time of 12 h. Once the phases were completely separated, samples were withdrawn with syringes to carry out the compositional analysis.

Compositions for ternary system limonene + linalool + $[C_2mim][Me(OEt)_2SO_4]$ were determined by gas chromatography. The method requires a previous calibration to relate the analytical signal obtained by the equipment with the concentration of the compounds in the studied sample. Among the most common calibration methods the internal standard method was used. This method allows determining the composition of limonene and linalool in the sample and the IL composition is determined by difference. Octane was used as the internal standard. A meticulous calibration during data acquisition provided estimated experimental uncertainty to be ±0.007 mole fraction for the IL-rich phase and ±0.005 for the limonene-rich phase.

Later, due to its simplicity, the compositional analysis by means of ^1H NMR spectroscopy was developed and used in the study of the equilibrium of all the other systems.

To do a selection of the peaks of each ternary system, several miscible samples were prepared by weight. The composition of these samples must cover the whole area in the proximities of the heterogeneous region. Afterwards, a drop of the sample was

introduced in a NMR tube with a deuterated solvent. Each tube was perfectly sealed to avoid losses of volatile components or moisture gain. The peaks in the spectra were assigned to the chemical structures of the species in the mixture. Figure 3.9 shows an example of a of this selection for the system limonene + linalool + [C_6mim][NTf_2].

The selected peaks for their integration were those which drove to a better concordance between the composition obtained by weight and the composition obtained by ^{1}H NMR. For example, the selected peaks in Figure 3.9 were the following: for the IL peaks 4 and 5; for the linalool peaks 12 and peaks from 11 to 17; and for the limonene, peaks 21 and 24. The maximum deviation between the compositions obtained by weight and the compositions obtained by ^{1}H NMR for all the ternary systems analysed by this method are summarized in Table 3.3.

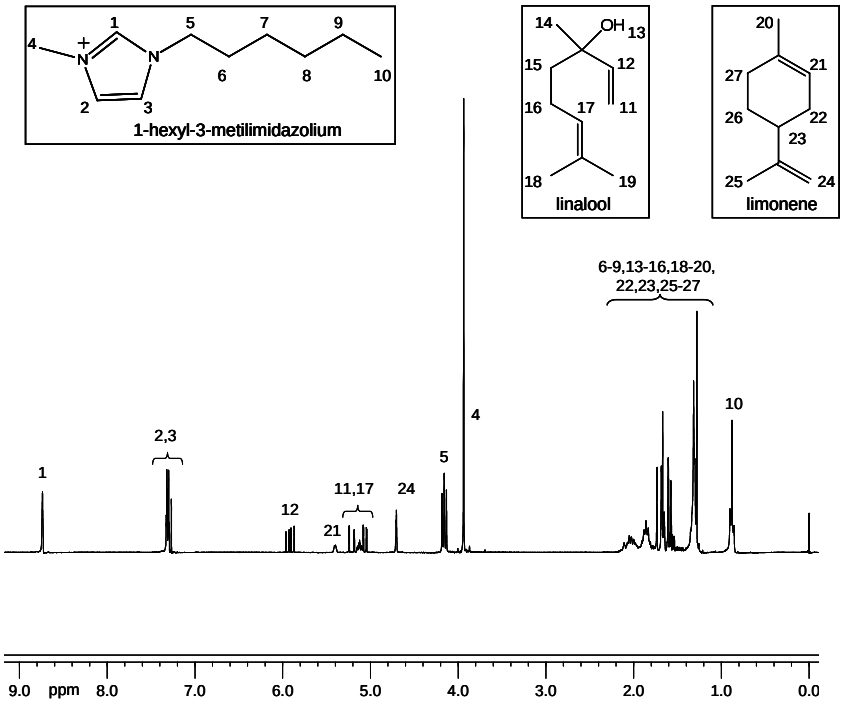

Figure 3.9. ^{1}H NMR spectrum for the ternary mixture limonene + linalool + [C_6mim][NTf_2], including structures of the chemical species and peak assignment (Note: the triflate anion of the IL was not considered, as it does not have any hydrogen atom and therefore does not generate any peak in the spectrum).

Table 3.3. Estimated uncertainty in the determination of the molar fraction compositions by ^{1}H NMR for the ternary systems limonene + linalool + IL.

Ternary system	Estimated uncertainty	
	Organic-rich phase	IL-rich phase
limonene + linalool + [C_2mim][OAc]	0.006	0.009
limonene + linalool + [C_4mim][OAc]	0.005	0.009
limonene + linalool + [C_2mim][NTf_2]	0.006	0.008
limonene + linalool + [C_6mim][NTf_2]	0.004	0.009
limonene + linalool + [C_{10}mim][NTf_2]	0.007	0.008
limonene + linalool + [C_1py][$MeSO_4$]	0.009	0.002
limonene + linalool + [C_2py][$EtSO_4$]	0.011	0.012

3.1.4. RESULTS AND DISCUSSION

Several ILs have been studied as possible solvents to deterpenate citrus essential oil by liquid-liquid extraction process: [C_2mim][Me(OEt)$_2$$SO_4$], [$C_2$mim][$NTf_2$], [$C_6$mim][$NTf_2$], [$C_{10}$mim][$NTf_2$], [$C_1$py][$MeSO_4$], [$C_2$py][$EtSO_4$], [$C_2$mim][OAc] and [$C_4$mim][OAc].

Citrus essential oil has been simulated as a mixture of two representatives of its main types of components: the terpene limonene and the oxyterpene linalool, being the last the main responsible of the organoleptic properties of the oil.

The suitability of each IL to extract the linalool from the essential oil mixture was evaluated from the experimental data by means of two classical parameters, namely solute distribution ratio (β) and selectivity (S), defined as:

$$\beta = \frac{x_s^{II}}{x_s^{I}} \qquad (3.1)$$

$$S = \frac{x_s^{II}}{x_s^{I}} \cdot \frac{x_i^{I}}{x_i^{II}} \qquad (3.2)$$

where x stands for molar fraction, subscripts s and i represent the solute (linalool) and the carrier (limonene), and superscripts I and II represent the organic-rich and IL-rich phases, respectively.

The LLE data for the studied systems are listed in Tables 3.4 to 3.11, along with the values of solute distribution ratio and selectivity, calculated according to Equations (3.1) and (3.2).

Table 3.4. Compositions of the experimental tie-line ends, solute distribution ratio (β) and selectivity (S) for the LLE of the ternary system limonene + linalool + [C_2mim][Me(OEt)$_2$SO$_4$] at several temperatures. The molar fractions of limonene, linalool and IL are represented by x_1, x_2 and x_3, respectively.

IL-rich phase			Organic-rich phase			β	S
x_1	x_2	x_3	x_1	x_2	x_3		
			T = 25 ºC				
0.018	0.000	0.982	1.000	0.000	0.000	-----	-----
0.023	0.039	0.938	0.936	0.064	0.000	0.61	24.8
0.036	0.109	0.855	0.838	0.162	0.000	0.67	15.7
0.042	0.163	0.795	0.804	0.196	0.000	0.83	15.9
0.109	0.283	0.608	0.712	0.288	0.000	0.98	6.42
0.120	0.329	0.551	0.672	0.328	0.000	1.00	5.62
0.156	0.392	0.452	0.613	0.387	0.000	1.01	3.98
0.183	0.419	0.398	0.587	0.413	0.000	1.01	3.25
0.220	0.481	0.299	0.540	0.460	0.000	1.05	2.57
0.230	0.505	0.265	0.503	0.497	0.000	1.02	2.22
			T = 35 ºC				
0.017	0.000	0.983	1.000	0.000	0.000	-----	-----
0.026	0.036	0.938	0.925	0.075	0.000	0.48	17.1
0.039	0.113	0.848	0.846	0.154	0.000	0.73	15.9
0.045	0.162	0.793	0.801	0.199	0.000	0.81	14.5
0.086	0.256	0.658	0.716	0.284	0.000	0.90	7.50
0.113	0.343	0.544	0.647	0.353	0.000	0.97	5.56
0.157	0.382	0.461	0.599	0.401	0.000	0.95	3.63
0.194	0.442	0.364	0.566	0.434	0.000	1.02	2.97
0.238	0.502	0.260	0.516	0.484	0.000	1.04	2.25
0.288	0.546	0.166	0.450	0.550	0.000	0.99	1.55
			T =45 ºC				
0.020	0.000	0.980	1.000	0.000	0.000	-----	-----
0.025	0.022	0.953	0.925	0.070	0.005	0.31	11.6
0.039	0.115	0.846	0.815	0.176	0.009	0.65	13.7
0.042	0.162	0.796	0.795	0.205	0.000	0.79	15.0
0.077	0.251	0.672	0.696	0.304	0.000	0.83	7.46
0.132	0.370	0.498	0.587	0.413	0.000	0.90	3.98
0.166	0.425	0.409	0.546	0.454	0.000	0.94	3.08
0.210	0.496	0.294	0.499	0.501	0.000	0.99	2.35
0.261	0.556	0.183	0.428	0.572	0.000	0.97	1.59

Table 3.5. Compositions of the experimental tie-line ends, solute distribution ratio (β) and selectivity (S) for the LLE of the ternary system limonene + linalool + [C_2mim][NTf_2] at 25 °C. The molar fractions of limonene, linalool and IL are represented by x_1, x_2 and x_3, respectively.

IL-rich phase			Organic-rich phase			β	S
x_1	x_2	x_3	x_1	x_2	x_3		
0.049	0.000	0.951	1.000	0.000	0.000	-----	-----
0.046	0.019	0.935	0.956	0.044	0.000	0.43	8.97
0.041	0.051	0.908	0.841	0.159	0.000	0.32	6.58
0.042	0.081	0.877	0.703	0.297	0.000	0.27	4.56
0.036	0.102	0.862	0.574	0.426	0.000	0.24	3.82
0.034	0.130	0.836	0.450	0.550	0.000	0.24	3.13
0.028	0.153	0.819	0.329	0.671	0.000	0.23	2.68
0.020	0.185	0.795	0.207	0.793	0.000	0.23	2.41
0.008	0.214	0.778	0.076	0.924	0.000	0.23	2.20
0.000	0.237	0.763	0.000	1.000	0.000	0.24	-----

Table 3.6. Compositions of the experimental tie-line ends, solute distribution ratio (β) and selectivity (S) for the LLE of the ternary system limonene + linalool + [C_6mim][NTf_2] at 25 °C. The molar fractions of limonene, linalool and IL are represented by x_1, x_2 and x_3, respectively.

IL-rich phase			Organic-rich phase			β	S
x_1	x_2	x_3	x_1	x_2	x_3		
0.160	0.000	0.840	1.000	0.000	0.000	-----	-----
0.161	0.028	0.811	0.972	0.028	0.000	1.00	6.04
0.165	0.082	0.753	0.906	0.094	0.000	0.87	4.79
0.158	0.153	0.689	0.782	0.218	0.000	0.70	3.47
0.163	0.229	0.608	0.645	0.355	0.000	0.65	2.55
0.155	0.284	0.561	0.530	0.470	0.000	0.60	2.07
0.143	0.320	0.537	0.456	0.544	0.000	0.59	1.88
0.133	0.349	0.518	0.385	0.615	0.000	0.57	1.64
0.116	0.377	0.507	0.336	0.664	0.000	0.57	1.64
0.091	0.428	0.481	0.232	0.768	0.000	0.56	1.42
0.059	0.486	0.455	0.148	0.852	0.000	0.57	1.43
0.000	0.573	0.427	0.000	0.998	0.002	0.57	-----

Table 3.7. Compositions of the experimental tie-line ends, solute distribution ratio (β) and selectivity (S) for the LLE of the ternary system limonene + linalool + [C_{10}mim][NTf_2] at 25 °C. The molar fractions of limonene, linalool and IL are represented by x_1, x_2 and x_3, respectively.

IL-rich phase			Organic-rich phase			β	S
x_1	x_2	x_3	x_1	x_2	x_3		
0.427	0.000	0.573	1.000	0.000	0.000	-----	-----
0.435	0.033	0.532	0.978	0.022	0.000	1.50	3.37
0.442	0.108	0.450	0.919	0.081	0.000	1.33	2.77
0.440	0.203	0.357	0.812	0.188	0.000	1.08	1.99
0.400	0.325	0.275	0.634	0.363	0.003	0.90	1.42
0.347	0.423	0.230	0.502	0.495	0.003	0.85	1.24
0.283	0.505	0.212	0.392	0.602	0006	0.84	1.16
0.221	0.591	0.188	0.292	0.701	0.007	0.84	1.11
0.187	0.629	0.184	0.239	0.752	0.009	0.84	1.07
0.126	0.708	0.166	0.160	0.828	0.012	0.86	1.09
0.080	0.756	0.164	0.102	0.886	0.012	0.85	1.09
0.032	0.817	0.151	0.039	0.946	0.015	0.86	1.05
0.000	0.851	0.149	0.000	0.984	0.016	0.86	-----

Table 3.8. Compositions of the experimental tie-line ends, solute distribution ratio (β) and selectivity (S) for the LLE of the ternary system limonene + linalool + [C_1py][$MeSO_4$] at 25 °C. The molar fractions of limonene, linalool and IL are represented by x_1, x_2 and x_3, respectively.

IL-rich phase			Organic-rich phase			β	S
x_1	x_2	x_3	x_1	x_2	x_3		
0.001	0.000	0.999	1.000	0.000	0.000	---	---
0.000	0.009	0.991	0.878	0.122	0.000	0.07	∞
0.000	0.015	0.985	0.770	0.230	0.000	0.07	∞
0.000	0.025	0.975	0.629	0.369	0.002	0.07	∞
0.000	0.038	0.962	0.502	0.497	0.001	0.08	∞
0.000	0.051	0.949	0.304	0.695	0.001	0.07	∞
0.000	0.052	0.948	0.000	0.995	0.005	0.05	∞

Table 3.9. Compositions of the experimental tie-line ends, solute distribution ratio (β) and selectivity (S) for the LLE of the ternary system limonene + linalool + [C_2py][$EtSO_4$] at 25 °C. The molar fractions of limonene, linalool and IL are represented by x_1, x_2 and x_3, respectively.

IL-rich phase			Organic-rich phase			β	S
x_1	x_2	x_3	x_1	x_2	x_3		
0.000	0.000	1.000	1.000	0.000	0.000	---	---
0.006	0.018	0.976	0.942	0.058	0.000	0.31	48.7
0.009	0.053	0.938	0.872	0.128	0.000	0.41	40.1
0.020	0.097	0.883	0.818	0.181	0.001	0.54	21.9
0.022	0.108	0.870	0.787	0.213	0.000	0.51	18.1
0.031	0.152	0.817	0.740	0.258	0.002	0.59	14.1
0.035	0.181	0.784	0.707	0.290	0.003	0.62	12.6
0.091	0.303	0.606	0.646	0.347	0.007	0.87	6.20
0.215	0.442	0.343	0.556	0.430	0.014	1.03	2.66
0.317	0.487	0.196	0.480	0.477	0.043	1.02	1.55

Table 3.10. Compositions of the experimental tie-line ends, solute distribution ratio (β) and selectivity (S) for the LLE of the ternary system limonene + linalool + [C_2mim][OAc] at 25 °C. The molar fractions of limonene, linalool and IL are represented by x_1, x_2 and x_3, respectively.

IL-rich phase			Organic-rich phase			β	S
x_1	x_2	x_3	x_1	x_2	x_3		
0.044	0.000	0.956	1.000	0.000	0.000	---	---
0.047	0.038	0.915	0.994	0.006	0.000	6.33	134
0.057	0.090	0.853	0.988	0.012	0.000	7.50	130
0.097	0.212	0.691	0.981	0.019	0.000	11.2	113
0.152	0.279	0.569	0.973	0.027	0.000	10.3	66.2
0.338	0.319	0.343	0.963	0.035	0.002	9.11	26.0
0.551	0.229	0.220	0.901	0.070	0.029	3.27	5.35

Table 3.11. Compositions of the experimental tie-line ends, solute distribution ratio (β) and selectivity (S) for the LLE of the ternary system limonene + linalool + [C_4mim][OAc] at 25 °C. The molar fractions of limonene, linalool and IL are represented by x_1, x_2 and x_3, respectively.

IL-rich phase			Organic-rich phase			β	S
x_1	x_2	x_3	x_1	x_2	x_3		
0.067	0.000	0.933	1.000	0.000	0.000	---	---
0.071	0.019	0.910	0.999	0.001	0.000	19.0	267
0.093	0.106	0.801	0.995	0.005	0.000	21.2	227
0.169	0.198	0.633	0.992	0.008	0.000	24.8	145
0.226	0.225	0.549	0.989	0.011	0.000	20.5	89.5
0.479	0.237	0.284	0.959	0.030	0.011	7.90	15.8
0.667	0.163	0.170	0.917	0.052	0.031	3.13	4.31

A first study was carried out to see how the temperature affects to the equilibrium. For this matter, the system limonene + linalool + [C_2mim][Me(OEt)$_2$$SO_4$] was studied at three different temperatures: 25, 35 and 45 °C [123]. Table 3.4 shows linalool solute distribution ratios and selectivities for this system. It can be noticed that β and S have very similar values at the studied temperatures, getting even slightly better results at 25 °C. At this temperature the results obtained for β and S are higher, especially at low concentrations of linalool. This is a region of particular interest, since the initial concentration of oxyterpenes (linalool) in the essential oil lies within it.

Due to the low influence of the temperature in the equilibrium data, and to the fact that an increase of this parameter would result in an increase in the operational costs, it was decided to carry out all the following studies at 25 °C, which is a recommended thermodynamic value or reference.

Figures 3.10 to 3.17 show the representation of the experimental and correlated LLE data in equilateral triangular diagrams. This kind of representation of ternary systems provides a good visualization of the shape and size of the immiscibility region, as well as the slopes of the tie-lines. The corresponding solute distribution ratios (β) and selectivities (S) for each system and their correlated values are also represented in these Figures.

According to the classification proposed by Sϕrensen *et al.* [124], the systems with [C_2mim][NTf_2], [C_6mim][NTf_2], [C_{10}mim][NTf_2] and [C_1py][$MeSO_4$] (Figures 3.11-3.14) correspond to Type II, since they present two immiscible pairs (limonene-IL, and linalool-IL), a completely miscible pair (limonene-linalool), and only one continuum immiscibility domain. In the same classification, the systems with [C_2mim][Me(OEt)$_2$$SO_4$], [$C_2$py][$EtSO_4$], [$C_2$mim][OAc] and [$C_4$mim][OAc] (Figures 3.10, 3.15-3.17) correspond to Type I, since they contain only one immiscible pair (limonene-IL).

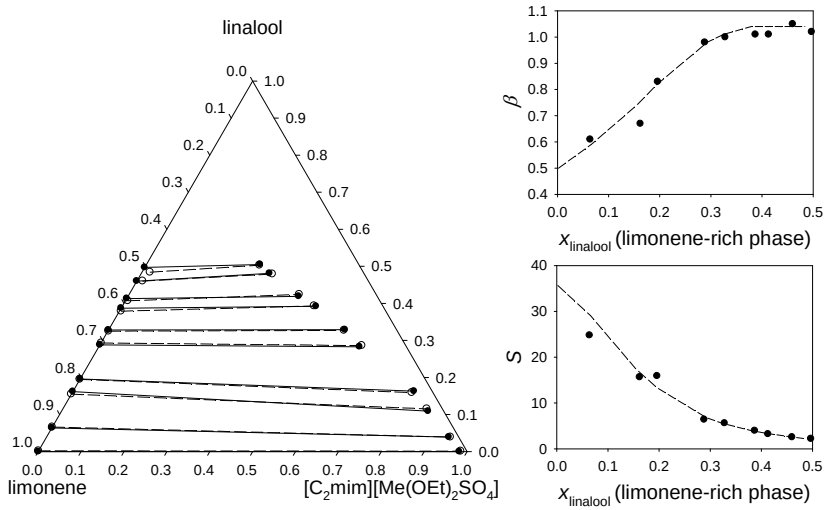

Figure 3.10. Triangular diagram representation of the experimental tie-lines (•, solid lines), and their corresponding correlated tie-lines (o, dashed lines), experimental solute distribution ratio (β) and selectivity (S) as a function of linalool in the organic-rich phase, and their corresponding correlated values (dashed line), for the ternary system limonene + linalool + $[C_2mim][Me(OEt)_2SO_4]$ at 25 °C. Correlated values were obtained with the NRTL model (α = 0.1) with a previously fixed value of β_∞.

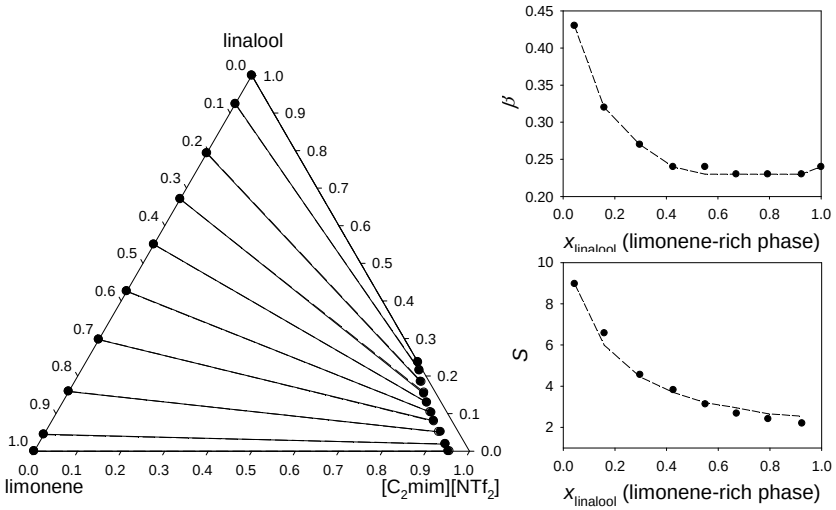

Figure 3.11. Triangular diagram representation of the experimental tie-lines (•, solid lines), and their corresponding correlated tie-lines (o, dashed lines), experimental solute distribution ratio (β) and selectivity (S) as a function of linalool in the organic-rich phase, and their corresponding correlated values (dashed line), for the ternary system limonene + linalool + $[C_2mim][NTf_2]$ at 25 °C. The correlated values were obtained with the UNIQUAC model with a previously fixed value of β_∞.

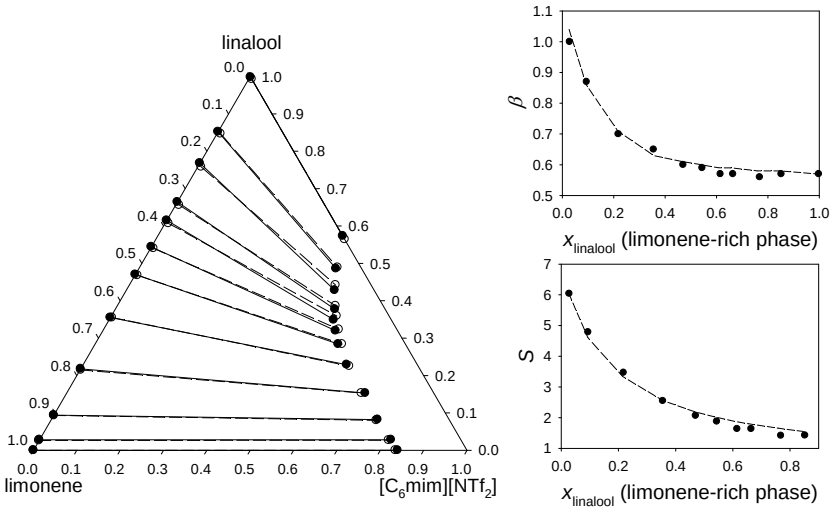

Figure 3.12. Triangular diagram representation of the experimental tie-lines (•, solid lines), and their corresponding correlated tie-lines (o, dashed lines), experimental solute distribution ratio (β) and selectivity (S) as a function of linalool in the organic-rich phase, and their corresponding correlated values (dashed line), for the ternary system limonene + linalool + $[C_6mim][NTf_2]$ at 25 °C. The correlated values were obtained with the UNIQUAC model with a previously fixed value of β_∞.

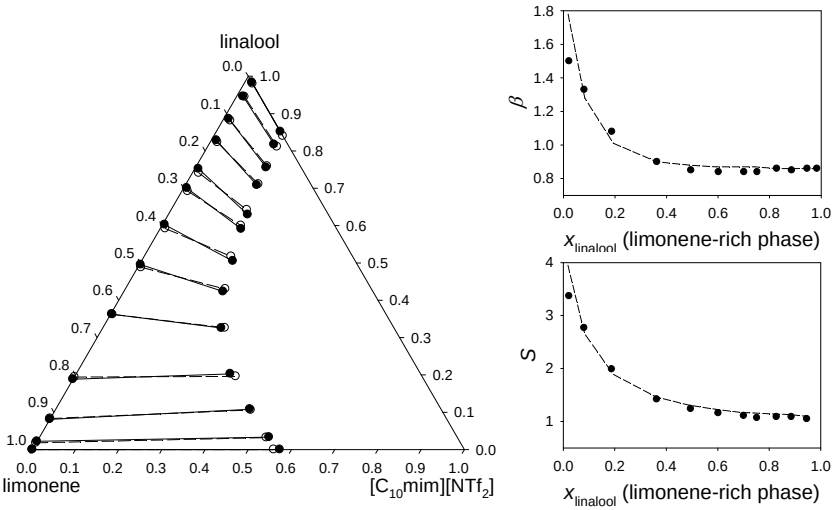

Figure 3.13. Triangular diagram representation of the experimental tie-lines (•, solid lines), and their corresponding correlated tie-lines (o, dashed lines), experimental solute distribution ratio (β) and selectivity (S) as a function of linalool in the organic-rich phase, and their corresponding correlated values (dashed line), for the ternary system limonene + linalool + $[C_{10}mim][NTf_2]$ at 25 °C. The correlated values were obtained with the UNIQUAC model with a previously fixed value of β_∞.

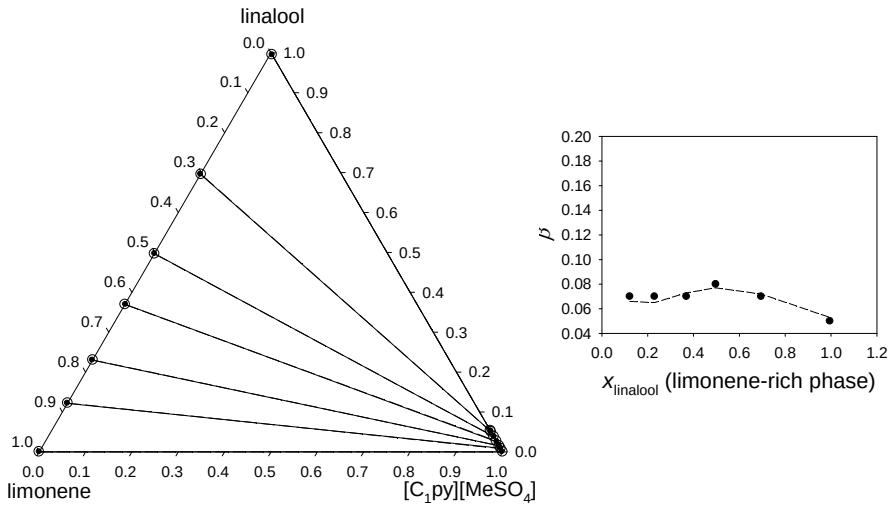

Figure 3.14. Triangular diagram representation of the experimental tie-lines (•, solid lines), and their corresponding correlated tie-lines (o, dashed lines) and experimental solute distribution ratio (β) as a function of linalool in the organic-rich phase, and its corresponding correlated values (dashed line), for the ternary system limonene + linalool + [C_1py][$MeSO_4$] at 25 ºC. The correlated values were obtained with the UNIQUAC model with a previously fixed value of β_∞ *(NOTE: Selectivities for this system were not plotted because of their infinite values)*

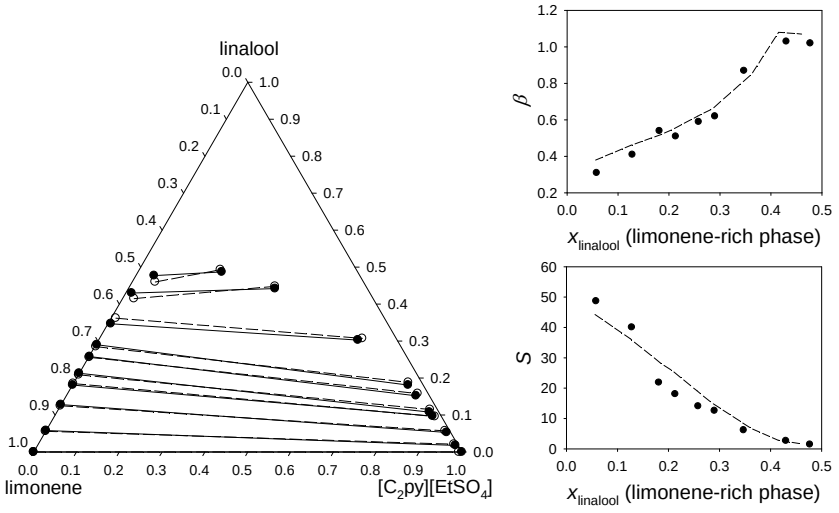

Figure 3.15. Triangular diagram representation of the experimental tie-lines (•, solid lines), and their corresponding correlated tie-lines (o, dashed lines), experimental solute distribution ratio (β) and selectivity (S) as a function of linalool in the organic-rich phase, and their corresponding correlated values (dashed line), for the ternary system limonene + linalool + [C_2py][$EtSO_4$] at 25 ºC. The correlated values were obtained with the UNIQUAC model with a previously fixed value of β_∞.

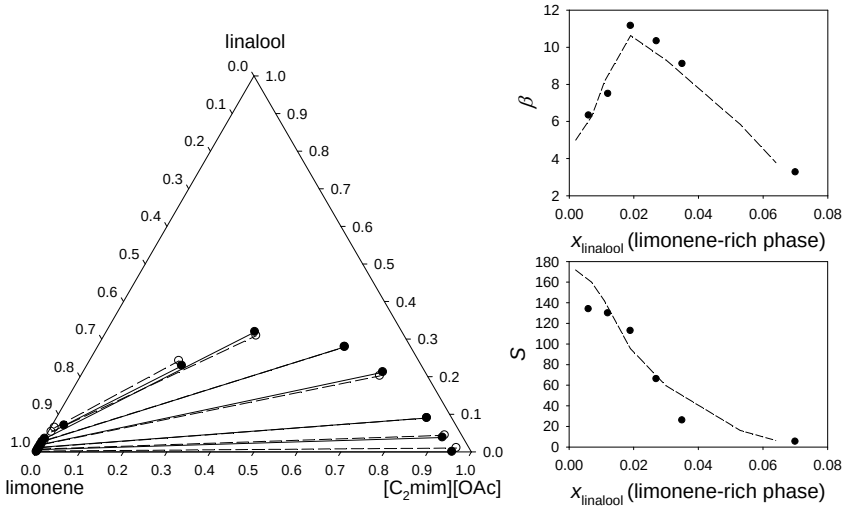

Figure 3.16. Triangular diagram representation of the experimental tie-lines (•, solid lines), and their corresponding correlated tie-lines (o, dashed lines), experimental solute distribution ratio (β) and selectivity (S) as a function of linalool in the organic-rich phase, and their corresponding correlated values (dashed line), for the ternary system limonene + linalool + [C_2mim][OAc] at 25 ºC. The correlated values were obtained with the NRTL model (α = 0.3) with a previously fixed value of β_∞.

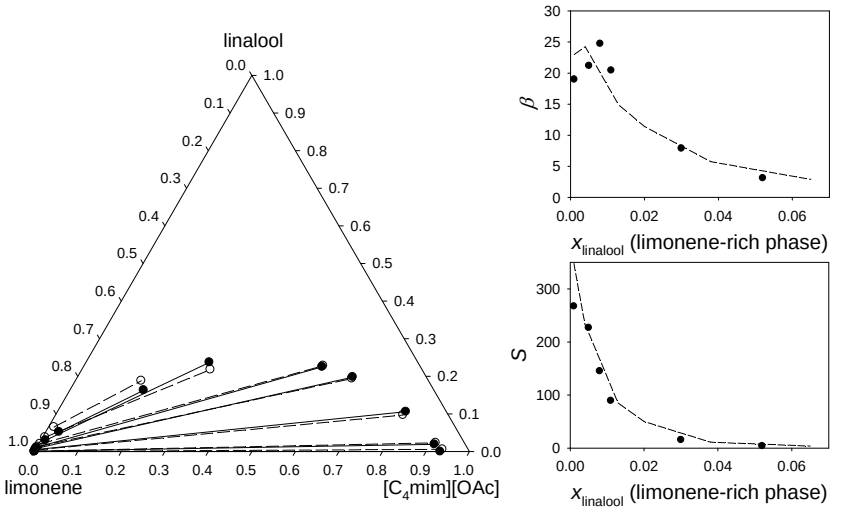

Figure 3.17. Triangular diagram representation of the experimental tie-lines (•, solid lines), and their corresponding correlated tie-lines (o, dashed lines), experimental solute distribution ratio (β), and selectivity (S) and their corresponding correlated values (dashed line), for the ternary system limonene + linalool + [C_4mim][OAc] at 25 ºC. The correlated values were obtained with the NRTL model (α = 0.3) with a previously fixed value of β_∞.

From a thermodynamic point of view, high values (always bigger than one) of solute distribution ratios and selectivities favour the desired separation. A higher value of β means that a smaller amount of solvent is needed to treat a given feed, and a higher value of S implies the need of fewer separation stages to achieve a specific degree of separation. For a better comprehension of the behaviour of ILs as solvents for the extraction of linalool from citrus essential oil, a comparison based on the influence of the cation and anion which constitute the ILs is going to be carried out.

The combined study of the [$C_n$mim][NTf_2] (n = 2, 6 or 10) [125] allows an analysis of the influence of the variation of the alkyl substituent chain in the imidazoliumcation on the deterpenation, being one of the most popular tuneable structural features in ILs, besides the own nature of the cation and the anion. Solute distribution ratio and selectivity for the systems limonene + linalool + [$C_n$mim][NTf_2] are plotted in Figure 3.18. Both parameters initially decrease, for all three systems, as the concentration of linalool increases, and they plateau at higher linalool concentrations (with perhaps the only exception of selectivity for the system [C_2mim][NTf_2], which monotonically decreases over the whole composition range). For a given molar fraction of linalool in the top phase, β increases as the length of the alkyl substituent chain of the IL increases, whereas the selectivity follows the opposite trend. The trends observed can be explained on the basis of segregated domains in the ILs. It is known that polar and nonpolar domains may exist in imidazolium ILs with alkyl substituent [126-128]. The presence of nonpolar domains increases as the length of the alkyl substituent increases. Therefore, as n increases in the [$C_n$mim][NTf_2] ILs, the most hydrophobic limonene will find better accommodation in the larger nonpolar domains of the IL phase. Linalool will also partition more easily to the IL phase with larger hydrophobic domains, resulting in a greater solute distribution ratio, although the overall effect will be a reduction in the selectivity. With an increasing presence of limonene and linalool in the extract, the two phases will get more similar in composition, causing a reduction in the difference of the interactions occurring within one phase and within the other one; thus, solute distribution ratio and selectivity vary to a minor extent when the global concentration of limonene and linalool in the systems is high enough.

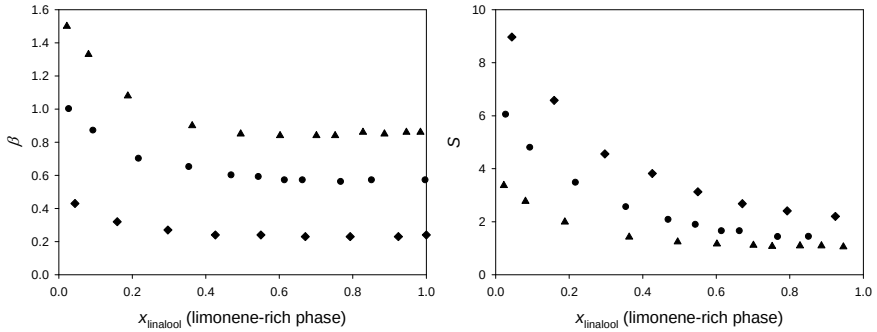

Figure 3.18. Solute distribution ratio (β) and selectivity (S) as a function of linalool in the organic-rich phase, for the systems limonene + linalool + [C_2mim][NTf_2] (◆), [C_6mim][NTf_2] (●) and [C_{10}mim][NTf_2] (▲), at 25 ºC.

A similar study, influence of the variation of the alkyl substituent chain in the imidazolium cation on the deterpenation, can be done from results found for systems with [C_2mim][OAc] and [C_4mim][OAc]. Figure 3.19 shows a comparison of β and S for the ternary systems limonene + linalool + [$C_n$mim][OAc]. In both cases, solubilities initially increase reaching a maximum at a determined concentration of linalool, and the parameter diminishes at higher concentrations. Selectivities, similar to systems with [NTf_2], decrease as the concentration of linalool increases, and they plateau at higher linalool concentrations. At low linalool concentrations (real interest), β and S increase as the length of the alkyl substituent chain of the IL increases, whereas at high linalool concentrations the parameters follow the opposite trend. The much higher solubilities and selectivities found with these ILs in comparison with [$C_n$mim][NTf_2], and the different qualitative behaviour (especially at low concentrations of linalool), is due to the introduction of the strongly interacting $[OAc]^-$ responsible of hydrogen bonds with the hydroxyl group of linalool.

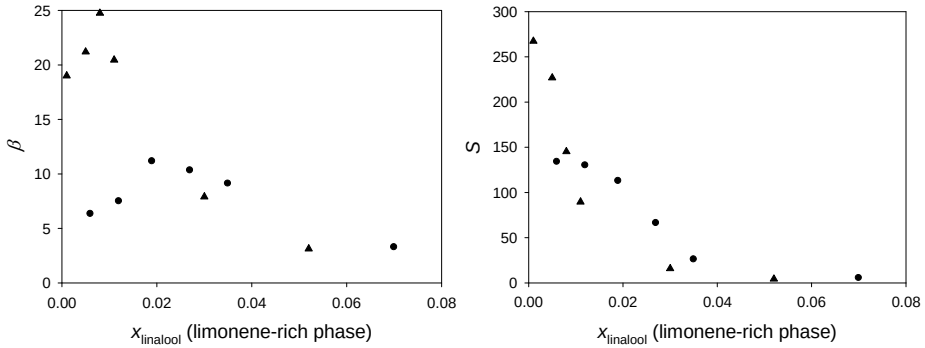

Figure 3.19. Solute distribution ratio (β) and selectivity (S) as a function of linalool in the organic-rich phase, for the systems limonene + linalool + [C_2mim][OAc] (●) or [C_4mim][OAc](▲), at 25 ºC.

Another interesting study is the influence of the cationic ring (pyridinium versus imidazolium) on the deterpenation ability. Figure 3.20 shows a comparison of both pyridinium ILs studied in this work [129] and the previously published 1-ethyl-3-methylimidazolium ethylsulfate ([C_2mim][$EtSO_4$]) [63]. The choice of the IL [C_2mim][$EtSO_4$] for this comparison is due to the structural analogy between [C_2mim][$EtSO_4$] and [C_2py][$EtSO_4$]. In the systems with these two ILs, there is an increase in β with an increase of linalool concentration. The values for the system with [C_2mim][$EtSO_4$] are higher, and tend to converge with those of the system with [C_2py][$EtSO_4$] as the plait points (almost positioned at the same concentration of linalool) are approached. It can also be highlighted, that selectivities in the systems with [C_2py][$EtSO_4$] and with [C_2mim][$EtSO_4$] follow similar trends; although it seems that, for low concentrations of linalool in the system, the performance of [C_2mim][$EtSO_4$] would be better. Therefore, since the selectivities are equivalent or better for the system with [C_2mim][$EtSO_4$], and its solute distribution ratios are also somewhat higher up to a practically coincident plait point, it can be stated that, from a thermodynamic perspective, this imidazolium IL would be a preferred solvent than its pyridinium analogous [C_2py][$EtSO_4$] for the deterpenation of citrus essential oil.

In addition to the effect of the cationic core, a comparison between the performances of the two pyridinium ILs can be done. In Figure 3.20, it can be observed that the system with [C_1py][$MeSO_4$] is clearly leading to the lowest values of β, which remain practically constant as the concentration of linalool in the system is varied. It must be noted that the selectivities for the system with [C_1py][$MeSO_4$] have not been plotted in Figure 3.20 because of their infinite value. In spite of this very large or infinite selectivity, the use of [C_1py][$MeSO_4$] as extracting solvent in the deterpenation of citrus essential would be impractical, due to the large amounts of solvent that would be needed as a result of the low solute distribution ratios.

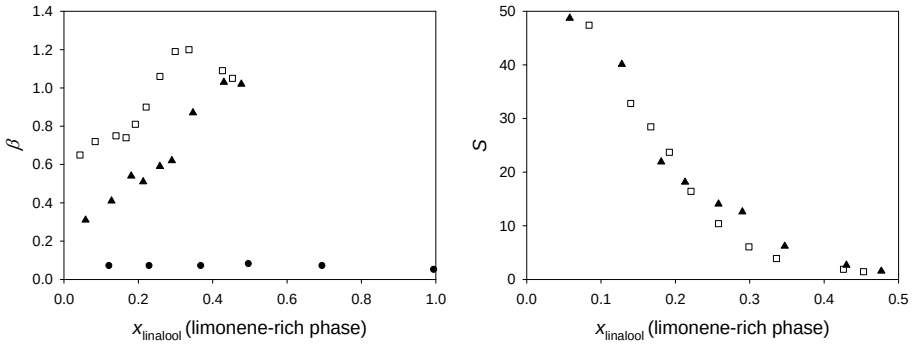

Figure 3.20. Solute distribution ratio (β) and selectivity (S) as a function of linalool in the organic-rich phase, for the systems limonene + linalool + [C_1py][$MeSO_4$] (•), [C_2py][$EtSO_4$] (▲) or [C_2mim][$EtSO_4$] (□), at 25 °C *(NOTE: Selectivities for the system with [C_1py][$MeSO_4$] were not plotted because of their infinite values).*

A direct comparison of the effect of the anion is possible by comparing the different 1-ethyl-3-methylimidazolium ILs studied in this work and published in bibliography. The anions previously studied in bibliography were ethylsulfate ($[EtSO_4]^-$) [63] and methanesulfonate ($[OMs]^-$) [55]. Figure 3.21 shows a comparison of β and S for the different systems limonene + linalool + $[C_2mim][X]$, namely, with $[X]^-$ being $[Me(OEt)_2SO_4]^-$, or $[NTf_2]^-$, or $[OAc]^-$, or $[OMs]^-$, or $[EtSO_4]^-$. Observing Figure 3.21 there is no evident pattern for the evolution of the β values, with most series increasing as the concentration of linalool in the system increases, and the one of the $[NTf_2]$-based IL slightly decreasing. The IL with the acetate anion exhibit the highest values of β, namely in the region of interest, at low concentrations of linalool in the organic-rich phase. It seems clear that the $[C_2mim][NTf_2]$ IL leads to the lowest values. Regarding the selectivity, the lowest values are also provided by the $[NTf_2]$-based IL, at least at low concentration of linalool in the system. In this range of solute concentration, the highest values of S correspond to the system with $[C_2mim][OMs]$ IL, followed by the $[C_2mim][OAc]$. At higher concentrations of linalool the values of S decrease and tend to converge. Despite this high value of selectivity achieved for $[C_2mim][OMs]$ IL, there is an important drawback in its supercooled state at 25 ºC at atmospheric pressure [130], with the implicit risk of crystallization at some point in the process. For this reason, and taking into account the considerably higher values of β for the IL $[C_2mim][OAc]$ (meaning smaller amount of solvent needed to treat a given feed), this last solvent would be chosen as preferable to carry out the targeted separation from the 1-ethyl-3-methylimidazolium ILs. Due to the short alkyl substituent in the imidazolium ring, the type of anion plays a definitive role in the citrus essential oil with these ILs. At this point, the reasons behind this different behaviour among anions remain unclear. Additional experimental work and computational simulations are needed in understanding the relevant interactions in the systems with ILs.

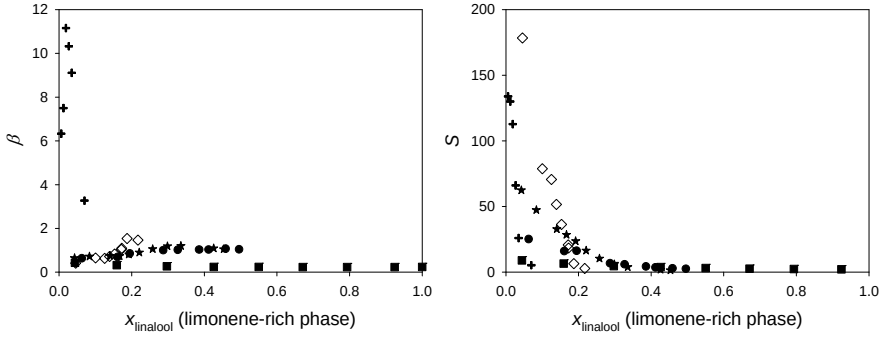

Figure 3.21. Solute distribution ratio, as a function of the mole fraction of linalool in the organic phase, for the ternary systems limonene + linalool + $[C_2mim][Me(OEt)_2SO_4]$ (•) or $[C_2mim][NTf_2]$ (■), or $[C_2mim][OAc]$ (+), or $[C_2mim][EtSO_4]$ (★), or $[C_2mim][OMs]$ (◇), at 25 ºC.

To finish with this study, the IL achieving the best results for the deterpenation of citrus essential oil ([C4mim][OAc]) has been compared with commonly used organic solvents found in the literature which better results achieved for the extraction of linalool. Namely, diethylene glycol [50] and a mixture ethanol and water with 85 wt% in ethanol [54]. Figure 3.22 shows the solution distribution ratio and selectivity, both in mass fraction, as a function of the mass fraction of linalool in the limonene-rich phase for the systems limonene + linalool + [C4mim][OAc], limonene + linalool + diethylene glycol and limonene + linalool + (water and ethanol), at 25 ºC. It can be highlighted that for the system with the diethylene glycol all the values of β are lower than the unit. Highest values of β are achieved for the system with the IL. Selectivity values are also much higher for the system including the IL, and the lowest values are achieved with the system with water and ethanol.

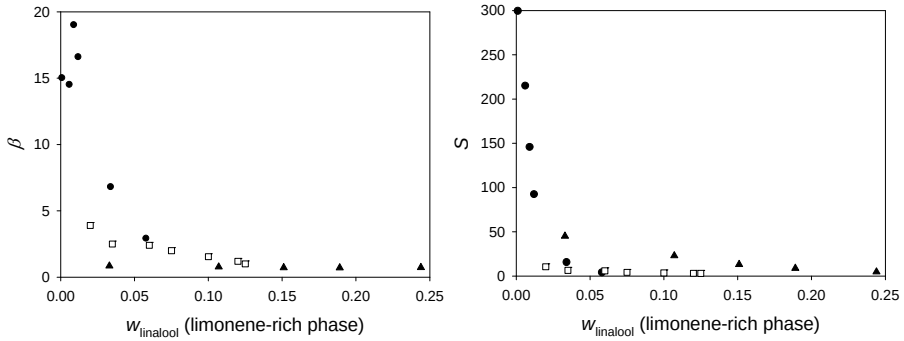

Figure 3.22. Solute distribution ratio (β) and selectivity (S) as a function of the mass fraction of linalool in the organic-rich phase, for the systems limonene + linalool + [C4mim][OAc] (•), diethylene glycol (▲) and (ethanol and water, 85 wt%) (□), at 25 ºC.

3.1.4.1. Data correlation

Equilibrium conditions are deduced from the First and Second Laws of Thermodynamics. A closed system, heterogeneous and multi-component, is at equilibrium when at constant temperature (T) and pressure (P), the Gibbs free energy (G) is a minimum. Mathematically:

$$d(G)_{T,P} = 0 \qquad (3.3)$$

and this expression can be considered as a criteria or definition of equilibrium.

From this equation, equilibrium conditions can be established in terms of activities. For a multi-phasic and multi-component system, the equilibrium conditions are:

$$T^{(1)} = T^{(2)} = \cdots = T^{(m)} \quad (3.4)$$

$$P^{(1)} = P^{(2)} = \cdots = P^{(m)} \quad (3.5)$$

$$a_i^{(1)} = a_i^{(2)} = \cdots = a_i^{(m)} \quad (3.6)$$

where i refers to all the components of the system and the superscripts make reference to all the distinct phases.

The activity is related to composition through the activity coefficient, which is defined as the ratio of the two, hence the expression turns into:

$$\left(x_i \cdot \gamma_i\right)^{(1)} = \left(x_i \cdot \gamma_i\right)^{(2)} = \cdots = \left(x_i \cdot \gamma_i\right)^{(m)} \quad (3.7)$$

which is probably the most practical expression of the equilibrium criterion.

To correlate the experimental data, a model of the activity coefficient as function of composition and temperature is needed. The *Non Random Two-Liquid* (NRTL) [131] and *Universal QUAsiChemical* (UNIQUAC) activity coefficient models [132] are widely used, even for systems with ILs, and implemented in most of simulation programs. For this reason, they are used in correlation of the experimental data presented in this work.

The NRTL equation was developed by Renon and Prausnitz (1968) [131]:

$$\ln \gamma_i = \frac{\sum x_j \tau_{ji} G_{ji}}{\sum x_k G_{ki}} + \sum \frac{x_j G_{ij}}{\sum x_k G_{kj}} \left(\tau_{ij} - \frac{\sum x_m G_{mj} \tau_{mj}}{\sum x_k G_{kj}} \right) \quad (3.8)$$

$$\tau_{ij} = (g_{ij} - g_{jj}) / RT = \Delta g_{ij} / RT \quad (3.9)$$

$$G_{ij} = \exp(-\alpha_{ij} \tau_{ij}) \quad (3.10)$$

where g_{ij} is the residual Gibbs free energy and $\alpha_{ij} = \alpha_{ji}$ is the parameter that takes into account the non-randomness aleatory disposition of the molecules. In principle, the non-randomness parameter can be specified (from 0.2 to 0.47) according to a set of rules devised by the authors [131] that depend on the chemical nature of the components in the mixture, but it is usually given a fixed value in an empirical way. The NRTL equation is applicable to multicomponent systems with only binary parameters (Δg_{ij}).

Abrams and Prausnitz [132] combined the theoretical concepts of the NRTL equation background with the quasi-chemical lattice model. The resulting UNIQUAC equation for the excess Gibbs energy consists of two parts, the first is a combinatorial part that attempt to describe the dominant entropic contribution, and the second is a residual part that is primarily due to intermolecular forces that are responsible for the enthalpy of mixing. For any component i, the expression of the activity coefficient provided by the UNIQUAC model is:

$$\ln \gamma_i = \ln \frac{\phi_i}{x_i} + \frac{z}{2} \cdot q_i \cdot \ln \frac{\theta_i}{\phi_i} + l_i - \frac{\phi_i}{x_i} \cdot \sum_{j=1}^{m} x_j \cdot l_j -$$

$$- q_i \cdot \ln\left(\sum_{j=1}^{m} \theta_j \cdot \tau_{ji} \right) + q_i - q_i \cdot \sum_{j=1}^{m} \left(\frac{\theta_j \cdot \tau_{ij}}{\sum_{k=1}^{m} \theta_k \cdot \tau_{kj}} \right) \quad (3.11)$$

$$l_j = \frac{z}{2} \cdot (r_j - q_j) - (r_j - 1) \quad (3.12)$$

where z is the lattice coordination number, arbitrarily given a value of 10; and the segment fraction ϕ, the area fraction θ and the parameter τ are given by:

$$\phi_i = \frac{r_i \cdot x_i}{\sum_{j=1}^{m} r_j \cdot x_j} \quad (3.13)$$

$$\theta_i = \frac{q_i \cdot x_i}{\sum_{j=1}^{m} q_j \cdot x_j} \quad (3.14)$$

$$\tau_{ij} = \exp\left(-\frac{u_{ij} - u_{jj}}{R \cdot T} \right) \quad (3.15)$$

where $(u_{ij} - u_{jj}) = \Delta u_{ij}$ are the adjusting parameters of the model and represent the description of the energy interaction between a molecule of i and a molecule of j, and the parameters r and q are pure-component molecular-structure constants depending on molecular size and external surface areas. These structural parameters can be obtained from crystallographic data, although it is also possible to estimate them through a group contribution method, using the Van der Waals volumes and areas of the functional groups and making them dimensionless by reference to the volume or area of a methylene element in an infinite hydrocarbon chain.

NRTL [131] and UNIQUAC [132] thermodynamic equations were used to correlate the obtained limonene + linalool + IL equilibrium data. The value of the non-randomness parameter, α, in the NRTL equation was pre-fixed at 0.1, 0.2 and 0.3 values, and the correlation was carried out for each of them. The structural parameters for applying the UNIQUAC model were obtained from literature and are shown in Table 3.12.

Table 3.12.UNIQUAC structural parameters

Compound	*r*	*q*	Ref.
Limonene	6.2783	5.2080	[133]
Linalool	7.0356	6.0600	[133]
[C_2mim][Me(OEt)$_2$$SO_4$]	7.2562	6.0054	[134]
[C_2mim][NTf_2]	9.8900	8.7800	[135]
[C_6mim][NTf_2]	12.970	10.920	[135]
[C_{10}mim][NTf_2]	15.6718	12.356	[134,135]
[C_1py][$MeSO_4$]	4.7214	4.3164	[134-136]
[C_2py][$EtSO_4$]	8.4649	7.0230	[134-137]
[C_2mim][OAc]	6.0191	5.5760	[134,135]
[C_4mim][OAc]	7.3291	6.9960	[134,135]

To obtain the binary interaction parameters, a program developed by Sorensen and Arlt [138] was used. It uses two objective functions to fit the experimental phase compositions. Data are fitted with F_a as objective function, not requiring any initial guess of parameters. Once it converges, the obtained parameters are used in the second fit using, F_b. Both parameters are defined as follows:

$$F_a = \sum_k \sum_i \left[\left(a_{ik}^I - a_{ik}^{II}\right) / \left(a_{ik}^I + a_{ik}^{II}\right)\right]^2 + Q\sum_n P_n^2 \qquad (3.16)$$

$$F_b = \sum_k \min \sum_i \sum_j (x_{ijk} - \hat{x}_{ijk})^2 + Q\sum_n P_n^2 + \left[\ln\left(\frac{\hat{\gamma}_{S\infty}^I}{\hat{\gamma}_{S\infty}^{II}}\beta_\infty\right)\right]^2 \qquad (3.17)$$

where a is the activity, x is the experimental molar fraction, "min" refers to a minimum obtained by the Nelder-Mead method, $\gamma_{S\infty}$ represents the solute activity coefficient at infinite dilution, and the symbol ^ on top of a variable indicates that it is a calculated value. Superscripts *I* y *II* refer to the phases in equilibrium, and subscripts *i*, *j* and *k* to the components, the phases and the tie-lines, respectively. Both functions include a penalisation term (second term on the right hand side of the equations) to reduce the risk of multiple solutions associated with large value parameters. In this penalisation term, Q is an empirical constant, which was given Sørensen's recommended values of 10^{-6} in Equation (3.16) and 10^{-10} in Equation (3.17) and P_n are the adjustable parameters (binary interaction parameters of the correlation model). F_b also includes a term that will only be relevant if a fixed value for the solute molar distribution ratio at infinite dilution, β_∞ ,is previously defined by the user. If this parameter is not fixed, then the last term in Equation (3.17) will be zero.

The quality of the correlations was measured by means of the residual function F and by the mean error of the solute distribution ratio, $\Delta\beta$, defined as:

$$F = 100\left[\sum_k \min \sum_i \sum_j \frac{(x_{ijk} - \hat{x}_{ijk})^2}{6M}\right]^{0.5} \quad (3.18)$$

$$\Delta\beta = 100\left[\sum_k \frac{((\beta_k - \hat{\beta}_k)/\beta_k)^2}{M}\right]^{0.5} \quad (3.19)$$

where M is the total number of tie-lines, and all other variables and symbols have already been defined.

In this work, experimental data have been correlated in two different ways: a) without previously fixing a value of β_∞, so annulling the last term of Equation (3.17), and b) specifying an optimum value for this parameter. Once an appropriate value of β_∞ is fixed, the fitting at low solute concentrations, interesting for practical applications, can be improved. The values of β_∞ which minimize $\Delta\beta$ were found by trial and error. It must be highlighted that minimum values of $\Delta\beta$ do not necessary imply lower values of F, which can slightly increase. Nevertheless, the obtaining of minimum values of $\Delta\beta$ has been set as the optimisation criterion.

Table 3.13 lists the root mean square deviations found with both models, NRTL (α optimised) and UNIQUAC, obtained defining the solute distribution ratio at infinite dilution, β_∞, or not. When the solute distribution ratio at infinite dilution, β_∞ is defined, the residual $\Delta\beta$ decreases extensively, and the residual F decreases or slightly increases. No convergence was found for the NRTL model for the systems limonene + linalool + alkylpyridinium alkylsulfate ILs. Binary interaction parameters for the correlation model selected for each case (Δg_{ij} and Δg_{ji} for the NRTL model, and Δu_{ij} and Δu_{ji} for the UNIQUAC model), defining the solute distribution ratio at infinite dilution, are summarised in Table 3.14.

A comparison between the experimental tie-lines and their correlated values obtained from the model which best fitting achieves is plotted in Figures 3.10 to 3.17, as well as the correlated solute distribution ratios and selectivities along with their experimental values. It can be seen a good agreement among experimental and correlated values, according to selected model, for limonene + linalool + IL equilibrium data.

Table 3.13. LLE data correlation for limonene + linalool + IL ternary systems at 25 ºC. Residual function F, and mean error of the solute distribution ratio, Δβ, for each model defining or not the solute distribution ratio at infinite dilution, β_∞.

IL	Model	β_∞	F	$\Delta\beta$
$[C_2mim][Me(OEt)_2EtSO_4]$	NRTL (α = 0.1)	-----	1.6636	5.3
		1.9	0.5429	2.9
	UNIQUAC	-----	0.4212	3.2
		0.83	0.4215	3.4
$[C_2mim][NTf_2]$	NRTL (α = 0.2)	-----	0.2467	10.6
		0.50	0.3058	1.9
	UNIQUAC	-----	0.1450	1.9
		0.50	0.1460	1.4
$[C_6mim][NTf_2]$	NRTL (α = 0.2)	-----	0.6896	3.0
		1.10	0.6918	2.4
	UNIQUAC	-----	0.6045	6.9
		1.12	0.5586	2.6
$[C_{10}mim][NTf_2]$	NRTL (α = 0.3)	-----	0.7465	3.4
		1.75	0.7465	3.5
	UNIQUAC	-----	0.4827	25.2
		2.00	0.6338	6.2
$[C_1py][MeSO_4]$	NRTL	-----	-----	-----
		-----	-----	-----
	UNIQUAC	-----	0.0731	9.9
		0.05	0.0815	5.5
$[C_2py][EtSO_4]$	NRTL	-----	-----	-----
		-----	-----	-----
	UNIQUAC	-----	0.6336	9.7
		0.33	1.0679	9.0
$[C_2mim][OAc]$	NRTL (α = 0.3)	-----	0.7924	84.7
		3.57	0.8741	15.8
	UNIQUAC	-----	1.9718	595
		1.80	1.4989	16.4
$[C_4mim][OAc]$	NRTL (α = 0.3)	-----	0.5817	40.0
		33.33	0.8335	26.7
	UNIQUAC	-----	0.7994	273
		40.00	0.8892	28.2

Table 3.14. LLE data correlation for limonene + linalool + IL ternary systems at 25 ºC. Binary interaction parameters for selected model, NRTL (Δg_{ij}, Δg_{ji}) or UNIQUAC (Δu_{ij}, Δu_{ji}),with the optimal value of the fixed solute distribution ratio at infinite dilution, β_∞.

IL	Model	*i-j*	Δg_{ij} or Δu_{ij}/J·mol^{-1}	Δg_{ji} or Δu_{ji}/J·mol^{-1}
[C_2mim][Me(OEt)$_2$$SO_4$]	NRTL	1-2	17825	-13306
	α = 0.1	1-3	39840	2816.2
		2-3	15911	11347
[C_2mim][NTf_2]	UNIQUAC	1-2	1791.9	-1131.8
		1-3	3821.1	-428.54
		2-3	3171.5	-1087.9
[C_6mim][NTf_2]	UNIQUAC	1-2	1718.2	-1134.1
		1-3	2636.6	-589.75
		2-3	2813.0	-1310.7
[C_{10}mim][NTf_2]	UNIQUAC	1-2	2793.3	-1771.6
		1-3	4419.3	-1567.1
		2-3	3088.2	-1686.5
[C_1py][$MeSO_4$]	UNIQUAC	1-2	-1963.7	4404.9
		1-3	2989.1	2115.4
		2-3	3797.6	-635.83
[C_2py][$EtSO_4$]	UNIQUAC	1-2	1178.4	-808.27
		1-3	7873.7	-390.24
		2-3	-1313.7	2459.8
[C_2mim][OAc]	NRTL	1-2	3260.0	4528.1
	α = 0.3	1-3	14732	7518.3
		2-3	-3914.4	9349.6
[C_4mim][OAc]	NRTL	1-2	2509.2	6288.1
	α = 0.3	1-3	13894	5773.6
		2-3	-5350.8	7329.3

3.2. ENHANCED OIL RECOVERY

3.2.1. CHEMICALS

Once inside the oil well, the reservoir fluid was simulated as a mixture of oil, water (or brine) and surfactant. In this work the oil was simulated as *n*-dodecane purchased from Merck with a nominal purity ≥ 99 wt%. In spite of its high purity, the small content of impurities drastically affects the interfacial tension measurements. Prior to its use, it was washed with fresh bidistilled water at least three times and passed several times through a column of alumina (Sigma-Aldrich, activated, basic, Brockman I) until its equilibrated mixture with water yielded and interfacial tension value in line with literature results. To study the effect of adding salt to the mixture, a 4 wt% solution of sodium chloride (Sigma-Aldrich, ≥ 99 wt%) in water was prepared. Any organic impurities contained in the salt were removed by heating up to 450 ºC for 12 h.

Two ILs with surfactant characteristics were used in this work; trihexyl(tetradecyl)phosphonium chloride ($[P_{6\ 6\ 6\ 14}]Cl$) and trihexyl(tetradecyl)phosphonium bis(trifluoromethylsulfonyl)imide ($[P_{6\ 6\ 6\ 14}][NTf_2]$).$[P_{6\ 6\ 6\ 14}]Cl$ was obtained from Cytec Industries Inc. with a purity of 96-97 wt%. Prior to use, this IL was dried under high vacuum (<0.1 mbar) at 70-80 ºC for a minimum of 24 h. Its purity was confirmed by ^{1}H NMR and ^{13}C NMR.

- ***Synthesis of trihexyl(tetradecyl)phosphonium bis(trifluoromehylsulfonyl)imide ($[P_{6\ 6\ 6\ 14}][NTf_2]$):***

The starting material was $[P_{6\ 6\ 6\ 14}]Cl$ obtained from Cytec and previously purified. $[P_{6\ 6\ 6\ 14}]Cl$ was dissolved in dichloromethane and afterwards added to an aqueous solution of $Li[NTf_2]$ [139]. The mixture was left stirring during 4 h. Extraction of the organic phase was carried out in a separating funnel. Then, the remaining dichloromethane and water were removed in a rotary evaporator and deep removal of volatiles under high vacuum was achieved at 80 ºC for more than 24 h. Its purity was confirmed by ^{1}H NMR and ^{13}C NMR. The final product was a colourless and viscous liquid product.

3.2.1.1. Physical properties of pure compounds

The CAS number, water content, density, viscosity and surface tension of the pure compounds used in the present section of this work are reported in Table 3.15 and compared with available literature data as a proof of their purity [82,109,140-142]. Due to the high hygroscopicity of $[P_{6\ 6\ 6\ 14}]Cl$, its water content was frequently checked and in case of obtaining higher values of water mass, put into the vacuum line.

3.2.1.2. Recoverability of ILs

The ILs used all along this experimental section were recovered in the laboratory for reuse, as it was explained in the 3.1.1.2 section.

Table 3.15. CAS number, water content (ω_{H2O}), and experimental and literature values for density (ρ), viscosity (η) and surface tension(γ) of the pure components at 25 °C and atmospheric pressure.

		ω_{H2O} (ppm)	ρ (g·cm^{-3})		η (mPa·s)		γ (mN·m^{-1})	
Compound	CAS Number	Exp	Exp	Lit	Exp	Lit	Exp	Lit
Water	7732-18-5	----	0.99704	0.99705[109]	0.904	0.890[109]	72.0	71.8[109]
n-Dodecane	112-40-3	74	0.74527	0.74518[109]	1.356	1.378[109]	24.9	24.9[109]
$[P_{6\,6\,6\,14}]Cl$	258864-54-9	898	0.89103	0.8899[140] 0.8826[141]	2014	2729.1[140] 2152[82]	32.3	33.6[140] 30.6[142]
$[P_{6\,6\,6\,14}][NTf_2]$	460092-03-9	180	1.06550	1.0661[140] 1.0501[141]	311.4	336.74[140]	30.9	33.08[141] 30.1[142]

3.2.2. EQUIPMENT

To determine the equilibrium compositions and physical properties of the different phases of the system, a large volume of sample is needed. For this reason, specially designed equilibrium cells were used with a total liquid capacity of 75 mL (Figure 3.23). A stirrer connected to a IKA RW 16 basic motor was used to ensure a perfect contact of the phases. Temperature was kept constant at 25ºC or 75ºC using a Selecta UltraTerm 6000383 thermostatic bath accurate to within ±0.02 ºC.

Figure 3.23. Equilibrium cell for EOR determinations.

The composition of each phase was analysed using a Hewlett–Packard HP 6890 Series gas chromatograph, equipped with a thermal conductivity detector and a HP-FFAP capillary column (25 m x 0.2 mm x 0.33 µm). Different chromatograph operation conditions were used for the analysis of the studied systems in this work: water + $[P_{6\,6\,6\,14}]Cl$ + *n*-dodecane and water + $[P_{6\,6\,6\,14}][NTf_2]$ + *n*-dodecane. These conditions are summarised in Tables 3.16 and 3.17, respectively. For calibration, all the weighing was carried out in a Mettler Toledo AE 240 analytic balance with a precision of 10^{-4} g.

When phases were practically pure *n*-dodecane or water, the IL content determined by chromatography was also contrasted by using ICP (optical) spectroscopy. Similarly, when water content in *n*-dodecane was very low, this concentration was determined by Karl-Fischer titration with a MetrOhm 737 KF coulometer.

Table 3.16. Gas chromatograph operation conditions for the analysis of the ternary system water + $[P_{6\,6\,6\,14}]Cl$ + *n*-dodecane.

Column	Type:	HP-FFAP
	Flux:	Constant flux of 1 mL/min
Detector	Type:	TCD
	Temperature:	230 ºC
Carrier gas		He
Injector	Temperature:	230 ºC
	Split rate:	200/1
	Injection volume:	2 µL
Oven	Temperature program:	80 ºC (3 min) → 100 ºC/min until 200 ºC (1 min)

Table 3.17. Gas chromatograph operation conditions for the analysis of the ternary system water + $[P_{6\,6\,6\,14}][NTf_2]$ + *n*-dodecane.

Column	Type:	HP-FFAP
	Flux:	Constant flux of 1.1 mL/min
Detector	Type:	TCD
	Temperature:	230 ºC
Carrier gas		He
Injector	Temperature:	230 ºC
	Split rate:	200/1
	Injection volume:	1µL
Oven	Temperature program:	100 ºC (1.90 min) → 100 ºC/min until 200 ºC (3.20 min)

The existence of micro-emulsions was proved by optical & confocal microscopy, using a spectral confocal microscope (Leica model TCS SP2).

As it was explained in the 3.1.2 section, densities were measured in an Anton Paar DMA 5000 densimeter (Figure 3.24) with viscosity correction and with self-control of temperature to ±0.01 K using the Peltier effect. The measurement was repeated at least three

times for each sample. The uncertainty in the density measurement is $\pm 10^{-5}$ g·cm^{-3}.

Kinematic viscosity (υ) was determined using a micro Ubbelohde viscosimeter technique. Previous to its use, the Newtonian character of the ILs was checked by using an Anton Paar Physica MCR 301 rheometer. Depending on the viscosity of the samples, two micro Ubbelohde viscosimeters (capillaries I and III) were used to measure the viscosity of the samples. The capillaries were calibrated and credited by the company and verified by measuring the viscosity of pure compounds with known viscosities. Flow time measurement was performed by Lauda Processor Viscosity system PVS1 (Figure 3.24) with a resolution of 0.01 s. The temperature of the viscosimeter was kept constant using a Lauda clear view thermostat D 20 KP with a through-flow cooler DLK 10. Viscosity measurements were repeated at least 3 times for each sample and were found to be reproducible to within ±0.04 s for times less than 100 s and ±0.4 s for longer times. Dynamic viscosity is given by the formula

$$\eta = \upsilon\rho = K(t-y)\rho \qquad (3.20)$$

where η and υ are the dynamic and kinematic viscosity respectively, ρ is the density of the sample, K is the capillary constant provided by the manufacturer, t is the flow time and y is the kinetic energy correction used if necessary. The uncertainty for the dynamic viscosity is estimated to be ±0.5%.

Figure 3.24. Densimeter, viscosimeter and tensiometer.

The interfacial tension of the samples was measured using a Krüss K11 tensiometer (Figure 3.24). The Wilhelmy plate method was adopted in which a specially adapted platinum plate with cylindrical shape (Krüs accessory reference PL22; dimensions: 10 mm height x 20 mm base perimeter x 0.1 mm width) was used to carry out reliable measurements with lower amounts of sample than a conventional plate. For the measurement of the interfacial tension sufficient samples were withdrawn from each phase in the equilibrium cells and stored at 25 ºC or 75 ºC, depending on the

experiment. Cylindrical open-top glass vessels with a diameter of 30 mm were used to place the lighter and denser phases during the different steps of the measuring procedure, which was performed according to the instructions of the manufacturer. The sample vessels were placed inside a jacketed oil bath through which refrigerating water from a Julabo F12 cryogenic thermostat was circulated. The actual temperature of the oil bath was determined by a built-in thermometer precise to within 0.1 ºC. Every interfacial tension data point reported in this work is the average of ten consecutive immersion measurements, after the first two immersion measurements were systematically discarded. The method described above has an estimated uncertainty of ±0.1 $mN \cdot m^{-1}$.

3.2.3. PROCEDURE

3.2.3.1. Solubility tests

$[P_{6\,6\,6\,14}][Cl]$ and $[P_{6\,6\,6\,14}][NTf_2]$ ILs were selected as possible surface active agents due to their long hydrocarbon chains attached to the charged head-group of the cation. To be sure that they were capable to form triphasic systems, samples of water, IL and *n*-dodecane at several concentrations were prepared in 2 mL vials. Following, each vial was vigorously stirred with a *vortex mixer* and left to settle down. The appearance at several concentrations, for both ILs, of three phases, confirmed the interest of studying the use of these ILs for EOR and the need of obtaining equilibrium data.

3.2.3.2. Equilibrium

The cloud point method cited previously (see section 3.1.3.2) was used to have an approximation of the shape of the solubility curve formed by the system water + IL + *n*-dodecane. LLE data for the studied systems were determined at 25 ºC and 75 ºC to analyse the effect of the temperature in the water + IL + *n*-dodecane phases diagram.

To perform the measurements, a known composition of the three components (or two in the case of the binary tie-lines) within the biphasic or triphasic region were prepared by weight to ensure that every repeated experiment had the same composition (very important feature to carry out interfacial tension data comparisons). The mixture was added into a specially designed jacked equilibrium cell (Figure 3.23). The content of each cell was vigorously stirred for 2 hours maintaining its temperature constant at 25 ºC or 75 ºC using a Selecta UltraTerm 6000383 thermostatic bath. The cells were then left to settle down for 48 hours for systems with $[P_{6\,6\,6\,14}]Cl$ and 72 h for systems involving the IL $[P_{6\,6\,6\,14}][NTf_2]$. This time ensures a complete separation of the phases. Previously, several tests with different settle down times were performed to ensure that 48 and 72 hours were sufficient to reach equilibrium and complete phase

separation. A sample of each phase was withdrawn to measure the composition and physical properties.

For both ternary systems, water and *n*-dodecane compositions of phases in equilibrium were analysed by gas chromatography using the internal standard method. The IL fraction was determined by difference. For the system water + $[P_{6\ 6\ 6\ 14}]Cl$ + *n*-dodecane, isopropanol was used as solvent and also acts as internal standard. For the system water + $[P_{6\,6\,6\,14}]NTf_2$ + *n*-dodecane, acetone was used as solvent and 1-decanol as internal standard. When by means of chromatography, IL compositions less than 0.1% were obtained, ICP (optical) spectroscopy was used to determine the exact composition. Similarly, when water content of organic phase was very low, this concentration was determined by Karl-Fischer titration with a MetrOhm 737 KF coulometer.

Samples of the micro-emulsion intermediate phase were taken and dyed with toluidine blue (Schaurlau Chemie) and/or rhodamine B (Sigma-Aldrich). Small samples were placed on a standard 76x26 mm glass slide and covered with a 22x22x0.17 mm coverslip. Both transmitted and reflected light images were captured lightning the sample with an Argon laser at 488 nm. Besides, optical microscope images were obtained for selected samples.

3.2.3.3 Physical properties

Density and viscosity were determined for homogeneous phases at 25 ºC and 75 ºC accordingly with temperature of equilibrium determination. Interfacial tension among phases in equilibrium was also determined. Samples were perfectly sealed to avoid losses by evaporation or pickup of moisture, and kept at the desired temperature of measurement to avoid phase separation. Special care was put in samples at 75 ºC. The withdrawn of these samples was done with hot syringes and keeping vials always at this temperature, placing a thermostatic bath next to the measurement apparatus.

3.2.4. RESULTS AND DISCUSSION

Two ILs presenting amphiphilic character have been studied as surfactants for EOR by microemulsion flooding. Namely, $[P_{6\,6\,6\,14}]Cl$ and $[P_{6\ 6\ 6\ 14}][NTf_2]$. To determine the suitability of these ILs as a potential replacement for conventional surface active agents in this application, the reservoir fluid was modeled as a mixture of water (or brine), surfactant (IL) and oil (*n*-dodecane).

LLE data for the systems water + $[P_{6\,6\,6\,14}]Cl$ + *n*-dodecane and water + $[P_{6\,6\,6\,14}][NTf_2]$ + *n*-dodecane at 25 ºC and 75 ºC are reported in Tables 3.18 to 3.21 (uncertainties in compositions determination are also presented) and represented in Figures 3.25 to 3.28.

All these ternary systems are Winsor type III, with a triphasic region and two biphasic regions around it, as well as a monophasic domain. Although the Winsor type III diagrams do 'nominally'

contain a third biphasic region, in most cases it has a negligible size and cannot be detected, as it is the case in the systems studied here. The first biphasic region (marked with circles) implies the coexistence of an excess-water phase and another phase where the IL solubilises a relevant amount of *n*-dodecane. The other biphasic region (marked with squares) corresponds to an excess-oil phase in equilibrium with another phase where the IL solubilises a relevant amount of water. In the triphasic region (under the dashed lines), there is an IL-rich middle phase coexisting with an excess-water phase (consisting of almost pure water) and an excess *n*-dodecane phase (consisting of almost pure *n*-dodecane). This situation is ideal to achieve ultralow interfacial tension values and is favourable for EOR.

The long alkyl side chains of the used phosphonium ILs classify them as hydrophobic. Nonetheless, there is a large influence of the anion on the water miscibility, which means that they can be substantially hygroscopic [143,144]. The chloride anion is more hydrophilic (through hydrogen bonding), resulting the water miscibility in $[P_{6\,6\,6\,14}]Cl$ larger than in $[P_{6\,6\,6\,14}]NTf_2$ at the studied temperatures. Solubility data here obtained at 25ºC for water-IL binaries are in good agreement with those found in the literature [144]. No comparative data have been found at 75ºC. On the other hand, the non-polar domains of these ILs have a large affinity for alkanes [145] through van der Waals interactions. The miscibility of the pair $[P_{6\,6\,6\,14}]Cl$ + *n*-dodecane is slightly larger than for the pair $[P_{6\,6\,6\,14}]NTf_2$ + *n*-dodecane, being the first completely miscible at 75ºC. Only solubility data for $[P_{6\,6\,6\,14}]Cl$ + *n*-dodecane at 25ºC have been found in the literature [146], and are in agreement with the data presented here.

For both ILs and both pairs, IL + water and IL + *n*-dodecane, miscibility increases with temperature, accordingly with the Upper Critical Solution Temperature found in the literature for these systems [144,146].

For the system with $[P_{6\,6\,6\,14}]Cl$, the maximum composition of IL in the water-rich phase (points near the left apex of triphasic system) was $2.1\cdot10^{-5}$ at 25 ºC and $4.5\cdot10^{-4}$ at 75 ºC, in mole fraction and obtained by ICP (optical) spectroscopy. Maximum water content in *n*-dodecane-rich phases, determined by Karl-Fischer titration, was $4.4\cdot10^{-4}$ at 25 ºC and $1.1\cdot10^{-3}$ at 75 ºC in mole fraction. In the case of system with $[P_{6\,6\,6\,14}]NTf_2$, for biphasic region 1 it is not possible to use the same nomenclature (upper and lower phases) that with $[P_{6\,6\,6\,14}]Cl$. This is due to the fact that depending on compositions of phase II, this in some cases is the upper phase but in others is the lower phase. Maximum mole fraction, obtained by ICP (optical) spectroscopy, of IL in water (points near the left apex of triphasic system) was $1.4\cdot10^{-6}$ at 25 ºC and $2.5\cdot10^{-5}$ at 75 ºC, and maximum IL content in *n*-dodecane (points near the right apex of triphasic system) at 25 ºC was $4.4\cdot10^{-4}$. Maximum water content, determined by Karl-Fischer titration, in *n*-dodecane was $4.7\cdot10^{-4}$ at 25 ºC and $9.9\cdot10^{-4}$ at 75 ºC.

Table 3.18. Experimental tie-lines for LLE of water (1) + [P6 6 6 14]Cl (2) + *n*-dodecane (3) ternary system at 25 ºC and atmospheric pressure.

Biphasic region 1

Upper Phase			Lower Phase		
x_1	x_2	x_3	x_1	x_2	x_3
0.824	0.176	0.000	1.000	0.000	0.000
0.777	0.176	0.048	1.000	0.000	0.000
0.718	0.182	0.010	1.000	0.000	0.000
0.683	0.173	0.144	1.000	0.000	0.000
$\delta(x_1)$=0.006	$\delta(x_2)$=0.004	$\delta(x_3)$=0.003	$\delta(x_1)$=0.001	$\delta(x_2)$=0.001	$\delta(x_3)$=0.001

Biphasic region 2

Upper Phase			Lower Phase		
x_1	x_2	x_3	x_1	x_2	x_3
0.000	0.005	0.995	0.000	0.259	0.741
0.000	0.006	0.994	0.043	0.267	0.690
0.000	0.003	0.997	0.083	0.275	0.642
0.000	0.004	0.996	0.148	0.279	0.573
0.000	0.003	0.997	0.195	0.270	0.535
0.000	0.008	0.992	0.292	0.256	0.452
0.000	0.006	0.994	0.424	0.221	0.355
0.000	0.007	0.993	0.506	0.209	0.285
0.000	0.003	0.997	0.562	0.190	0.249
$\delta(x_1)$=0.001	$\delta(x_2)$=0.001	$\delta(x_3)$=0.001	$\delta(x_1)$=0.006	$\delta(x_2)$=0.004	$\delta(x_3)$=0.003

Triphasic region

Upper Phase			Medium Phase			Lower Phase		
x_1	x_2	x_3	x_1	x_2	x_3	x_1	x_2	x_3
0.000	0.005	0.995	0.654	0.158	0.188	1.000	0.000	0.000
$\delta(x_1)$=0.001	$\delta(x_2)$=0.001	$\delta(x_3)$=0.001	$\delta(x_1)$=0.004	$\delta(x_2)$=0.001	$\delta(x_3)$=0.003	$\delta(x_1)$=0.001	$\delta(x_2)$=0.001	$\delta(x_3)$=0.001

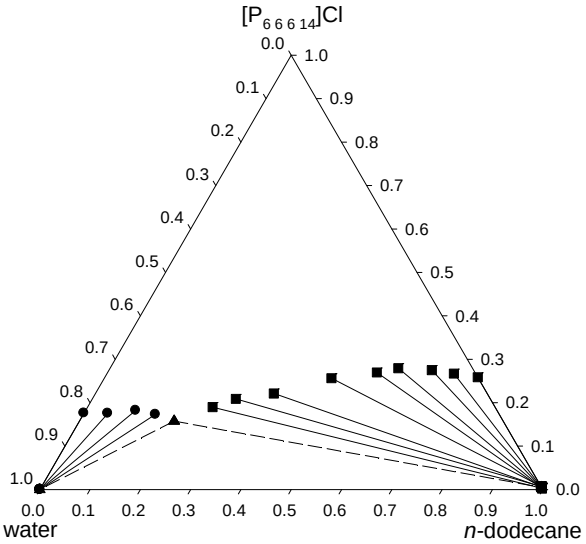

Figure 3.25. Experimental tie-lines for the water + [P6 6 6 14]Cl + *n*-dodecane ternary system at 25 ºC. Biphasic region 1 (●), biphasic region 2 (■) and triphasic region (▲ and dashed lines).

Table 3.19. Experimental tie-lines for LLE of (water (1) + $[P_{6\,6\,6\,14}]Cl$ (2) + *n*-dodecane (3)) ternary system at 75 ºC and atmospheric pressure.

Biphasic region 1					
Upper Phase			Lower Phase		
x_1	x_2	x_3	x_1	x_2	x_3
0.830	0.170	0.000	1.000	0.000	0.000
0.781	0.179	0.040	1.000	0.000	0.000
0.735	0.176	0.089	1.000	0.000	0.000
0.689	0.169	0.142	1.000	0.000	0.000
$\delta(x_1)$=0.006	$\delta(x_2)$=0.004	$\delta(x_3)$=0.003	$\delta(x_1)$=0.001	$\delta(x_2)$=0.001	$\delta(x_3)$=0.001

Biphasic region 2					
Upper Phase			Lower Phase		
x_1	x_2	x_3	x_1	x_2	x_3
0.001	0.011	0.988	0.171	0.189	0.640
0.001	0.010	0.989	0.274	0.194	0.532
0.001	0.010	0.989	0.371	0.183	0.446
0.001	0.009	0.990	0.481	0.184	0.335
0.001	0.008	0.991	0.577	0.169	0.254
$\delta(x_1)$=0.001	$\delta(x_2)$=0.001	$\delta(x_3)$=0.001	$\delta(x_1)$=0.006	$\delta(x_2)$=0.004	$\delta(x_3)$=0.003

Triphasic region								
Upper Phase			Medium Phase			Lower Phase		
x_1	x_2	x_3	x_1	x_2	x_3	x_1	x_2	x_3
0.001	0.009	0.990	0.643	0.150	0.207	1.000	0.000	0.000
$\delta(x_1)$=0.001	$\delta(x_2)$=0.001	$\delta(x_3)$=0.001	$\delta(x_1)$=0.004	$\delta(x_2)$=0.001	$\delta(x_3)$=0.003	$\delta(x_1)$=0.001	$\delta(x_2)$=0.001	$\delta(x_3)$=0.001

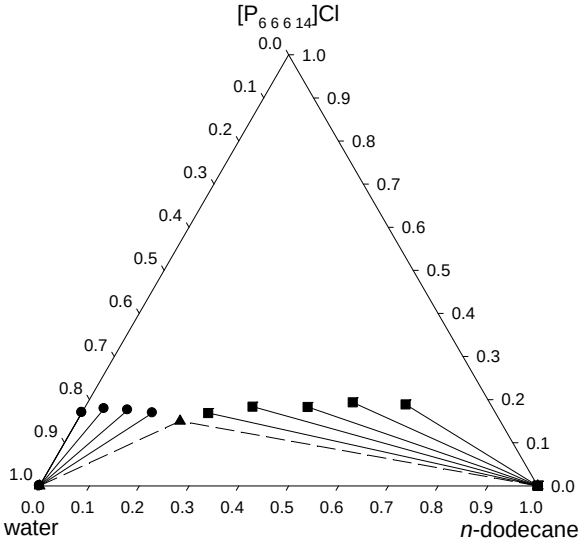

Figure 3.26. Experimental tie-lines for water + $[P_{6\,6\,6\,14}]Cl$ + *n*-dodecane ternary system at 75 ºC. Biphasic region 1 (●), biphasic region 2 (■) and triphasic region (▲ and dashed lines).

Table 3.20. Experimental tie-lines for LLE of (water (1) + $[P_{6\,6\,6\,14}][NTf_2]$ (2) + *n*-dodecane (3)) ternary system at 25 ºC and atmospheric pressure.

Biphasic region 1					
Phase I			Phase II		
x_1	x_2	x_3	x_1	x_2	x_3
1.000	0.000	0.000	0.072	0.928	0.000
1.000	0.000	0.000	0.071	0.873	0.056
1.000	0.000	0.000	0.065	0.785	0.150
1.000	0.000	0.000	0.053	0.596	0.351
1.000	0.000	0.000	0.042	0.519	0.439
1.000	0.000	0.000	0.041	0.500	0.459
1.000	0.000	0.000	0.028	0.431	0.541
$\delta(x_1)$=0.001	$\delta(x_2)$=0.001	$\delta(x_3)$=0.001	$\delta(x_1)$=0.001	$\delta(x_2)$=0.002	$\delta(x_3)$=0.002

Biphasic region 2					
Phase I			Phase II		
x_1	x_2	x_3	x_1	x_2	x_3
0.000	0.000	1.000	0.004	0.343	0.653
$\delta(x_1)$=0.001	$\delta(x_2)$=0.001	$\delta(x_3)$=0.001	$\delta(x_1)$=0.001	$\delta(x_2)$=0.002	$\delta(x_3)$=0.002

Triphasic region								
Upper Phase			Medium Phase			Lower Phase		
x_1	x_2	x_3	x_1	x_2	x_3	x_1	x_2	x_3
0.000	0.000	1.000	0.024	0.336	0.640	1.000	0.000	0.000
$\delta(x_1)$=0.001	$\delta(x_2)$=0.001	$\delta(x_3)$=0.001	$\delta(x_1)$=0.001	$\delta(x_2)$=0.002	$\delta(x_3)$=0.002	$\delta(x_1)$=0.001	$\delta(x_2)$=0.001	$\delta(x_3)$=0.001

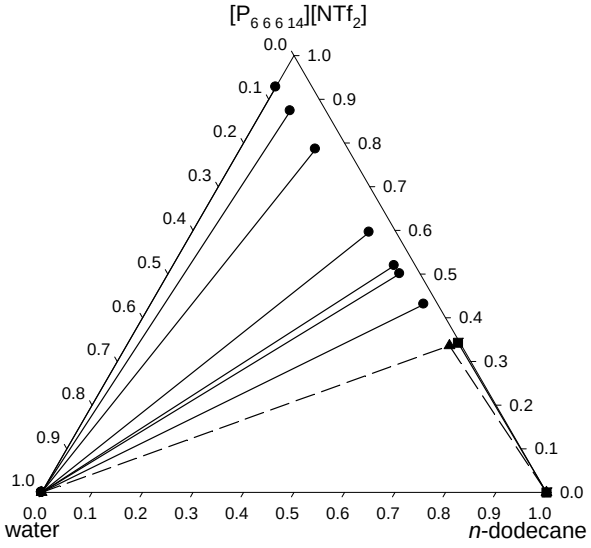

Figure 3.27. Experimental tie-lines for water + $[P_{6\,6\,6\,14}][NTf_2]$ + *n*-dodecane ternary system at 25 ºC. Biphasic region 1 (•), biphasic region 2 (■) and triphasic region (▲ and dashed lines).

Table 3.21. Experimental tie-lines for LLE of (water (1) + $[P_{6\,6\,6\,14}][NTf_2]$ (2) + *n*-dodecane (3)) ternary system at 75 °C and atmospheric pressure.

Biphasic region 1

Phase I			Phase II		
x_1	x_2	x_3	x_1	x_2	x_3
1.000	0.000	0.000	0.177	0.823	0.000
1.000	0.000	0.000	0.163	0.774	0.063
1.000	0.000	0.000	0.149	0.729	0.122
1.000	0.000	0.000	0.120	0.679	0.201
1.000	0.000	0.000	0.099	0.624	0.277
1.000	0.000	0.000	0.071	0.542	0.387
1.000	0.000	0.000	0.059	0.502	0.439
1.000	0.000	0.000	0.052	0.453	0.495
1.000	0.000	0.000	0.050	0.422	0.528
1.000	0.000	0.000	0.047	0.282	0.671
$\delta(x_1)$=0.001	$\delta(x_2)$=0.001	$\delta(x_3)$=0.001	$\delta(x_1)$=0.001	$\delta(x_2)$=0.002	$\delta(x_3)$=0.002

Biphasic region 2

Phase I			Phase II		
x_1	x_2	x_3	x_1	x_2	x_3
0.001	0.002	0.997	0.004	0.256	0.740
$\delta(x_1)$=0.001	$\delta(x_2)$=0.001	$\delta(x_3)$=0.001	$\delta(x_1)$=0.001	$\delta(x_2)$=0.002	$\delta(x_3)$=0.002

Triphasic region

Upper Phase			Medium Phase			Lower Phase		
x_1	x_2	x_3	x_1	x_2	x_3	x_1	x_2	x_3
0.001	0.002	0.997	0.042	0.260	0.698	1.000	0.000	0.000
$\delta(x_1)$=0.001	$\delta(x_2)$=0.001	$\delta(x_3)$=0.001	$\delta(x_1)$=0.001	$\delta(x_2)$=0.002	$\delta(x_3)$=0.002	$\delta(x_1)$=0.001	$\delta(x_2)$=0.001	$\delta(x_3)$=0.001

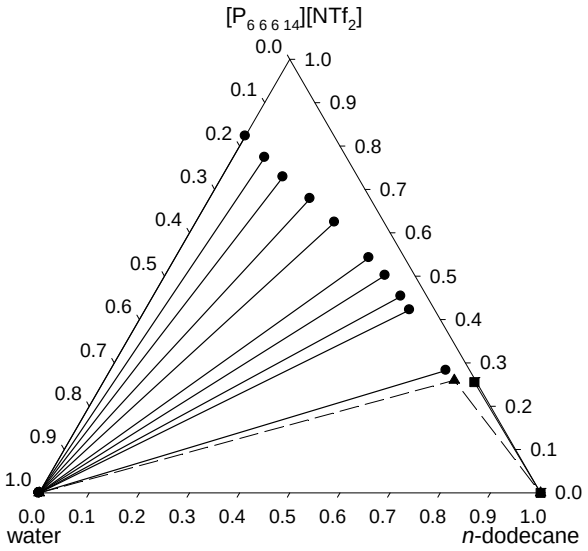

Figure 3.28. Experimental tie-lines for water + $[P_{6\,6\,6\,14}][NTf_2]$ + *n*-dodecane ternary system at 75 °C . Biphasic region 1 (•), biphasic region 2 (■) and triphasic region (▲ and dashed lines).

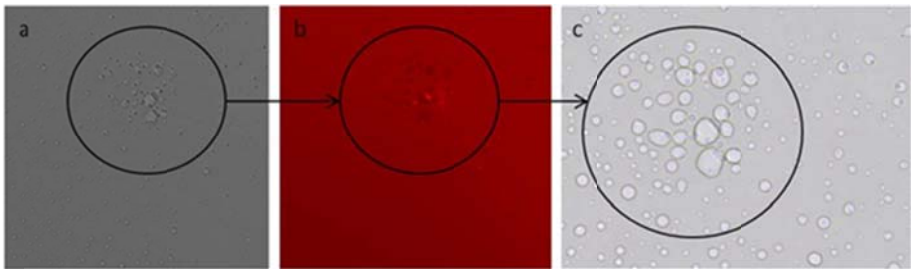

Figure 3.29. Images of the [$P_{6\ 6\ 6\ 14}$][Cl] micro-emulsion, dyed with rhodamine B, obtained by (a) transmission confocal microscopy, (b) fluorescence confocal microscopy, (c) optical microscopy.

Samples of the middle phases in triphasic systems were analysed by optical&confocal microscopy. First, micro-emulsions for the IL [$P_{6\ 6\ 6\ 14}$][Cl] were analysed. Sample was dyed with rhodamine B, which is soluble in both water and the IL. Figure 3.29 shows the images obtained by confocal microscopy (a: transmission, b: fluorescence). Figure 3.29c shows the image obtained by optical microscopy for a selected region of the previous images (b and c). It is clear from inspection of any images in Figure 3.29 that there are different micro-domains (micro-drops) in the sample. The comparison of Figures 3.29a and 3.29b shows that these micro-drops are indeed different, and there are two different types of micro-drops: Some of these micro-drops are composed by water, were rhodamine B is soluble and thus appear darker in the transmission image and emitted fluorescent light in Figure 3.29b. The other drops are composed by *n*-dodecane, rhodamine B is not soluble and thus appear dark in Figure 1b but clearer in Figure 1a (transmitted light). Figure 1c shows a magnification of the central area, obtained by optical microscopy, which confirms the existence of darker (aqueous) and clearer (*n*-dodecane) micro-drops.

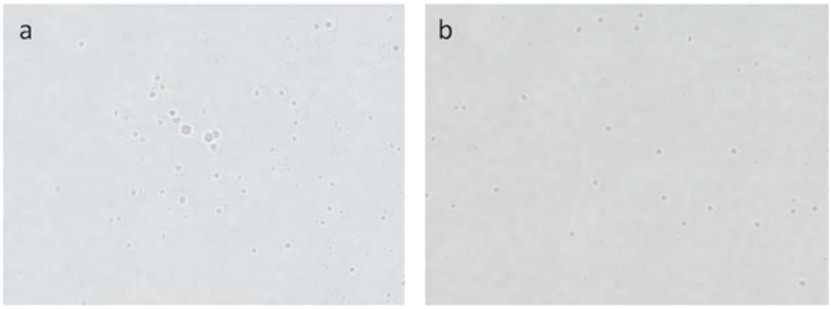

Figure 3.30. Images of the [$P_{6\ 6\ 6\ 14}$][NTf_2] micro-emulsion, dyed with (a) rhodamine B, or (b) toluidine blue, obtained by optical microscopy.

Samples of the micro-emulsions obtained with the IL $[P_{6\,6\,6\,14}][NTf_2]$ were also analysed by confocal microscopy. Samples were dyed with either rhodamine B or toluidine blue. As rhodamine B is highly soluble in this IL and water content in the micro-emulsion is low, no fluorescence emission images could be taken. Thus, only optical microscope images are shown here. Figure 3.30 presents the images of samples dyed with rhodamine B (Figure 3.30a and with toluidine blue (Figure 3.30b. As the water content is too low, the differences in the micro-drops cannot be appreciated visually.

It is important to highlight that Winsor Type III diagrams were obtained with both studied phosphonium ILs and at both temperatures, 25ºC and 75ºC. This is interesting because it indicates that these ILs act as surfactants, solubilising both water and oil. Further, the middle phase exists as a microemulsion without the need of adding any co-surfactant in a wide range of temperatures. Both, low interfacial tensions and a high degree of solubilisation are considered desirable for oil recovery. From this point, an analysis of these parameters will be done for both studied systems.

Table 3.22. Mass fraction compositions of the vertices of three-phase tie triangles (w_1 = water, w_2 = IL, w_3 = *n*-dodecane).

$[P_{6\,6\,6\,14}]Cl$, 25ºC								
Upper Phase			Medium Phase			Lower Phase		
w_1	w_2	w_3	w_1	w_2	w_3	w_1	w_2	w_3
0.000	0.015	0.985	0.094	0.652	0.254	1.000	0.000	0.000
$[P_{6\,6\,6\,14}]Cl$, 75ºC								
Upper Phase			Medium Phase			Lower Phase		
w_1	w_2	w_3	w_1	w_2	w_3	w_1	w_2	w_3
0.000	0.027	0.973	0.093	0.624	0.283	1.000	0.000	0.000
$[P_{6\,6\,6\,14}]NTf_2$, 25ºC								
Upper Phase			Medium Phase			Lower Phase		
w_1	w_2	w_3	w_1	w_2	w_3	w_1	w_2	w_3
0.000	0.000	1.000	0.001	0.701	0.298	1.000	0.000	0.000
$[P_{6\,6\,6\,14}]NTf_2$, 75ºC								
Upper Phase			Medium Phase			Lower Phase		
w_1	w_2	w_3	w_1	w_2	w_3	w_1	w_2	w_3
0.000	0.009	0.991	0.002	0.624	0.374	1.000	0.000	0.000

In both cases, using $[P_{6\,6\,6\,14}]Cl$ or $[P_{6\,6\,6\,14}]NTf_2$ ILs as surface active agents, small amounts of surfactant have to be added to the water and *n*-dodecane mixture to form the triphasic system. These quantities increase slightly with temperature. In the case of $[P_{6\,6\,6\,14}]NTf_2$ at 25ºC, the IL content of the base of the three-phase triangle is undetectable by gas chromatography.

For a better visualization, Table 3.22 shows the compositions of the vertices of the tie triangles in mass fractions. As it can be seen in this table, for the water + $[P_{6\ 6\ 6\ 14}]Cl$ + *n*-dodecane ternary system mass compositions of the apex of the three-phase tie triangle are 0.094 in water and 0.652 in IL at 25 °C. Increasing the temperature makes the apex of the three-phase tie-triangle shift to slightly lower IL contents and increases the quantity of solubilized *n*-dodecane. For the water + $[P_{6\ 6\ 6\ 14}]NTf_2$ + *n*-dodecane ternary system, mass compositions of the apex of the three-phase tie triangle are 0.001 in water and 0.701 in IL at 25 °C. Similarly to the previous case, the increase of temperature shifts the apex of the three-phase triangle towards lower values of IL and oil content increases. With both ILs, an important quantity of surfactant is needed to solubilize the water-oil mixture. Despite IL composition for the apex triangle is larger in the case of $[P_{6\ 6\ 6\ 14}]NTf_2$, this IL dissolves a larger amount of oil (apex forward to the right), being the water composition in this intermediate phase very low.

Density and viscosity were determined for homogeneous phases corresponding to biphasic or triphasic systems, at 25 °C and 75 °C, accordingly with temperature of equilibrium determination. Interfacial tension among phases in equilibrium was also determined. Figures 3.31 to 3.34 show the localisation of the samples and Tables 3.23, 3.25, 3.27 and 3.29 the obtained results. Due to the presence of salts in the oilfield, the same study was carried out by substituting the water with a brine solution (4 wt% NaCl). Results with this brine solution are showed in Tables 3.24, 3.26, 3.28 and 3.30.

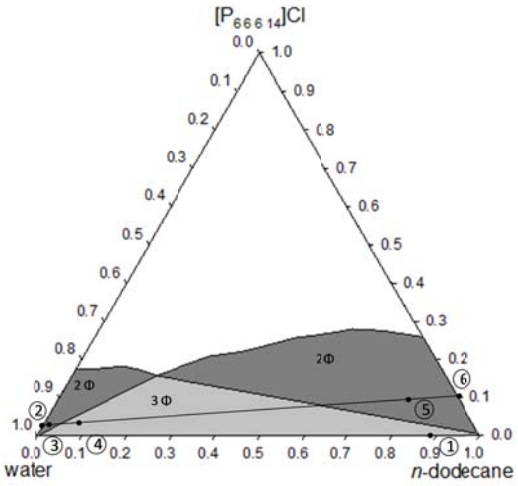

Figure 3.31. Localisation of the samples used to measure physical properties for the system water + $[P_{6\ 6\ 6\ 14}]Cl$ + *n*-dodecane at 25 °C

Table 3.23. Physical properties of involved phases (x_1 = water, x_2 = $[P_{6\,6\,6\,14}]Cl$, x_3 = *n*-dodecane): density (ρ), viscosity (η) and interfacial tension (γ) at 25 °C.

	Phase	ρ (g·cm^{-3})	η (mPa·s)	γ (mN·m^{-1})
Experiment 1 x_1 =0.890 , x_2 = 0.000 , x_3 = 0.110	Upper	0.74527	1.356	52.2
	Lower	0.99704	0.904	
Experiment 2 x_1 = 0.970 , x_2 = 0.030 , x_3 = 0.000	Upper	0.90408	113.3	1.8*
	Lower	1.00092	0.908	
Experiment 3 x_1 = 0.950, x_2 = 0.025 , x_3 = 0.025	Upper	0.86244	49.34	1.4*
	Lower	1.00047	0.910	
Experiment 4 x_1 = 0.885, x_2 = 0.025 , x_3 = 0.090	Upper	0.74578	1.363	0.3 1.4*
	Middle	0.85795	44.99	
	Lower	0.99829	0.904	
Experiment 5 x_1 = 0.118, x_2 = 0.088 , x_3 = 0.794	Upper	0.74583	1.370	0.4
	Lower	0.83619	77.73	
Experiment 6 x_1 = 0.000 , x_2 = 0.100, x_3 = 0.900	Upper	0.74605	1.368	0.5
	Lower	0.81508	84.20	

* Negative values are reported by tensiometer due to light phase is the wetting fluid

Table 3.24. Physical properties of involved phases (x_1 = brine, x_2 = $[P_{6\,6\,6\,14}]Cl$, x_3 = *n*-dodecane): density (ρ), viscosity (η) and interfacial tension (γ) at 25 °C.

	Phase	ρ (g·cm^{-3})	η (mPa·s)	γ (mN·m^{-1})
Experiment 1 x_1 =0.890 , x_2 = 0.000 , x_3 = 0.110	Upper	0.74526	1.353	53.2
	Lower	1.02544	0.957	
Experiment 2 x_1 = 0.970 , x_2 = 0.030 , x_3 = 0.000	Upper	0.90356	122.2	2.4*
	Lower	1.03248	0.971	
Experiment 3 x_1 = 0.950, x_2 = 0.025 , x_3 = 0.025	Upper	0.86168	51.36	2.0*
	Lower	1.03186	0.968	
Experiment 4 x_1 = 0.885, x_2 = 0.025 , x_3 = 0.090	Upper	0.74590	1.365	0.5 1.7*
	Middle	0.85607	46.54	
	Lower	1.03228	0.978	
Experiment 5 x_1 = 0.118, x_2 = 0.088 , x_3 = 0.794	Upper	0.74598	1.368	0.6
	Lower	0.91003	78.48	
Experiment 6 x_1 = 0.000 , x_2 = 0.100, x_3 = 0.900	Upper	0.74605	1.368	0.5
	Lower	0.81508	84.20	

* Negative values are reported by tensiometer due to light phase is the wetting fluid

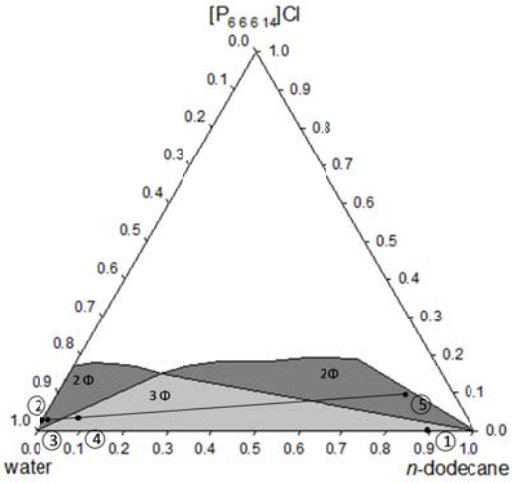

Figure 3.32. Localisation of the samples used to measure properties for the system water + [P6 6 6 14]Cl + *n*-dodecane at 75°C.

Table 3.25. Physical properties of involved phases (x_1 = water, x_2 = [P6 6 6 14]Cl, x_3 = *n*-dodecane): density (ρ), viscosity (η) and interfacial tension (γ) at 75 °C.

	Phase	ρ (g·cm^{-3})	η (mPa·s)	γ (mN·m^{-1})
Experiment 1 x_1 =0.890 , x_2 = 0.000 , x_3 = 0.110	Upper	0.70851	0.660	49.6
	Lower	0.97498	0.389	
Experiment 2 x_1 = 0.970 , x_2 = 0.030 , x_3 = 0.000	Upper	0.86515	22.69	1.5*
	Lower	0.97496	0.388	
Experiment 3 x_1 = 0.950, x_2 = 0.025 , x_3 = 0.025	Upper	0.82689	10.33	1.2*
	Lower	0.97491	0.385	
Experiment 4 x_1 = 0.885, x_2 = 0.025 , x_3 = 0.090	Upper	0.70929	0.676	0.1
	Middle	0.81307	6.959	0.4*
	Lower	0.97479	0.385	
Experiment 5 x_1 = 0.118, x_2 = 0.088 , x_3 = 0.794	Upper	0.70921	0.681	0.1
	Lower	0.75915	5.412	

* Negative values are reported by tensiometer due to light phase is the wetting fluid

Table 3.26. Physical properties of involved phases (x_1 = brine, x_2 = $[P_{6\,6\,6\,14}]Cl$, x_3 = *n*-dodecane): density (ρ), viscosity (η) and interfacial tension (γ) at 75 °C.

	Phase	ρ (g·cm^{-3})	η (mPa·s)	γ (mN·m^{-1})
Experiment 1 x_1 =0.890 , x_2 = 0.000 , x_3 = 0.110	Upper	0.70851	0.660	51.2
	Lower	1.00971	0.447	
Experiment 2 x_1 = 0.970 , x_2 = 0.030 , x_3 = 0.000	Upper	0.87932	21.37	1.7*
	Lower	1.00969	0.445	
Experiment 3 x_1 = 0.950, x_2 = 0.025 , x_3 = 0.025	Upper	0.82634	8.816	1.3*
	Lower	1.00975	0.449	
Experiment 4 x_1 = 0.885, x_2 = 0.025 , x_3 = 0.090	Upper	0.70951	0.683	0.09 0.7*
	Middle	0.80199	6.303	
	Lower	1.00969	0.439	
Experiment 5 x_1 = 0.118, x_2 = 0.088 , x_3 = 0.794	Upper	0.70970	0.687	0.1
	Lower	0.77313	5.547	

* Negative values are reported by tensiometer due to light phase is the wetting fluid

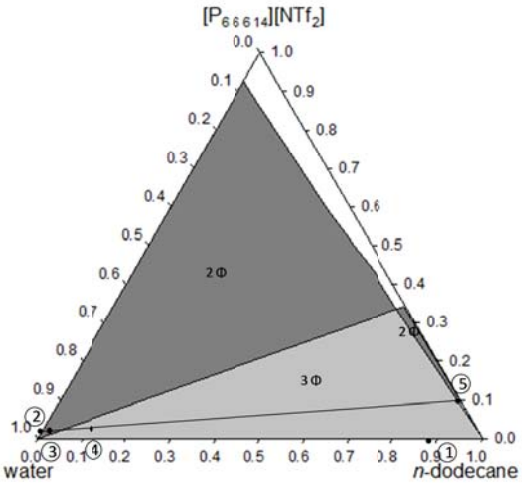

Figure 3.33. Localisation of the samples used to measure properties for the system water + $[P_{6\,6\,6\,14}][NTf_2]$+ *n*-dodecane at 25 °C.

Table 3.27. Physical properties of involved phases (x_1 = water, x_2 = $[P_{6\,6\,6\,14}][NTf_2]$, x_3 = *n*-dodecane): density (ρ), viscosity (η) and interfacial tension (γ) 25 °C.

	Phase	ρ (g·cm^{-3})	η (mPa·s)	γ (mN·m^{-1})
Experiment 1 x_1 =0.890 , x_2 = 0.000 , x_3 = 0.110	Upper	0.74527	1.356	52.2
	Lower	0.99704	0.904	
Experiment 2 x_1 = 0.970 , x_2 = 0.030 , x_3 =0.000	Upper	0.99707	0.900	27.1
	Lower	1.06386	293.6	
Experiment 3 x_1 = 0.950 , x_2 = 0.025 , x_3 = 0.025	Upper	0.99709	0.897	25.3
	Lower	1.00815	104.0	
Experiment 4 x_1 = 0.885 , x_2 = 0.025 , x_3 = 0.090	Upper	0.74537	1.354	0.6 23.5
	Middle	0.94806	44.49	
	Lower	0.99708	0.907	
Experiment 5 x_1 = 0.000, x_2 = 0.100 , x_3 = 0.900	Upper	0.74530	1.355	0.9
	Lower	0.94703	43.78	

Table 3.28. Physical properties of involved phases (x_1 = brine, x_2 = $[P_{6\,6\,6\,14}][NTf_2]$, x_3 = *n*-dodecane): density (ρ), viscosity (η) and interfacial tension (γ) at 25 °C.

	Phase	ρ (g·cm^{-3})	η (mPa·s)	γ (mN·m^{-1})
Experiment 1 x_1 =0.890 , x_2 = 0.000 , x_3 = 0.110	Upper	0.74526	1.353	53.2
	Lower	1.02544	0.957	
Experiment 2 x_1 = 0.970 , x_2 = 0.030 , x_3 =0.000	Upper	1.02548	0.954	26.2
	Lower	1.06464	301.9	
Experiment 3 x_1 = 0.950 , x_2 = 0.025 , x_3 = 0.025	Upper	1.00667	103.5	24.9
	Lower	1.02548	0.958	
Experiment 4 x_1 = 0.885 , x_2 = 0.025 , x_3 = 0.090	Upper	0.74525	1.355	0.5 23.1
	Middle	0.94567	43.67	
	Lower	1.02542	0.957	
Experiment 5 x_1 = 0.000, x_2 = 0.100 , x_3 = 0.900	Upper	0.74528	1.351	0.9
	Lower	0.94703	43.78	

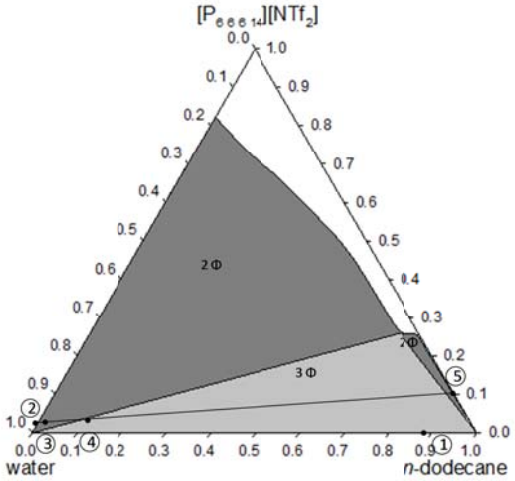

Figure 3.34. Localisation of the samples used to measure properties for the system water + $[P_{6\,6\,6\,14}][NTf_2]$ + *n*-dodecane at 75 °C.

Table 3.29. Physical properties of involved phases (x_1 = water, x_2 = $[P_{6\,6\,6\,14}][NTf_2]$, x_3 = *n*-dodecane): density (**(**ρ), viscosity (η) and interfacial tension (γ) at 75 °C.

	Phase	ρ (g·cm^{-3})	η (mPa·s)	γ (mN·m^{-1})
Experiment 1 x_1 =0.890 , x_2 = 0.000 , x_3 = 0.110	Upper	0.70851	0.660	49.6
	Lower	0.97498	0.389	
Experiment 2 x_1 = 0.970 , x_2 = 0.030 , x_3 =0.000	Upper	0.97501	0.391	25.6
	Lower	1.02117	32.23	
Experiment 3 x_1 = 0.950 , x_2 = 0.025 , x_3 = 0.025	Upper	0.97498	0.391	23.8
	Lower	0.98753	19.53	
Experiment 4 x_1 = 0.885 , x_2 = 0.025 , x_3 = 0.090	Upper	0.71028	0.679	0.4 22.2
	Middle	0.87426	5.802	
	Lower	0.97503	0.394	
Experiment 5 x_1 = 0.000, x_2 = 0.100 , x_3 = 0.900	Upper	0.71019	0.676	0.6
	Lower	0.87212	6.316	

Table 3.30. Physical properties of involved phases (x_1 = brine, x_2 = $[P_{6\,6\,6\,14}][NTf_2]$, x_3 = *n*-dodecane): density (ρ), viscosity (η) and interfacial tension (γ) at 75 ºC.

	Phase	ρ (g·cm^{-3})	η (mPa·s)	γ (mN·m^{-1})
Experiment 1 x_1 =0.890 , x_2 = 0.000 , x_3 = 0.110	Upper	0.70851	0.660	51.2
	Lower	1.00971	0.447	
Experiment 2 x_1 = 0.970 , x_2 = 0.030 , x_3 =0.000	Upper	1.00979	0.443	25.0
	Lower	1.02519	29.15	
Experiment 3 x_1 = 0.950 , x_2 = 0.025 , x_3 = 0.025	Upper	0.97225	15.28	23.7
	Lower	1.00975	0.448	
Experiment 4 x_1 = 0.885 , x_2 = 0.025 , x_3 = 0.090	Upper	0.71135	0.673	0.3
	Middle	0.87080	5.441	22.1
	Lower	1.00980	0.447	
Experiment 5 x_1 = 0.000, x_2 = 0.100 , x_3 = 0.900	Upper	0.71019	0.676	0.6
	Lower	0.87212	6.316	

The high water-oil interfacial tension is responsible for the need of adding a surface active agent to reduce it and dissolve oil, sweeping trapped oil out of the rock pore spaces. The interfacial tension obtained for water + *n*-dodecane system at 25 and 75 ºC is in good agreement with bibliographic data [147,148]. Literature also shows that in presence of NaCl, the interfacial tension of this binary increases [149]. According to Tables 3.23 and 3.25, interfacial tensions of 1.8 mN·m^{-1}at 25 ºC and 1.5 at 75 ºC were found for the water + $[P_{6\,6\,6\,14}]Cl$ binary system. A considerable deviation was found with data reported by Carrera *et al.* [150], who found an interfacial tension of 6.11 mN·m^{-1} at 20ºC. This is probably due to the different method used in the measurement. These authors used a pendant drop method, which requires knowledge of the density of the phases in equilibrium, in order to calculate the interfacial tension. In the case of the IL phase, it is well known that this physical property is substantially affected by the presence of impurities; in particular, of the water content, which is not stated by Carrera *et al.* in their work. No comparative data have been found in bibliography for systems with $[P_{6\,6\,6\,14}]NTf_2$.

The interfacial tension water/brine + *n*-dodecane is reduced by adding any of the ILs. The presence of $[P_{6\,6\,6\,14}]Cl$ at 25 ºC reduces this interfacial tension from 52.2 mN·m^{-1} (53.2 with brine) down to 1.0 mN·m^{-1} (1.9 with brine) and at 75 ºC from 49.6 (51.2 with brine) down to 0.3 mN·m^{-1} (0.6 with brine). The comparative values are given for the interfacial tension measured among the aqueous and *n*-dodecane phase of the triphasic system. In the case of $[P_{6\,6\,6\,14}][NTf_2]$ the reduction at 25 ºC is from 52.2 mN·m^{-1} (53.2 with brine) down to

21.7 mN·m^{-1} (21.5 with brine) and at 75 ºC from 49.6 mN·m^{-1} (51.2 with brine) down to 20.1 mN·m^{-1} (19.9 with brine). The IL [$P_{6\,6\,6\,14}$]Cl shows a bigger surfactant character than [$P_{6\,6\,6\,14}$][NTf_2]. This can be due to the more polar character of chloride anion against bis(trifluoromehylsulfonyl)imide.

In the literature, the interfacial tensions between water and *n*-dodecane in the triphasic systems are not usually measured, because these phases are not in contact at equilibrium (there is a microemulsion as middle phase). This middle phase is a continuous layer containing the surfactant together with the dissolved water and *n*-dodecane. For this reason, the discussion that follows is established according to phases in contact (as it is usual in bibliography).

Figure 3.35 shows the variation with temperature of the microemulsion-oil and microemulsion-water interfacial tension in the triphasic system with water or brine when using IL [$P_{6\,6\,6\,14}$]Cl as surfactant. The presence of salt increases the value of this property. There is an important decrease of the microemulsion-water/brine interfacial tension with temperature, and a less significative decrease in the case of the microemulsion-oil.

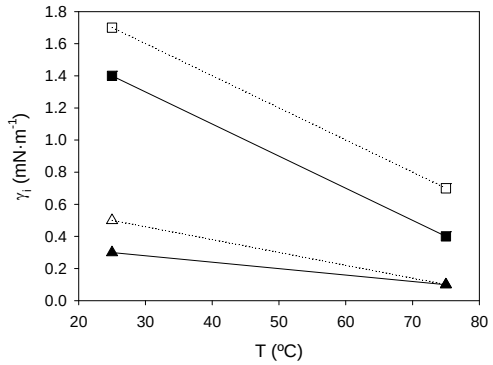

Figure 3.35. Effect of temperature on the interfacial tension of water-microemulsion (■ water, □ brine), microemulsion-oil (▲ water, Δ brine) of the triphasic system water/brine + [$P_{6\,6\,6\,14}$]Cl + *n*-dodecane. The lines are included for visual guidance.

A similar analysis can be done through Figure 3.36 for water + [$P_{6\,6\,6\,14}$]NTf_2 + *n*-dodecane ternary system. Similarly to the other system, there is a decrease of the microemulsion-water/brine and microemulsion-oil interfacial tensions with temperature, being more noticeable for the first. Nonetheless, in this case the influence of the presence of NaCl on the interfacial tensions is negligible. There is little information in bibliography about interactions among ILs and inorganic salts in water. The addition of an electrolyte to aqueous solutions of a surfactant diminishes the solvation of the hydrophilic

part of the surfactant. This effect is most noticeable in the case of the most polar IL, the $[P_{6\ 6\ 6\ 14}]Cl$, justifying the larger effect of the inorganic salt in their interfacial tensions.

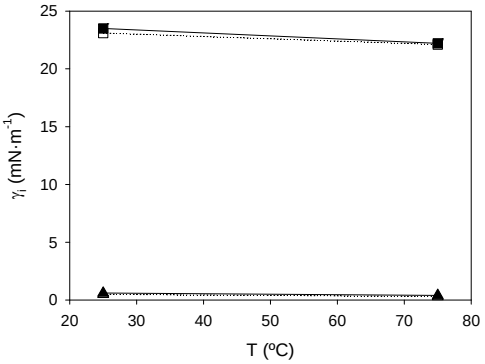

Figure 3.36. Effect of temperature on the interfacial tension of water-microemulsion (■ water, □ brine), microemulsion-oil (▲ water, Δ brine) of the triphasic system water/brine + $[P_{6\ 6\ 6\ 14}][NTf_2]$ + *n*-dodecane. The lines are included for visual guidance.

Finally, it should be noted that viscosity (a property that, as expected, decreases with temperature) of aqueous phases, increases when mixed with any of the ILs due to the higher viscosity of these compounds. Regarding to EOR applications, this can be useful to get a more homogeneous front and reduce fingering. These viscosity results, however, must be taken with particular care since it is hard to extrapolate viscous behaviour from the use of *n*-dodecane in the model systems to a real field case, with real (and much more viscous) oil.

3.3. BIOMASS PROCESSING

3.3.1. CHEMICALS

For the preparation of the DESs, different starting materials were used as hydrogen bond donors and acceptors. DL-malic acid (M) and glycerol (Gly) were purchased from Merck with a nominal purity of ≥ 99 wt%. Choline chloride (C), proline (P), alanine (A), oxalic acid (O), tetramethylammonium chloride (TMAC) and 2-chloroethyltrimethylammonium chloride (CEAC) were obtained from Sigma-Aldrich and their purity was ≥ 98 wt%. Finally, lactic acid (L) was purchased from PURAC Biochem BV at pharmaceutical grade (≥ 99 wt%). All the materials were used without further purification, apart from the choline chloride and lactic acid which were previously dried under vacuum due to their high hygroscopicity.

Wheat straw was produced in Spain under controlled conditions. Before usage, the material was milled using a Tomado stick blender set and sieved with a mesh size <1mm. The straw was analysed by the Klason method [151] and it was found to consist of 30 wt% cellulose, 32 wt% hemicellulose and 38 wt% lignin.

Pine wood pellets were purchased from Energy Pellets Moerdijk (the Netherlands) and were milled using a Retsch ZM-200 ultra-centrifugal mill. The wood powder was sieved with a mesh size < 1mm. Klason analysis [151] indicated the following composition for the wood: 39 wt% cellulose, 26 wt% hemicellulose and 35 wt% lignin.

3.3.2. EQUIPMENT

All the weighing was done with a Mettler AX205 balance with a precision of ±0.02 mg.

Proton Nuclear Magnetic Resonance (^{1}H-NMR) spectra of DESs were obtained from a Bruker BZH 400/52 with Varian Mercury and the Fourier Transform Infra-Red (FT-IR) spectra on a PerkinElmer Spectrum One.

To keep a constant temperature when mixing, a thermostatic oil bath with an IKA ETS-D5 temperature controller (uncertainty of ±0.1 °C) was used. Phase separation was carried out by means of a MSE Mistral 3000 E-Bench model centrifuge.

3.3.3. PROCEDURE

Several DESs which were previously proved as being useful for pure lignin solubilisation [38], and some other hitherto not synthetized, were tested for biomass processing.

3.3.3.1. DESs preparation

The preparation of the DESs (Figure 3.37) was done by mixing one hydrogen bond donor with a hydrogen bond acceptor in the solid

state, followed by melting them at 65 ºC for the mixtures containing lactic or oxalic acid and at 130 ºC for the malic acid mixtures. The selected temperatures depend on the stability and melting point of the different precursors. Table 3.31 shows the different DESs prepared to be tested as biomass fractionation solvents.

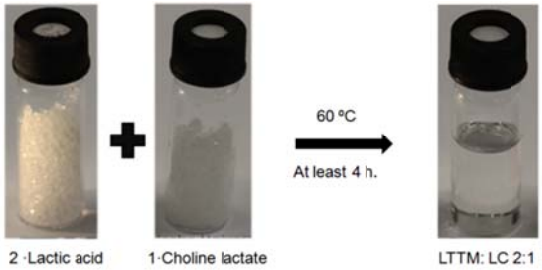

Figure 3.37. Preparation of lactic acid-chloline lactate DES, with a molar ratio 2:1 of the starting materials.

Table 3.31. Combination of different H-bond donors and H-bond aceptors to prepare the corresponding DESs.

H-bond donor	H-bond acceptor	Ratio	DES
lactic acid	choline chloride	2:1	LC 2:1
	choline chloride	9:1	LC 9:1
	tetramethylammonium chloride	2:1	LTMAC 2:1
	tetramethylammonium chloride	3:1	LTMAC 3:1
	2-chloroethyltrimethylammonium chloride	2:1	LCEAC 2:1
	2-chloroethyltrimethylammonium chloride	5:1	LCEAC 5:1
malic acid	alanine	1:1	MA 1:1
	choline chloride	1:1	MC 1:1
	glycine	1:1	MGly 1:1
	proline	1:3	MP 1:3
oxalyc acid	choline chloride	1:1	OC 1:1

3.3.3.2. Biomass treating

Following the same procedure as that reported by Spronsen *et al.* [27], different samples containing 10 g of the corresponding DES and 0.5 g of biomass (pine wood or wheat straw) were prepared in 15 mL vials. Samples were sealed to avoid water uptake from the atmosphere.

The vials were placed in a silicon oil thermostatic bath and left stirring overnight (at least 14 hours) at 60 ºC for samples containing lactic or oxalic acid, and at 85 ºC for malic acid mixtures due to its higher viscosity. After this period of time the samples were left to cool down. Figure 3.38 shows a scheme of the biomass treatment. Following, they were centrifuged (30 minutes at 3000 rpm) to promote settling down of the biomass suspended in the DES. For the less viscous samples, the supernatant (DES with dissolved biomass)

was withdrawn with a Pasteur pipette and stored in a Falcon tube. For the most viscous samples the withdrawn of the supernatant was not possible without adding ethanol (5 mL), which is miscible with the DES and decreases its viscosity. The separated supernatant is subsequently used for lignin precipitation.

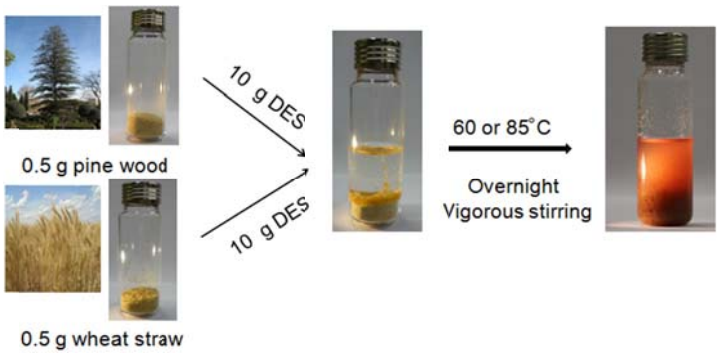

Figure 3.38. Biomass processing with DESs.

Once the supernatant was withdrawn, ethanol was added to the sample in order to wash the solid biomass particles, and mixed thoroughly by means of a Vortex mixer. It was then centrifuged for 30 minutes at 3000 rpm. The top layer was removed with a syringe. Each biomass sample was washed two to four times.

The remaining wet biomass was transferred to a Petri-dish and dried over-night in the oven at 90 °C. Dried samples were weighted twice to ensure a complete elimination of any remaining ethanol.

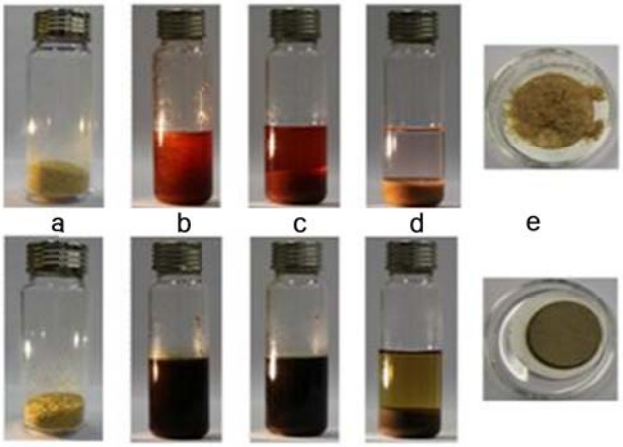

Figure 3.39. Pine wood (top) and wheat straw (bottom) biomass processing with LC9:1: (a) raw biomass samples, (b) after overnight pretreatment with DESs, (c) after centrifuging,(d) after washing twice with ethanol and centrifuging and (e) after filtration.

Figure 3.39 shows the biomass processing with LC 9:1 after the above mentioned steps (treating and washing). In the last picture of this figure, the pine wood and wheat straw precipitated biomass is shown.

3.3.3.3. Lignin precipitation

The supernatant (mixed with ethanol for the most viscous DESs), was precipitated by adding 10 g of water to the Falcon tube and vigorously stirring by means of a vortex mixer. Afterwards, the mixture was filtered to retain lignin with a 0.22 µm glass fibre filter on a vacuum filtration kit. Lignin was dried overnight in an oven and weighted twice to verify a complete elimination of water. As an example, Figure 3.40 shows the different steps in the precipitation of lignin from pine wood solved in LC 9:1.

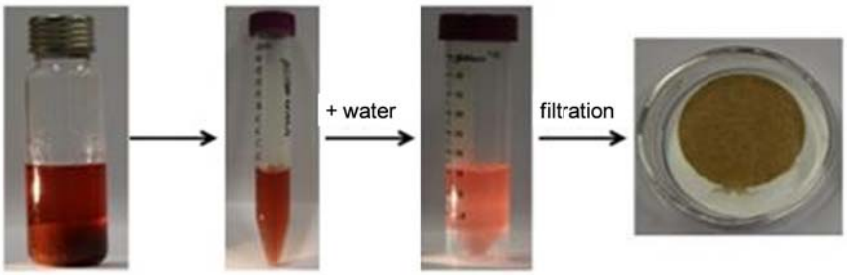

Figure 3.40. Lignin precipitation after pine wood biomass treatment using LC9:1.

3.3.4. RESULTS AND DISCUSSION

Mixtures of high melting temperature starting materials, according to ratios showed in Table 3.31, form DESs (actually low transition temperature mixtures) which are colourless liquids. These DESs are natural and biorenewable solvents which have been tested for the processing of biomass.

The biomass used in this work consists on pine wood or wheat straw. When treated with the DESs, the later become coloured. As conjecture, it can be assumed that lignin was extracted from the biomass, since lignin has a deep dark colour. Moreover, Francisco *et al.* [38] showed a high solubility of lignin on this kind of DESs, being the solubility of cellulose or starch small or practically null in most of the cases. Figure 3.41 shows the processed biomass after their overnight treatment with all the tested DESs. A different colour can be observed for pine wood or wheat straw treatment. This effect can be related with the type of biomass: different kinds of lignin are present in different types of biomass.

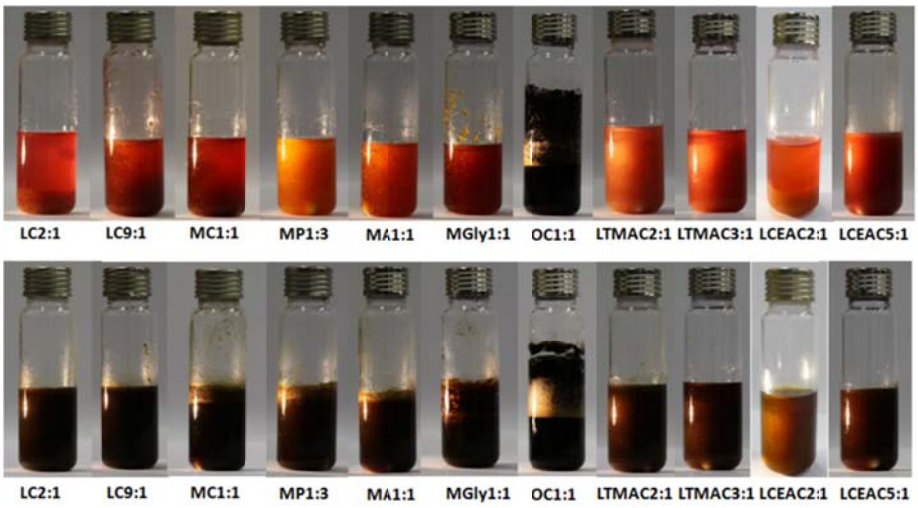

Figure 3.41. Processed samples after overnight stirring. Top pictures: pine wood; bottom pictures: wheat straw.

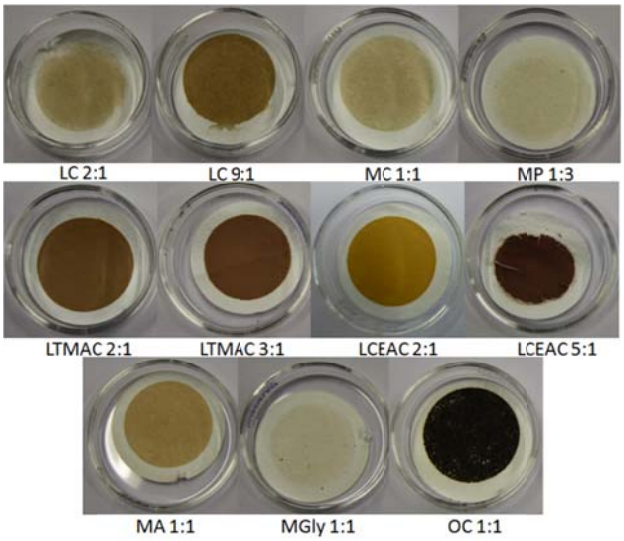

Figure 3.42. Precipitated lignin obtained from pine wood biomass fractionation with DESs.

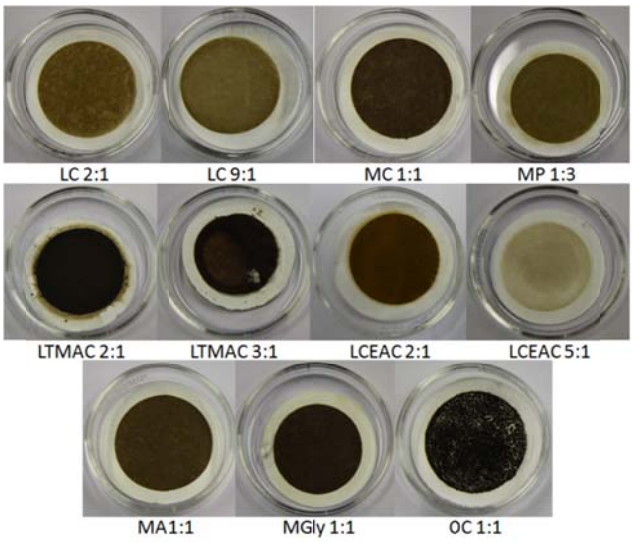

Figure 3.43. Precipitated lignin obtained from wheat straw biomass fractionation with DESs.

Lignin has been precipitated from the supernatant (mixed with ethanol for the most viscous DESs) by addition of water. This has been confirmed by the FT-IR spectra of the precipitated lignin, showing a spectra similar to alkali lignin.

Figures 3.42 and 3.43 show the precipitated lignin obtained from pine wood and wheat straw deconstruction, respectively. Numerical results of these experiments are recorded in Table 3.32, where the mass of obtained lignin as percentage of total initial biomass is presented for several DESs.

Table 3.32. Percentage of lignin obtained after processing of pine wood and wheat straw raw biomass with different DESs.

	Pine wood	Wheat straw
LTTM	Lignin (wt %)	Lignin (wt %)
LC 2:1	1.7	1.5
LC 9:1	3.4	3.0
MC 1:1	0.6	1.1
OC 1:1	3.4	7.1
LTMAC 2:1	2.9	7.3
LTMAC 3:1	4.4	9.5
LCEAC 2:1	3.2	5.7
LCEAC 5:1	7.8	0.6

Data for MA 1:1, MGly 1:1 and MP 1:3 do not appear in Table 3.32. The high viscosity of these DESs led to difficulties during the

experimental work. Ethanol was added to the supernatant phase to lower the viscosity and help the precipitation of the biomass. Nonetheless, this alcohol is not miscible with these DESs in all the range of concentrations and precipitation of the solvent was observed in the filtered biomass (Figure 3.44) for these three DESs, it is not possible to extract any conclusions from the mass balances of lignin along the pretreatment process. For these cases, the amount of ethanol added to the samples must be optimised in order to obtain a viscosity low enough to make the withdrawn of samples possible, or a different solvent should be explored.

Results for LC2:1, LC9:1, MC1:1 and OC1:1 shown in Table 3.32 are in agreement with tested solubilities of pure lignin in these DESs [38], being the OC 1:1 the DES which allows the major recovery of lignin. Results obtained for LTMAC2:1, LTMAC3:1, LCEAC2:1 and LCEAC 5:1 (no lignin solubility data available), show that these DESs can solubilise the biopolymer, even with better results that those previously cited.

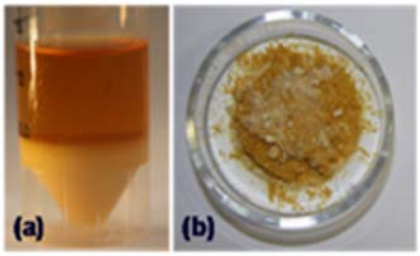

Figure 3.44. Precipitation of MP1:3 when washing the processed samples with 5 mL of ethanol. (a) supernatant and (b) filtered biomass.

It can be observed that for DES formed by lactic acid and choline chloride, the solubility of lignin increases with increasing the relative ratio of lactic acid, and higher amount of lignin has been recovered. This behaviour is observed for both studied types of biomass and it is in agreement with solubility results obtained by Francisco *et al.* [38]. The same behaviour has been found for mixtures of lactic acid and tetramethylammonium chloride or 2-chloroethyltrimethylammonium chloride (except in the case of this last mixture treating wheat straw).

The two different kinds of biomass show different values of lignin solubility for each DES, due to the different structure and type of lignin found in each kind of biomass. For pine wood, the following trend has been found for solubilisation of lignin: LCEAC 5:1 > LTMAC 3:1>LC 9:1~ OC 1:1 > LCEAC 2:1>LTMAC 2:1> LC 2:1 > MC 1:1. In the case of wheat straw the trend is: LTMAC 3:1 > LTMAC 2:1 > OC 1:1 > LCEAC 2:1 >LC 9:1 >LC 2:1 > MC 1:1 > LCEAC 5:1.

Cellulose and hemicellulose are polysaccharides and can be seen as the most valuable components of lignocellulosic biomass. In the conversion to bioethanol or other high value products, both

enzymatic hydrolysis and yeast fermentation are hindered or inhibited by lignin, so delignification is a step necessary during the process.

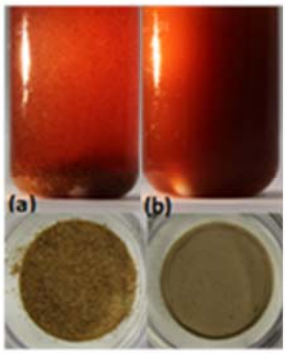

Figure 3.45. Pine wood biomass samples after pretreatment with (a) MC1:1 at 85°C and (b) LCEAC5:1 at 60°C, overnight.

Once the lignin has been extracted with the DESs, the remaining biomass is rich in cellulose and hemicellulose. It must be noted that even though cellulose solubility was found to be negligible for most of the studied solvents, there was a noticeable change in cellulose crystallinity in most cases. Figure 3.45 shows an example of the change of biomass crystallinity for MC1:1 and LCEAC5:1 when processing pine wood.

This study constitutes a small introduction in early stage to what it seems to be a promising investigation process to use new and bio-renewable solvents to deconstruct raw biomass into its valuable biopolymer constituents. Further and deeper investigation has to be carried out yet to obtain organized and clear conclusions about this process and the best DESs to carry out this task.

4 Conclusions

4. CONCLUSIONS

In this thesis, the suitability of using designer solvents to develop greener and/or more efficient chemical processes was proved through thermodynamic studies. The main advantages of the proposed solvents, ILs and DESs, are: the liquid ranges exhibited, their very low vapour pressure (which avoids atmospheric contamination), their thermal and chemical stability, and their tuneability, which allows them to be optimized for a specific application as low toxicity and high biodegradability are sought simultaneously. The main conclusions drawn from the results obtained in the three different sections of this work are summarized below.

– Citrus essential oil deterpenation

The feasibility of ILs to carry out the separation of the mixtures limonene and linalool (characteristic compounds of the citrus essential oil) by solvent extraction, was investigated through the determination of the LLE of ternary systems limonene + linalool + IL. The following ILs were specifically investigated: $[C_2mim][Me(OEt)_2SO_4]$, $[C_2mim][NTf_2]$, $[C_6mim][NTf_2]$, $[C_{10}mim][NTf_2]$, $[C_1py][MeSO_4]$, $[C_2py][EtSO_4]$, $[C_2mim][OAc]$ and $[C_4mim][OAc]$. The suitability of each IL to extract the linalool was evaluated by means of the solute distribution ratio (β) and selectivity (S). It is important to highlight that all the conclusions set in this section are established for β and S values at low concentrations of linalool, in accordance with the essential oil composition.

From obtained limonene + linalool + $[C_2mim][Me(OEt)_2SO_4]$ LLE data, it can be concluded that temperature has a slight effect on the equilibrium, this means that the separation could be carried out at room temperature. For this reason the other equilibria were determined only at 25ºC.

Several conclusions can be drawn from the structure of the studied ILs. The influence of the length of the alkyl substituent in a 1-alkyl-3-methylimidazolium cation depends on the type of anion. In the case of the $[NTf_2]$ anion, β increases as the length of the alkyl substituent increases whereas S follows the opposite trend. In the case of the [OAc] anion, both parameters increase with the length of the alkyl substituent.

Comparing the results obtained for $[C_2py][EtSO_4]$ with those of the previously studied $[C_2mim][EtSO_4]$, it can be confirmed that imidazolium IL shows slightly better results for β than its analogous pyridinium, with S values being very similar.

In any case, the type of anion seems to be the key factor to achieve the high desired values for these thermodynamic parameters. Conclusions can be established through the comparison of results obtained with ILs based in the [C_2mim] cation. Several of them showed good selectivities, clearly higher than one, ranking as follows: [OMs]> [OAc]> [$EtSO_4$]> [C_2mim][$Me(OEt)_2SO_4$]> [NTf_2]. Nonetheless, among these ILs the only solubilities clearly higher than one were found with the IL [C_2mim][OAc]. This is due to the linalool susceptibility of establishing hydrogen bonding with the IL which has a strong capacity to act as a hydrogen bond acceptor.

The final conclusion is that among all the tested ILs and those found in the bibliography, the IL [C_4mim][OAc] is the most apt to carry out the deterpenation of citrus essential oil by LLE. Moreover, β and S values obtained with this IL are clearly higher to those obtained with solvents proposed in the bibliography of this application (diethylene glycol and a mixture ethanol and water with 85 wt% in ethanol). The practically null vapour pressure of the IL makes the recoverability of linalool easy by applying high vacuum and low temperatures. In addition, the proposed IL has moderately low viscosity and toxicity, in comparison to other ILs. This proposal avoids the need of a distillation process, which implies two stages, high energetic requirements, and the possible degradation of the oil.

The NRTL and UNIQUAC equations were found to provide good correlations of the LLE, in spite of being a model not intended for systems involving electrolytes. Depending on the system, one of the two models provided slightly better results. Nevertheless no convergence was found for the NRTL model with the systems limonene + linalool + alkylpyridinium alkylsulfate IL. For this reason, UNIQUAC would be selected for the data treatment and its incorporation to simulation software.

– Enhanced oil recovery

The possibility of using surfactant ILs to improve the surfactant flooding EOR methods was evaluated by simulating the reservoir fluid as a mixture of water/brine, *n*-dodecane (oil) and IL. LLE data and interfacial tension among equilibrium phases were determined. Concretely, the ILs [$P_{6\,6\,6\,14}$]Cl and [$P_{6\,6\,6\,14}$][NTf_2] were investigated for this aim.

Both ILs could be used in EOR as in presence of water/brine and oil, they form a Winsor type III system, with a triphasic region consisting of a microemulsion (middle phase) coexisting with excess-water and excess-*n*-dodecane phases. In this middle phase, the IL solubilises a relevant amount of water and *n*-dodecane. This is associated to a drastic reduction of the water-oil interfacial tension, as was shown by means of the measurement of this property. Therefore, during the EOR process, these ILs could eliminate the capillary forces that hold the oil in the porous medium, thus improving the oil recovery. The advantages of ILs being liquids at room temperature, and avoiding the addition of any co-surfactant

must be highlighted. This last point could be a particularly important improvement over traditional surfactants.

The temperature and the presence of salt play an important role when looking for an optimal formulation water-oil-surfactant to be used in surfactant flooding EOR processes. There is a small influence of the temperature on the composition of the apex's three-phase tie triangle. Thus, with any of the ILs, the triphasic system is stable in a wide range of temperatures and in presence of salt. This stability greatly enhances the use of ILs to this application.

Moreover, water or brine viscosity increases when mixed with the IL due to the high viscosity of this compound. Regarding EOR applications, a reduced difference among water and oil viscosities reduces the mobility ratio between the heavy oil and the water, resulting in a more homogeneous front and reducing fingering. This results in a more efficient oil recovery.

Establishing a comparison among the two proposed ILs, the less amphiphilic character of the IL with the [NTf_2] anion makes the microemulsion solubilise practically only *n*-dodecane, and therefore, the water-oil interfacial tension is slightly decreased. The IL [$P_{6\,6\,6\,14}$]Cl shows a bigger surfactant character (it reduces the water-oil interfacial tension by 98% at 25°C and by 99% at 75°C) and solubilises both water and oil.

Concluding, due to the fact that these ILs can form a triphasic system, in a wide temperature range without the need of co-surfactant and in presence of salt, this can encourage further research on the use of ILs as surface active agents in EOR. Among the two studied ILs, the [$P_{6\,6\,6\,14}$]Cl showed the best properties for this purpose. This is an initial study. The capability of tuning the ILs must be used to increase the oil solubilisation and to get the extremely low interfacial tensions needed in this application, while simultaneously looking for an environmental friendly IL. Further investigation on the influence of pressure, adsorption of ILs in rocks, behaviour of real oil, and many others are needed before envisioning in situ research in the oilfield.

– Biomass processing

The capability of using bio-renewable DESs as solvents for lignocellulosic biomass processing was proved through solubility studies of pine wood and wheat straw. Different hydrogen bond donors (lactic, malic and oxalic acid), and different hydrogen bond acceptors (glycerol, choline chloride, proline, alanine, tetramethylammonium chloride and 2-chloroethyltrimethylammonium chloride) were combined to prepare the DESs.

The solid-liquid extraction (carried out under mild conditions), allowed the obtaining of a supernatant (DESs-rich phase) of a brown-reddish colour associated to the presence of lignin, as it was posteriorly confirmed by FT-IR spectra. Lignin was precipitated from

the supernatant (mixed with ethanol for the most viscous DESs) by water addition. Nonetheless, the method must be improved for DESs which are immiscible with ethanol, because this fact produces the precipitation of the solvent which was detected with the filtered biomass.

The tested DESs show high lignin solubility and very poor or negligible cellulose or hemicellulose solubility. Hence, the selectivity of the process is very high, a promising feature for delignification processes. The cellulose which remained in the biomass showed a noticeable change in its crystallinity in most cases.

It can be concluded that the best DES to carry out this separation depends on the nature of the biomass (different structures of lignin). Thus, in the case of pine wood, best results were found with LCEAC 5:1, and in the case of wheat straw, best results were found with LTMAC 3:1.

To sum up, tested DESs are promising solvents for biomass processing due to the high lignin solubility achieved over cellulose and hemicellulose. Nevertheless, further research needs to be carried out. Some of the parameters to be optimised are: the pretreatment process, new DESs components, the use of additives, other anti-solvents, and different temperature or pressure.

LIST OF SYMBOLS

LIST OF SYMBOLS

a	activity
CAS	Chemical Abstracts Service
DES	Deep Eutectic Solvent
EOR	Enhanced Oil Recovery
F	residual function
F_a	objective function (activities)
F_b	objective function (compositions)
G	Gibbs energy
g	binary energy interaction parameter in the NRTL model
IL	Ionic Liquid
i	generic species
j	generic species
K	capillary constant
k	generic species
k	kinetic energy correction
LLE	Liquid-Liquid Equilibrium
LTTM	Low Transition Temperature Mixtures
l	parameter in the UNIQUAC model
M	number of tie-lines
m	number of phases
NMR	Nuclear Magnetic Resonance
NRTL	*Non Random Two-Liquid* activity coefficient model
n	number of carbon atoms in an alkyl substituent chain of the imidazolium and pyridinium cation of an ionic liquid
n_D	refractive index
P	pressure
P_n	binary interaction parameter
Q	empirical constant, in the expression of F_a
q	area molecular-structure constant in the UNIQUAC model

R	universal constant of gases
R	hydrocarbon chain substituent
RTILs	Room Temperature Ionic Liquids
r	volume molecular-structure constant in the UNIQUAC model
S	selectivity
T	temperature
t	flow time
UNIQUAC	*Universal QUAsiChemical* activity coefficient model
u_{ij}	binary energy interaction parameter in the UNIQUAC model
w	mass fraction
X	halide
x	molar fraction
y	kinetic energy correction
z	lattice coordination number

Subscripts

a	in function of activity
b	in function of compositions
i	component
i	inert
i	counter
j	component
j	counter
k	component
k	counter
m	phase
n	counter
P	constant pressure
s	solute
T	constant temperature
∞	infinite dilution

Superscripts

I	organic-rich phase
II	IL-rich phase
m	generic phase

Greek letters

α	non-randomness parameter in the NRTL model
β	solute distribution ratio
Δ	Variation
$\Delta\beta$	mean error of the solute distribution ratio
δ	uncertainty
ϕ	number of phases
ϕ	segment fraction in the UNIQUAC model
γ	activity coefficient
γ	interfacial tension
η	dynamic viscosity
θ	area fraction in the UNIQUAC model
ν	kinematic viscosity
ρ	density
τ_{ij}	parameter in the NRTL or UNIQUAC models
ω_{H2O}	water content

Symbols on top

^	calculated value

REFERENCES

REFERENCES

[1] R. D. Rogers, K. R. Seddon. *Science* **302** (2003) 792.

[2] J. F. Brennecke, E. J. Maginn. *AIChE J.* **47** (2001) 2384.

[3] R. D. Rogers, K. R. Seddon (Eds.). In the *preface to Ionic Liquids as Green Solvents - Progress and Prospects*, ACS Symposium Series vol. 856, American Chemical Society, Washington DC, 2003.

[4] S. Gabriel, J. Weiner. *Ber.* **21** (1888) 2669.

[5] P. Walden. *Bull. Acad. Impér. Sci. St. Petersburg* (1914) 405.

[6] J. S. Wilkes, M.J. Zaworotko. *J. Chem. Soc. Chem. Commun.* (1992) 965.

[7] M. J. Earle, K. R. Seddon. *Pure Appl. Chem.* **72** (2000) 1391.

[8] W. Kunz, E. Maurer, R. Klein, D. Touraud, D. Rengsti, A. Harrar, S. Dengler, O. Zech. *J. Disp. Sci. Technol.* **32** (2011) 1694.

[9] J. D. Holbrey, K. R. Seddon. *Clean Prod. Proc.* **1** (1999) 223.

[10] J. S. Wilkes. *Green Chem.* **4** (2002) 73.

[11] M. J. Earle, J. M. S. S. Esperança, M. A. Gilea, J. N. Canongia, L. P. N. Rebelo, J. W. Magee, K. R. Seddon, J. A. Widegren. *Nature* **439** (2006) 831.

[12] N. V. Plechkova, K. R. Seddon. *Ionic liquids: "designer" solvents for green chemistry.* In: P. Tundo, A. Perosa, F. Zecchini (Eds.). Methods and Reagents for Green Chemistry, John Wiley & Sons, New Jersey, 2007.

[13] K. R. Seddon. *J. Chem. Tech. Biotechnol.* **68** (1997) 351.

[14] T. Welton. *Chem. Rev.* **99** (1999) 2071.

[15] M. Freemantle. *An Introduction to Ionic Liquids*, RSC Publishing, Cambridge, 2010.

[16] N. V. Plechkova, K. R. Seddon. *Chem. Soc. Rev.* **37** (2008)123.

[17] R. D. Rogers, K. R. Seddon, S. Volkov (Eds.). In the *Preface to Green Industrial Applications of Ionic Liquids*, Kluwer, Dordrecht, 2002.

[18] W. W. Meindersma, A. B. De Haan, A. B. In: N. V. Plechkova and K. R. Seddon. *Separation Processes with Ionic Liquids, in Ionic Liquids Uncoiled: Critical Expert Overviews,* John Wiley & Sons, New Jersey, 2012.

[19] M. Ramdin, T. W. de Loos, and T. J. H. Vlugt. *Ind. Eng. Chem. Res.* **51** (2012) 8149.

[20] D. Gorri, A. Urtiaga, I. Ortiz. *Supported liquid membranes for pervaporation processes.* In: E. Drioli and L. Giorno (Eds.).

Comprehensive Membrane Science and Engineering, vol. 2, Elsevier, Oxford, 2010.

[21] E. Santos, J. Albo, C. I. Daniel, C. A. M. Portugal, J. G. Crespo, A. Irabien. *J. Membr. Sci.* **430** (2013) 56.

[22] Y. S. Liu and G. B. Pan. *Ionic Liquids for the Future Electrochemical Applications.* In: A. Kokorin (Ed.). Ionic Liquids: Applications and perspectives, InTech, Croatia, 2011.

[23] A. Lewandowski, A. Świderska-Mocek. *J. Power Sources* **194** (2009) 601.

[24] J. D. Stenger-Smith, A. P. Chafin, Jr. Kline, F. Clare, G. S. Ostrom, R. L. Quintana. *Ionic Liquids in Charge Storage Devices: Effect of Purification on Performance*. T. Sato, S. Marukane, T. Morinaga. *Ionic Liquids for the Electric Double Layer Capacitor Applications.* In: S. T. Handy (Ed.). Applications of Ionic Liquids in Science and Technology, InTech, Croatia, 2011.

[25] A. P. Abbott, K. J. McKenzie, *Phys. Chem. Chem. Phys.* **8** (2006) 4265.

[26] R. P. Swatloski, S. K. Spear, J. D. Holbrey, R. D. Rogers. *J. Am. Chem. Soc.* **124** (2002) 4974.

[27] J. van Spronsen, M. A. Tavares-Cardoso, G. J. Witkamp, W. de Jong, M. C. Kroon. *Chem. Eng. Proces: Proces Intens.* **50** (2011) 196.

[28] A. V. Mudring, T. Alammar, T. Baecker, K. Richter. *Nanoparticle Synthesis in Ionic Liquids,* ACS Symposium Series vol. 1030, American Chemical Society , Washington D.C., 2009.

[29] J.D. Scholten, M. H. G. Prechtl, J. Dupont. *Formation of Nanoparticles assisted by Ionic Liquids.* In: P. T. Anastas (Ed) Handbook of Green Chemistry, John Wiley and Sons, Weinheim, 2012.

[30] J. A. Murillo-Hernández, J. Aburto. *Current knoweledge and potential applications of ionic liquids in the petroleum industry.* In: A. Kokorin (Ed.). Ionic liquids: applications and perspectives, Intech-Open, 2011.

[31] M. Boukherissa, F. Mutelet, A. Modarressi, A. Dicko, D. Dafri, M. Rogalski. *Energ. Fuel.* **23** (2009) 2557.

[32] Y. F. Hu, T. M. Guo. *Langmuir* **21** (2005) 8168.

[33] R. C. B. Lemos, E. B. da Silva, A. dos Santos, R. C. L. Guimaraes, B. M. S. Ferreira, R. A. Guarnieri, C. Dariva, E. Franceschi, A. F. Santos, M. Fortuny. *Energ. Fuel.* **24** (2010) 4439.

[34] D. Guzmám-Lucero, P. Flores, T. Rojo, R. Martínez-Palou. *Energ. Fuel.* **24** (2010) 3610.

[35] P.S. Kulkarni, C.A.M. Afonso, *Green Chem.* **12** (2010) 1139.

[36] M. Abai, M. P. Atkins, K. Y. Cheun, J. D. Holbrey, P. Nockemann, K. R. Seddon, G. Srinivasan, Y. Zou. *Process for*

removing metals from hydrocarbons by using ionic liquids. PTC Int. Appl. WO 2012/046057 A2.

[37] C. Capello, U. Fischer, K. Hungerbühler. *Green Chem.* **9** (2007) 927.

[38] M. Francisco, A. van den Bruinhorstand, C. Kroon, *Green Chem.* **14** (2012) 2153.

[39] A. P. Abbott, G. Capper, D. L. Davies, R. K. Rasheed, V. Tambyrajah. *Chem. Commun.* (2003) 70.

[40] A. P. Abbott, D. Boothby, G. Capper, D. L. Davies, R. K. Rasheed. *J. Am. Chem. Soc.* **126** (2004) 9142.

[41] C. Ruß, B. König. *Green Chem.* **14** (2012) 2969.

[42] Q. Zhang, K. Oliveira-Vigier, S. Royer, F. Jerome. *Chem. Soc. Rev.* **41** (2012) 7108.

[43] M. Francisco, A. van den Bruinhorst, M. C. Kroon. *Angew. Chem. Intl. Ed.* **52** (2013) 3074.

[44] J. Lawless. *The Encyclopedia of Essential Oils*, Harper Collins, London, 2002.

[45] A. Verzera, A. Trozzi, G. Dugo, G. Di Bella, A. Cotroneo. *Flavour Fragr. J.* **19** (2004) 544.

[46] A. Arce, A. Soto. Citrus *Essential oils: Extraction and Deterpenation.* In: N. Benkeblia, P. Tennant (Eds.). Tree and Forestry Science and Biotechnology, Special Issue 1, vol. 2, Global Sciences Books, London, 2009.

[47] M. Kondo, M. Goto, A. Kodama, T. Hirose. *Ind. Eng. Chem. Res.* **39** (2000) 4745.

[48] J. Owusu-Yaw, R. F.Matthews. *J. Food Sci.* **51** (1986) 1180.

[49] G. R. Stuart, D. Lopes, J. V. Oliveira. *J. Am. Oil Chem. Soc.* **78** (2001) 1041.

[50] A. Arce, A. Marchiaro, O. Rodríguez, A. Soto. *Chem. Eng. J.* **89** (2002) 223.

[51] A. Arce, A. Machiaro, A. Soto. *Fluid Phase Equilib.* **211** (2003) 129.

[52] A. Arce, A. Marchiaro, A. Soto. *J. Sol. Chem.* **33** (2004) 559.

[53] A. Arce, A. Marchiaro, A. Soto. *Fluid Phase Equilib.* **226** (2004)121.

[54] A. Arce, A. Marchiaro, J. M. Martínez-Ageitos, A. Soto. *Can. J. Chem. Eng.* **83** (2005) 366.

[55] A. Arce, A. Marchiaro, O. Rodríguez, A. Soto. *AIChE J.* **52** (2006) 2089.

[56] M. B. Gramajo de Oz, A. M. Cases, H. N. Sólimo. *J. Chem. Thermodyn.* **40** (2008) 1575.

[57] L. M. Sevgili, S. Sahin, S. I. Kirbaslar. *J. Chem. Eng. Data* **53** (2008) 737.

[58] D. J. Brose, M. B. Chidlaw, D. T. Friesen, E. D. LaChapelle, P. van Eikeren. *Biotechnol. Prog.* **11** (1995) 214.

[59] K. Sakamoto, K. Fujii, A. Inoue, H. Kozuka, H. Ohta. *Food Sci. Technol. Res.* **9** (2003) 11.

[60] S. Díaz, S. Espinosa, E. A. Brignole. *J. Supercrit. Fluids* **35** (2005) 49.

[61] F. Gironi, M. Maschietti. *Chem. Eng. Sci.* **63** (2008) 651.

[62] F. Benvenuti, F. Gironi, L. Lamberti. *J. Supercrit. Fluids* **20** (2001) 129.

[63] A. Arce, A. Pobudkowska, O. Rodríguez, A. Soto. *Chem. Eng. J.* **133** (2007) 213.

[64] E.C. Donaldson, G.V. Chilingarian, T.F. Yen. *Enhanced oil recovery, II: processes and operations*, Elsevier, Amsterdam 1989.

[65] J. L. Salager. *Recuperación mejorada del petróleo* (Cuaderno FIRP S357-C), Universidad de los Andes, Mérida-Venezuela, 2005.

[66] J. G. Speight. *Enhanced oil recovery methods for heavy oil and tar sands*, GULF Publishing Company, Houston, 2009.

[67] L. W. Lake, R. L. Schmidt, P. B. Venuto, *Oilfield Rev.* **4** (1992) 55.

[68] P. A. Winsor. *Trans. Faraday Soc.* **44** (1948) 376.

[69] P. A. Winsor. *Solvent Properties of Amphiphilic Compounds*, Butherworth& Co., London, 1954.

[70] J, L. Salager, J. C. Morgan, R. S. Schechter, W. H. Wade, E. Vasquez. *SPE J.* **19** (1979) 107.

[71] J.L. Salager. *Physicochemical Properties of Surfactant-oil-water Mixtures: Phase Behaviour, Microemulsion Formation and Interfacial Tension*, Tesis PhD, Univ. Texas, USA, 1977.

[72] V. Pino, M. Germán-Hernández, A. Martín-Pérez, J. L. Anderson. *Sep. Sci. Technol.* **47** (2012) 264.

[73] I. R. Collins, M. J. Earle, S. P. Exton, N. V. Plechkova, K. R. Seddon. *Ionic liquids and uses thereof*, PTC Int. Appl. WO 2006/111712 A2.

[74] J. Bowers, C. P. Butts, P. J. Martin, M. C. Vergara-Gutierrez. *Langmuir* **20** (2004) 2191.

[75] M. Blesic, M. H. Marques, N. V. Plechkova, K. R. Seddon, L. P. Rebelo, A. Lopes. *Green Chem.* **9** (2007) 481.

[76] M. Blesic, A. Lopes, E. Melo, Z. Petrovski, N. V. Plechkova, J. N. Canongia-Lopes, K. R. Seddon, L. P. Rebelo. *J. Phys. Chem. B.* **112** (2008) 8645.

[77] M. Blesic, M. Swadzba-Kwasny, J. D. Holbrey, J. N. Canongia Lopes, K. R. Seddon, L. P. Rebelo. *Phys. Chem. Chem. Phys.* **11** (2009) 4260.

[78] Z. X. Fan, T. F. Wang, Y. H. He. J. *Fuel Chem. Technol.* **37** (2009) 690.

[79] Y. Z. Shang, W. J. Song, N. Zhao, H. Li, H. I. Liu. *You tian huaxue* **27** (2010) 306.

[80] G. Zhang, X. Chen, Y. Zhao, Y. Xie, H. Qiu. *J. Phys. Chem. B.* **111** (2007) 11708.

[81] J. Liu, Y. Li, J. L. Chai, C. K. Kin, X. Y. Yu, Y. Xia. *Tenside Surf. Det.* **46** (2009) 306.

[82] K. Anderson, H. Rodríguez, K. R. Seddon. *Green Chem.* **11** (2009) 780.

[83] S. Lago, H. Rodríguez, A. Soto, A. Arce, M. Khoshkbarchi. *RSC Advanc.* **2** (2012) 9392.

[84] M. Siskin, M. A. Francisco, R. M. Billimora. *Upgrading of petroleum residues, bitumen, or heavy oils by separation of asphaltenes and resins using ionic liquids*. PCT Int. Appl. WO 2008/124042 A1 20081016.

[85] M. Siti-Qurratu'Aini, I. Mohd-Saaid. *A review of ionic liquids used for upgrading of heavy oils*, 3rd CUTSE International Conference, Miri, Sarawak, 2011.

[86] A. Zeinolabedini-Hezave, S. Dorostkar, S. Ayatollahi, M. Nabipour, B. Hemmateenejad, *Colloid Surface A* **421** (2013) 63.

[87] J.B. Binder, R. T. Raines. *J. Am. Chem. Soc.* **131** (2009)1979.

[88] Z. Zhang, Z. K. Zhao. *Bioresource Technol.* **101** (2010) 1111.

[89] N. Jiang, A. J Ragauskas. *Perdeuterated Pyridinium Ionic Liquids for Direct Biomass Dissolution and Characterization*, In: A. Kokorin (Ed.). Ionic liquids: applications and perspectives, Intech-Open, 2011.

[90] Md. M. Hossain, L. Aldous. *Aust. J. Chem.* **65** (2012) 1465.

[91] E. M. Rubin. *Nature* **454** (2008) 841.

[92] N. Sun, H. Rodríguez, M. Rahman, R. D. Rogers. *Chem. Commun.* **47** (2011) 1405.

[93] Y. Zheng, Z. Pan, R. Zhang. *Int. J. Agric. Biol. Eng.* **2** (2009) 51.

[94] M. Mazza, D. A. Catana, C. Vaca-García, C. Cecutti. *Cellulose* **16** (2009) 207.

[95] J. Holm, U. Lassi. *Ionic Liquids in the Pretreatment of Lignocellulosic Biomass*, In: A. Kokorin (Ed.). Ionic liquids: applications and perspectives, Intech-Open, 2011.

[96] A. Pinkert, K. N. Marsh, S. S. Pang, M. P. Staiger. *Chem. Rev.* **109** (2009) 6712.

[97] P. Maki-Arvela, I. Anugwom, P. Virtanen, R. Sjoeholm, J. P. Mikkola. *Ind. Crops Prod.* **32** (2010)175.

[98] A. Stark. *Energ. Environ. Sci.* **4** (2011) 19.

[99] H. Tadesse, R. Luque. *Energy Environ. Sci.* **4** (2011) 3913.

[100] M. Mora-Pale, L. Meli, T. V. Doherty, R. J. Linhardt, J. S. Dordick. *Biotechnol. Bioeng.* **108** (2011) 1229.

[101] N. Muhammad, Z. Man, M. A. Bustam-Khalil. Eur. *J. Wood Prod.* **70** (2012) 125.

[102] H. Wang, G. Gurau, R. D. Rogers. *Chem. Soc. Rev.* **41** (2012) 1519.

[103] A. Brandt, J. Graesvik, J. Hallett, T. Welton. *Green Chem.* **15** (2013) 550.

[104] Q. P. Liu, X. D. Hou, N. Li, M. H. Zong. *Green Chem.* **14** (2012) 304.

[105] P. Bonhôte, A. P. Dias, N. Papageorgiou, K. Kalyanasundaram, M. Grätzel. *Inorg. Chem.* **35** (1996)1168.

[106] S. Himmler, S. Hormann, R. van Hal, P. S. Schulz, P. Wasserscheid. *Green Chem.* **8** (2006) 887.

[107] A. Arce, E. Rodil, A. Soto. *J. Chem. Eng. Data* **51** (2006) 1453.

[108] K. R. Seddon, A. Stark, M. J. Torres. *Pure Appl. Chem.* **72** (2000) 2275.

[109] J. A. Riddick, W. B. Bunger y T. K. Sakano, *Organic Solvents – Physical Properties and Methods of Purification*, 4ª ed., Wiley, New York, 1986.

[110] F. Comelli, S. Ottani. *J. Chem. Eng. Data* **47** (2002) 93.

[111] R. Francesconi, C. Castellari. *J. Chem. Eng. Data* **46** (2001)1520.

[112] M. G. Freire, A. R. Teles, M. A. Rocha, B. Schröder, C. M. Neves, P. J. Carvalho, D. V. Evtuguin, L. M. Santos, J. A. Coutinho. *J. Chem. Eng. Data* **56** (2011) 4813¬.

[113] M. Tariq, P.A. Forte, M.F. Costa Gomes, J.N. Canongia Lopes, L.P. Rebelo. *J. Chem. Thermodyn.* **41** (2009) 790.

[114] A. N. Soriano, B. T. Doma Jr., M. H. Li. *J. Chem. Thermodyn.* **40** (2008) 1654.

[115] A. P. Fröba, H. Kremer, A. Leipertz. *J. Phys. Chem. B* **112** (2008) 12420.

[116] A. Muhammad, M. I. Mutalib, C. D. Wilfred, T. Murugesan, A. Shafeeq. *J. Chem. Thermodyn.* **40** (2008) 1433.

[117] K. Shimizu, M. Tariq, M. F. Costa Gomes, L. P. Rebelo, J. N. Canongia Lopes. *J. Phys. Chem. B* **114** (2010) 5831.

[118] E. Gómez, N. Calvar, A. Domínguez, E. A. Macedo. *J. Chem. Thermodyn.* **42** (2010) 1324.

[119] E. Gómez, I. Domínguez, B. González, A. Domínguez. *J. Chem. Eng. Data* **55** (2010) 5169.

[120] A. Arce, M. Earle, H. Rodriguez, K. R. Seddon. *J. Phys. Chem. B* **111** (2007) 4732.

[121] U. Domanska, Z. Zolek-Tryznowska, A. Pobudkowska. *J. Chem. Eng. Data* **54** (2009) 972.

[122] R. Anantharaj, T. Banerjee. *Fluid Phase Equilibr.* **312** (2011) 20.

[123] M. Francisco, S. Lago, A. Soto, A. Arce. *Fluid Phase Equilibr.* **296** (2010) 149.

[124] J. M. Sørensen, T. Magnussen, P. Rasmussen, A. Fredenslund. *Fluid Phase Equilib.* **2** (1979) 297.

[125] S. Lago, H. Rodríguez, A. Soto, A. Arce. *J. Chem. Eng. Data* **56** (2011) 1273

[126] Y. A. Wang, G. A. Voth. *J. Am. Chem. Soc.* **127** (2005) 12192.

[127] J. N. Canongia-Lopes, A. A. Pádua. *J. Phys. Chem. B* **110** (2006) 3330.

[128] J. N. Canongia-Lopes, M. F. Costa-Gomes, A. A. Pádua. *J. Phys. Chem. B* **110** (2006) 16816.

[129] S. Lago, H. Rodríguez, A. Soto, A. Arce. *Sep. Sci. Technol.* **47** (2012) 292.

[130] http://www.merckmillipore.com/chemicals/1-ethyl-3-methylimidazolium-methanesulfonate/MDA_CHEM-490286/p_sLusHfETyAcAAAE852pCX8kx (Last accessed, July 2013).

[131] H. Renon, J. M. Prausnitz. *AIChE J.* **14** (1968) 135.

[132] D. S. Abrams, J. M. Prausnitz. *AIChE J.* **21** (1975) 116.

[133] A. Bondi. *Physical Properties of Molecular Crystals, Liquids and Glasses,* Wiley, New York, 1968.

[134] Z. Lei, J. Zhang, Q. Li, B. Chen. *Ind. Eng. Chem. Res.* **48** (2009) 2697.

[135] R. Kato, J. Gmehling. *J. Chem. Thermodyn.* **37** (2005) 603.

[136] T. Banerjee, M. K. Singh, R. K. Sahoo, A. Khanna, A. *Fluid Phase Equilib.* **234** (2005) 64.

[137] R. S. Santiago, G. R. Santos, M. Aznar. *Fluid Phase Equilib.* **293** (2010) 66.

[138] J. M. Sørensen, W. Arlt. *Liquid-Liquid Equilibrium Data Collection*, DECHEMA Chemistry Data Series, Frankfurt, 1980.

[139] P. Bonhôte, A. P. Dias, M. Armand, N. Papageorgiou, K. Kalyanasundaram, M. Grätzel. *Inorg. Chem.* **37** (1998) 166.

[140] C. M. Neves, P.J. Carvalho, M.G. Freire, J.A. Coutinho. *J. Chem. Thermodyn.* **43** (2011) 948-957.

[141] P. Kilaru, G. A. Baker, P. Scovazzo. *J. Chem. Eng. Data* **52** (2007) 2306.

[142] H.F. Almeida, J.A. Lopes-da-Silva, M.G. Freire, J.A. Countinho. *J. Chem. Thermodyn.* **57** (2013) 372.

[143] M. G. Freire, C. M. Neves, P. J. Carvalho, R. L. Gardas, A. M. Fernandes, I. M. Marrucho, L. M. Santos, J. A. Coutinho. *J. Phys. Chem. B.* **111** (2007)13082.

[144] M. G. Freire, P. J. Carvalho, R. L. Gardas, L. M. Santos, I. M. Marrucho, J. A. Coutinho. *J. Chem. Eng. Data* **53** (2008) 2378.

[145] M. Blesic, J. N. Canongia-Lopes, M. F. Costa-Gomes, L. P. Rebelo. *Phys. Chem. Chem. Phys.* **12** (2010) 9685.

[146] A. Makowska, A. Siporska, P. Oracz, J. Szydlowski. *J. Chem. Eng. Data* **55** (2010) 2829.

[147] S. Zeppieri, J. Rodríguez, A. L. López-Ramos. *J. Chem. Eng. Data* **46** (2001) 1086.

[148] D. M. Mitrinovic, A. M. Tikhonov, M. Li, Z. Huang, M. L. Schlossman. *Phys. Ver. Lett.* **85** (2000) 582.

[149] R. Aveyard, S. M. Saleem. *J. Chem. Soc. Farad. T* **172** (1976) 1609.

[150] G. V. Carrera, C. A. Afonso, L. C. Branco. *J. Chem. Eng. Data* **55** (2010) 609.

[151] Y. C. Chung, A. Bakalinsky, M. H. Penner. *Appl. Biochem. Biotechnol.* **66** (1997) 249.

APENDIX A: PUBLICATIONS

APENDIX A: PUBLICATIONS

1.- M. Francisco, **S. Lago**, A. Soto and A. Arce

Essential oil deterpenation by solvent extraction using 1-ethyl-3-methylimidazolium 2-(2-methoxyethoxy) ethylsulphate ionic liquid.

Fluid Phase Equilibria, vol. 296, 149-153 (2010)

2.- **S. Lago**, H. Rodríguez, A. Soto and A. Arce

Deterpenation of Citrus Essential Oil by Liquid-Liquid Extraction with 1-Alkyl-3-methyl-imidazolium bis(trifluoromethylsulfonyl)amide ionic liquids

Journal of Chemical and Engineering Data, vol. 56, 1273-1281 (2011)

3.- **S. Lago**, H. Rodríguez, A. Soto and A. Arce

Alkylpyridinium Alkylsulfate Ionic Liquids as Solvents for the Deterpenation of Citrus Essential Oil

Separation Science and Technology, vol. 47, 292-299 (2012)

4.- **S. Lago**, H. Rodríguez, A. Soto, A. Arce, and M. Khoshkbarchi.

Study of phase behavior and transport properties of trihexyl(tetradecyl)phosphonium chloride ionic liquid for enhanced oil recovery.

RSC Advances, vol.2, 9392-9397 (2012)

5.- M. Francisco, A. S. B. González, **S. Lago García de Dios**, W. Weggemans, M. C. Kroon

Comparison of choline-based low transition temperature mixtures (LTTMs) with choline-based ionic liquids and salts: physical properties and vapour-liquid equilibria of mixtures containing water and ethanol.

RSC Advances. Major revision July 2013

6.- A. S. B. González, M. Francisco, G. Jimeno, **S. Lago García de Dios**, M. C. Kroon

Liquid – liquid equilibrium data for the systems {LTTM + benzene + hexane} and {LTTM + ethyl acetate + hexane} at different temperatures and atmospheric pressure

Fluid Phase Equilibria. Sent to be published June 2013

7.- **S. Lago**, M. Francisco, A. Arce, and A. Soto

The effect of the temperature on enhanced oil recovery with the ionic liquid trihexyl(tetradecyl)phosphonium chloride: thermal stability and properties of a three-phase system

Energy and Fuels. Sent to be published June 2013

8.- **S. Lago**, H. Rodríguez, A. Soto and A. Arce

Improved concentration of citrus essential oil by solvent extraction with acetate ionic liquids

Green Chemistry. Sent to be published July 2013

APPENDIX B:
RESUMEN
(Summary, in Spanish)

APPENDIX B: RESUMEN (Summary, in Spanish)

El principal objetivo de esta tesis consiste en analizar la viabilidad de la utilización de diferentes tipos de disolventes de diseño, Líquidos Iónicos (LIs) y Disolventes Eutécticos (DEs), para mejorar la sostenibilidad y/o eficiencia de diferentes procesos químicos.

La definición más comúnmente utilizada para los LIs es la de sales con un punto de fusión por debajo de los 100 ºC. El gran interés que estas sales han despertado en las últimas décadas se debe principalmente a sus prometedoras propiedades. Entre otras: amplio intervalo de temperaturas en el cual se encuentran en estado líquido, su prácticamente despreciable presión de vapor (lo que evita problemas de olores y contaminación atmosférica), y que la mayoría no son inflamables y presentan una gran estabilidad térmica y química. Hay que mencionar, además, la posibilidad de "diseñar a medida" estas sales, combinando distintos cationes y aniones, cambiando la longitud de cadena o sus ramificaciones, e incluso mezclando diferentes LIs, lo que permite obtener distintas propiedades físicas, químicas y bilógicas. Por todo ello, estas sales están sustituyendo a los disolventes orgánicos tradicionales a nivel de laboratorio y, poco a poco, a nivel industrial.

Los DEs podrían definirse como fluidos iónicos constituidos por un dador de hidrógeno asociado, mediante enlace de puente de hidrógeno, a un aceptor de hidrógeno. Normalmente los compuestos iniciales están en estado sólido y al mezclarse forman un eutéctico con un punto de fusión más bajo que el de los precursores. Al igual que los LIs, estos disolventes presentan numerosas ventajas con respecto a los disolventes orgánicos tradicionales, se consideran no inflamables y su volatilidad es baja. Pero sus características más atractivas son sus bajas toxicidad y biodegradabilidad, debido a que generalmente sus precursores son de origen natural y renovable. Por este motivo su precio suele ser claramente inferior al de los LIs. Son también disolventes de diseño, a partir de una correcta selección de los precursores. Los DEs son normalmente líquidos a temperaturas por debajo de 150 ºC, sin embargo el número de DEs líquidos a temperatura ambiente hasta ahora conocido es escaso.

En esta Tesis se analiza la posibilidad de utilizar LIs en la mejora de dos procesos muy diferentes: la desterpenación de aceites esenciales de cítricos y la extracción mejorada del petróleo. En cuanto a los DEs, se realiza un estudio introductorio sobre su uso como disolventes para el fraccionamiento de la biomasa. A continuación se resume el trabajo experimental y los resultados obtenidos en estas aplicaciones.

Desterpenación de aceites esenciales de cítricos

Se define aceite esencial como la fracción volátil obtenida a partir de una planta, o parte de la misma, mediante un proceso de separación física. Ese método físico suele ser destilación o prensado. Esta pequeña porción del material de la planta proporciona su olor y sabor característico. En el caso de los cítricos, los aceites están contenidos mayoritariamente en pequeñas glándulas presentes en la piel de los frutos.

Los aceites esenciales son mezclas complejas de hasta más de 100 componentes entre los que se encuentran: monoterpenos, sesquiterpenos, sus derivados oxigenados y compuestos alifáticos de bajo peso molecular (alcanos, alcoholes, aldehidos, cetonas, ésteres y ácidos), además de residuos no volátiles (parafinas, ceras…). Los aceites esenciales de la piel de los frutos cítricos tienen alrededor de un 95% de hidrocarburos monoterpénicos. Los hidrocarburos terpénicos contribuyen muy poco a los perfiles de olor y sabor. Además pueden generar problemas a causa de su insolubilidad en disoluciones acuosas y alcohólicas, oxidación en presencia de oxígeno y resinificación, que causan el deterioro del olor y el sabor del aceite. Las características organolépticas de los aceites de cítricos se deben fundamentalmente a los derivados oxigenados de los compuestos terpénicos y a ciertos compuestos oxigenados como compuestos carbonílicos y ésteres, que se encuentran en el aceite en muy baja concentración.

La eliminación total o parcial de los hidrocarburos terpénicos de los aceites esenciales naturales se denomina desterpenación y se efectúan principalmente con los siguientes fines:

- Aumentar la concentración de los componentes que contribuyen en mayor medida al aroma.

- Aumentar la estabilidad de los aceites pues el contenido de terpenos se reduce, ralentizando reacciones de oxidación y resinificación. De esta forma, se elimina la aparición de olores desagradables.

- Incrementar la solubilidad del aceite esencial de cítricos en agua, etanol (incluso de baja graduación) y, así mismo, en disolventes aptos para tecnología alimentaria.

Para el tratamiento de volúmenes importantes de aceite, el método más habitual de desterpenación es la destilación fraccionada a vacío. Sin embargo, se produce una incompleta separación de los constituyentes debido a que sus puntos de ebullición son próximos, y se necesita trabajar al menos en dos etapas con grandes requerimientos energéticos, lo que conlleva cierta degradación del aceite durante el tiempo de calentamiento. Todo ello se traduce en una disminución de la calidad del aceite obtenido.

Una alternativa que evita esos problemas es la extracción mediante alcohol diluido u otros disolventes. Sin embargo, los

disolventes ensayados hasta el momento no son muy eficaces (bajas solubilidades y selectividades).

Experimental

El aceite esencial de cítrico se simuló como una mezcla binaria de limoneno y linalool (terpeno y oxiterpeno característicos de dicho aceite). La capacidad de los LIs como disolventes para llevar a cabo la desterpenación del aceite se determinó a través del estudio del equilibrio líquido-líquido del sistema limoneno + linalool + LI.

Para la selección de los disolventes se realizaron pruebas de solubilidad mediante ensayos de turbidez. Se escogieron aquellos que presentaron altas solubilidades del linalool y bajas para el limoneno. Concretamente: $[C_2mim][Me(OEt)_2SO_4]$, $[C_2mim][NTf_2]$, $[C_6mim][NTf_2]$, $[C_{10}mim][NTf_2]$, $[C_1py][MeSO_4]$, $[C_2py][EtSO_4]$, $[C_2mim][OAc]$ y $[C_4mim][OAc]$. Excepto los dos últimos que fueron comprados, los demás se sintetizaron en el laboratorio.

Para cada sistema limoneno + linalool + LI, el estudio se inició con la determinación de las curvas de solubilidad, a la temperatura de trabajo, mediante el método del punto de niebla. Para la determinación de las rectas de reparto, se introdujeron mezclas de los tres componentes con composición global comprendida en la región inmiscible del sistema en una célula de vidrio termostatizada a la temperatura de trabajo. Se agitó el contenido vigorosamente durante al menos 2 h. El tiempo de reposo se estableció en 5 h para asegurar una correcta separación de las fases generadas, a excepción de los sistemas con $[C_npy][RSO_4]$ y $[C_nmim][OAc]$ que necesitaron 12 h (estudios previos demostraron que tiempos superiores no implicaban variación en los resultados obtenidos). Una vez que las fases se separaron correctamente, se procedió a la extracción de las muestras con ayuda de jeringas.

En el caso del sistema con $[C_2mim][Me(OEt)_2SO_4]$ se utilizó cromatografía de gases (HP 6890) para la determinación de la composición de las distintas fases. Para el resto de los sistemas se utilizó espectroscopía de resonancia magnética nuclear de protón (Varian Mercury 300), una técnica que proporciona la precisión necesaria e implica un desarrollo analítico más simple. La validez cuantitativa de ambas técnicas se comprobó mediante la preparación de diferentes muestras, con composiciones próximas a la región de inmiscibilidad por pesada, y mediante comparación de las composiciones determinadas analíticamente con las reales.

Resultados y discusión

Además de presentar los diagramas triangulares de todos los equilibrios determinados, la capacidad de los LIs para llevar a cabo la desterpenación se evaluó mediante dos parámetros termodinámicos: el coeficiente de distribución de soluto (β) y la selectividad (S). Valores superiores a la unidad en ambos parámetros implican la bondad de la extracción planteada (menor cantidad de disolvente y menor número de etapas en la separación).

Los datos de equilibrio para el sistema limoneno + linalool + $[C_2mim][Me(OEt)_2SO_4]$ se determinaron a 25, 35 y 45 ºC, para ver el efecto que la temperatura ejerce en el equilibrio. Dado que los valores de β y S prácticamente no se vieron afectados por la temperatura, obteniéndose incluso ligeramente mejores resultados a temperatura ambiente, el resto de los estudios se realizó a 25 ºC.

Se determinó el equilibrio con diferentes LIs con catión imidazólico dialquilsustituido ($[C_nmim]$), siendo estos radicales un metilo y una cadena lineal hidrocarbonada de longitud variable. Se encontró que la influencia del tamaño de dicha cadena en β y S depende del tipo de anión del LI. Así en los líquidos iónicos con anión $[NTf_2]$, al aumentar la longitud de la cadena β aumenta y S disminuye. Sin embargo, con el anión [OAc], al aumentar el tamaño de la cadena, ambos parámetros aumentan para bajas concentraciones de linalool que son las existentes en el aceite esencial previo a su desterpenación.

Comparando los resultados obtenidos con los LIs $[C_2mim][EtSO_4]$, previamente estudiado, y $[C_2py][EtSO_4]$, se encontraron solubilidades superiores con el primero (de menor coste) y selectividades similares con ambos.

El análisis de los datos obtenidos con diferentes LIs del tipo $[C_2mim]X$, siendo X el anión ($[Me(OEt)_2SO_4]$, $[NTf_2]$, [OAc], [OMs] y $[EtSO_4]$), permite establecer que la influencia de este ión no es clara. Con todos ellos, se obtuvieron selectividades claramente superiores a la unidad, pero los coeficientes de distribución de soluto dieron valores favorables únicamente en el caso de los acetatos. La formación de puentes de hidrógeno entre el linalool y el LI resultó ser un parámetro clave en el aumento de esa solubilidad.

Los valores de β y S más favorables (obtenidos para el $[C_4mim][OAc]$) se compararon con los valores obtenidos en la bibliografía para los disolventes tradicionales propuestos para este proceso (dietilenglicol y la mezcla etanol-agua con un 85% en masa de etanol). Los resultados mostraron que el líquido iónico es indiscutiblemente el mejor extractor de linalool. Además, su prácticamente nula volatilidad permitiría su recuperación con relativa facilidad.

Finalmente, los datos experimentales de equilibrio obtenidos para cada sistema limoneno + linalool + LI se correlacionaron mediante los modelos termodinámicos NRTL y UNIQUAC, obteniendo los correspondientes parámetros binarios de interacción energética, con el fin de modelar el comportamiento de las mezclas consideradas para el diseño de las unidades de separación. Aunque, en general, ambas ecuaciones proporcionaron resultados adecuados, obteniendo resultados ligeramente mejores con un modelo u otro dependiendo del sistema estudiado, no se consiguió convergencia para los sistemas con $[C_npy][RSO_4]$ correlacionados con el modelo NRTL.

Extracción mejorada del petróleo

Los métodos tradicionales de extracción primaria y secundaria del petróleo extraen aproximadamente la tercera parte del petróleo de un yacimiento. En los últimos años, la escasez de crudo ha llevado a la necesidad de recuperar más petróleo de yacimientos ya explotados. La extracción terciaria o mejorada del petróleo ("Enhanced Oil Recovery"), consiste en la utilización de medios que aumentan la movilidad del fluido en el pozo conjuntamente con los métodos de extracción secundaria (inyección de fluidos para generar un gradiente de presión), permitiendo una extracción mucho más eficaz en el yacimiento.

Dentro de los métodos de extracción mejorada del petróleo, hay que citar: los métodos térmicos, los métodos de desplazamiento mediante fluido miscible (CO_2 el más utilizado) y los métodos químicos. Estos últimos se consideran los más eficaces, sin embargo su coste es elevado, y es necesario mejorar su aplicabilidad puesto que estos métodos se ven afectados por múltiples parámetros como: tipo de crudo, temperatura, presión, porosidad del pozo, permeabilidad de los fluidos, naturaleza de los productos químicos, necesidad de aditivos, etc.

El método de extracción terciaria mediante drenaje micelar es un método químico que se basa en la inyección de una disolución acuosa de baja concentración de surfactante dentro de la reserva de petróleo, con el fin de reducir la tensión interfacial existente entre el agua y el petróleo contenido en los poros de las rocas. De esta forma se mejora la movilidad del petróleo atrapado dentro de la reserva pudiendo ser arrastrado a la superficie mediante agua. El control de la movilidad es importante para que el proceso sea efectivo, por eso, habitualmente tras la inyección del sistema micelar, se introduce una fase acuosa de polímero, éste aumenta la viscosidad del agua y la eficiencia de barrido evitando la formación de digitaciones.

Una aproximación válida para el estudio de sistemas de interés en la extracción del petróleo, a pesar de que éstas son mezclas complejas (agua, sales, surfactante, co-surfactante, componentes del petróleo…), es considerarlos como un sistema pseudo-ternario surfactante – agua – aceite. Así, a temperatura y presión constante, Winsor definió tres tipos de diagramas básicos (Winsor tipo I, tipo II y tipo III). El diagrama tipo III comprende una región trifásica rodeada por tres zonas bifásicas y una región monofásica. En lo que concierne a los sistemas cuya composición global se encuentra en la zona trifásica, se separan en tres fases en equilibrio: una fase acuosa y una fase aceitosa que contienen esencialmente agua y aceite, respectivamente, y también una fase media de densidad intermedia entre las fases anteriores. En el diagrama tipo III, las interacciones se equilibran y el surfactante está en lo que se llama la formulación óptima, ya que dicha situación físico-química corresponde a la existencia de una tensión interfacial extremadamente baja y por

tanto a la eliminación casi total de las fuerzas capilares que atrapan el petróleo en el medio poroso.

Experimental

El sistema en el interior del yacimiento se simuló como una mezcla de surfactante (LI), aceite (*n*-dodecano) y agua/agua salada. La capacidad de algunos LIs surfactantes para mejorar los métodos existentes de recuperación mejorada del petróleo, se estudió a través de la determinación del equilibrio líquido-líquido de los sistemas ternarios agua + *n*-dodecano + LI. Se determinaron también la viscosidad y densidad de las distintas fases obtenidas en las diferentes regiones del equilibrio, así como las tensiones interfaciales existentes entre las fases. Los LIs seleccionados fueron $[P_{6\,6\,6\,14}][Cl]$ y $[P_{6\,6\,6\,14}][NTf_2]$, por su carácter surfactante y por ser líquidos a temperatura ambiente.

Para cada sistema agua + *n*-dodecano + LI, el estudio se inició con la determinación de las curvas de solubilidad a la temperatura de trabajo mediante el método del punto de niebla. Posteriormente, se determinó el equilibrio líquido-líquido (a 25 y 75 ºC), de manera similar al procedimiento explicado en el apartado anterior, pero en celdas termostatizadas especialmente diseñadas con una capacidad suficiente para abarcar los volúmenes necesarios de líquido para la determinación de las rectas de reparto, propiedades físicas y tensiones interfaciales. El tiempo de agitación fue de 2h, y el de reposo 48 h para los sistemas con $[P_{6\,6\,6\,14}]Cl$ y 72 h para los sistemas que contienen el LI $[P_{6\,6\,6\,14}][NTf_2]$.

Las composiciones de equilibrio de agua y *n*-dodecano se determinaron mediante cromatografía de gases (HP 6890) utilizando el método del patrón interno. La composición del LI se estableció por diferencia. Cuando la composición del LI obtenido era menor que el 0.1 %, se utilizó el método de espectroscopia ICP (óptico) para determinar las composiciones exactas. De una forma similar, cuando el contenido en agua de la fase orgánica era muy pequeño, éste fue determinado mediante valoración (Karl-Fischer).

La densidad y la viscosidad de las fases homogéneas se determinaron a 25 ºC y 75 ºC mediante un densímetro (Anton Paar DMA 5000) con corrección de viscosidad y autocontrol de temperatura y un viscosímetro capilar (Ubbelohde), respectivamente. La medida de las tensiones interfaciales entre las diferentes fases se llevó a cabo en un tensiómetro (Krüss K11) utilizando el método de la placa Wilhelmy.

Resultados y discusión

A partir de los datos de equilibrio se puede confirmar que en presencia de agua y *n*-dodecano, ambos LIs forman sistemas de Winsor Tipo III. Se encontró que la fase intermedia es una microemulsión donde el LI, en el caso del $[P_{6\,6\,6\,14}]Cl$ solubiliza una cantidad considerable de n-dodecano y agua, y en el caso del $[P_{6\,6\,6\,14}][NTf_2]$ se solubiliza prácticamente sólo *n*-dodecano.

A partir de la medida de las tensiones interfaciales se confirmó que el sistema trifásico está asociado a una importante reducción de la tensión interfacial, mucho mayor en el caso del LI con el anión Cl, probablemente debido al mayor carácter polar de este anión. Se observó también un aumento de la viscosidad del agua/agua salada al mezclarla con el LI. Esto constituye una ventaja en esta aplicación, ya que el aumento de este parámetro reduce la diferencia de movilidad entre el agua y el aceite, viéndose disminuida la formación de digitaciones, y por tanto se mejora la eficacia del proceso.

Se encontró también que con el aumento de temperatura se mantiene el sistema trifásico. La variación en la composición del vértice del triángulo que representa a dicho sistema es muy pequeña con esta variable. Así mismo, en presencia de sal se mantienen las tres fases encontradas.

Fraccionamiento de biomasa

Los principales recursos energéticos utilizados hoy en día (carbón, petróleo, gas natural, etc.) son limitados y, por lo tanto, pueden agotarse. Esta limitación ha generado, además de una investigación para el mejor aprovechamiento de los recursos existentes, un interés creciente por el desarrollo de nuevas tecnologías para la utilización de fuentes de energía renovables alternativas que, aunque actualmente son poco rentables, tienen la ventaja de ser poco contaminantes e inagotables.

La biomasa es la energía solar convertida por la vegetación en materia orgánica. Esa energía puede ser recuperada por combustión directa o transformando la materia orgánica en otros combustibles. La biomasa lignocelulósica está constituida fundamentalmente por celulosa, hemicelulosa y lignina. Las interacciones intermoleculares de estos polímeros son muy difíciles de romper, consistiendo este hecho el mayor reto a la hora de obtener combustibles y productos químicos a partir de la biomasa. Los procesos convencionales de pretratamiento de la biomasa muestran conversiones relativamente altas, sin embargo la eficiencia energética y el impacto medioambiental necesitan ser mejorados.

Una investigación puntera hoy en día se centra en el uso de LIs para el fraccionamiento de la biomasa en sus principales biopolímeros, evitando las condiciones tóxicas y peligrosas de los procesos actuales y convirtiéndolos en métodos más sostenibles medioambientalmente. Como alternativa, los DEs en general presentan costes inferiores, menor toxicidad y mayor biodegradabilidad. Sin embargo, los estudios encontrados en la bibliografía sobre el uso de estos disolventes para el fraccionamiento de la biomasa son muy escasos y en su mayoría teóricos.

Experimental

El trabajo experimental de esta sección se inicia con la preparación de varios DEs a partir de diferentes precursores. Para ello, se utilizaron distintos dadores de hidrógeno (ácido láctico, málico y oxálico) y aceptores de hidrógeno (glicerol, cloruro de colina, prolina, alanina, cloruro de tetrametilamonio y cloruro de 2-cloroetiltrimetilamonio). La capacidad de estos DEs para fraccionar la biomasa se analizó a partir de diferentes ensayos de solubilidad de dos materiales lignocelulósicos: paja de trigo y madera de pino.

La biomasa se sometió a un proceso de molienda manual y otro posterior de tamizado. Se mezcló con el disolvente y las muestras se agitaron vigorosamente durante por lo menos 14 h y a 60 ºC para las muestras con ácido láctico u oxálico, y a 85 ºC para las muestras con ácido málico (debido a su alta viscosidad). A continuación, las muestras se dejaron enfriar y posteriormente se centrifugaron para facilitar el precipitado de la biomasa suspendida en el DEs. El sobrenadante fue directamente retirado en los casos en los que fue posible, y mezclado con etanol en el caso de las muestras más viscosas. El sobrenadante fue utilizado para una posterior precipitación del biopolímero disuelto mediante el uso de agua como anti-disolvente.

Resultados y discusión

Al mezclar el material lignocelulósico con el DEs, el sobrenadante adquirió un color entre rojo y marrón, dependiendo del tipo de biomasa, asociado a la disolución de lignina. La separación de este biopolímero fue comprobada posteriormente mediante espectroscopía FT-IR.

Se encontró una alta solubilidad de lignina en los disolventes sintetizados, al mismo tiempo que una solubilidad casi despreciable de celulosa y hemicelulosa. Estos resultados coinciden con estudios previos de la bibliografía sobre la solubilidad de estos biopolímeros en alguno de los DEs ensayados, investigación que dio origen al trabajo realizado en esta sección de la tesis. Por tanto, el proceso presenta una alta selectividad, mostrándose prometedor como proceso de deslignificación de biomasa. Se encontró que, una vez extraída la lignina, la celulosa que permanece en la biomasa sufre un cambio en su cristalinidad. Esto podría ser de interés, por ejemplo, para un posterior proceso de sacarificación.

El mejor DES para llevar a cabo esta separación depende de la naturaleza de la biomasa. Sin embargo, en mezclas de ácido láctico y un aceptor de hidrógeno (cloruro de colina, cloruro de tetrametilamonio o cloruro de 2-cloroetiltrimetilamonio) la disolución de lignina aumenta con la proporción del ácido.

El método utilizado debe ser optimizado, especialmente en el caso de los DEs más viscosos, puesto que la adición de etanol produce a veces problemas de inmiscibilidad con la consecuente precipitación del disolvente, según se detectó en la biomasa filtrada.

Conclusiones y trabajo futuro

La investigación realizada en esta Tesis permite concluir que los disolventes de diseño, LIs y DEs, pueden sustituir a los disolventes orgánicos tradicionales dando lugar a procesos más sostenibles y/o de mayor eficacia.

La desterpenación de aceites esenciales de cítrico puede llevarse a cabo mediante extracción líquido-líquido utilizando el LI [C_4mim][OAc] como disolvente, puesto que las solubilidades y selectividades obtenidas son muy favorables y el LI sería relativamente fácil de recuperar. Se evitarían así los inconvenientes de la destilación fraccionada utilizada hoy en día (altos requerimientos energéticos y pérdida de calidad del producto).

Ciertos LIs con carácter surfactante pueden ser empleados con el objetivo de mejorar las técnicas de drenaje micelar-polímero puesto que:

- Permiten la formación de un sistema trifásico, asociado a una drástica reducción de la tensión interfacial agua-aceite, que liberaría el crudo atrapado en las rocas. Además, para la formación de este sistema, y a diferencia de los surfactantes tradicionales, no es necesaria la adición de co-surfactantes.
- El sistema trifásico obtenido es estable ante cambios de temperatura y en presencia de sal.
- La alta viscosidad de los LIs, al mezclarse con el agua, podrían evitar la formación de digitaciones permitiendo un avance homogéneo de la mezcla agua y crudo.

De los dos LIs utilizados en este trabajo, los mejores resultados se obtuvieron con el [$P_{6\ 6\ 6\ 14}$]Cl, reduciendo la tensión interfacial agua-n-dodecano un 98 % a 25 ºC y un 99% a 75 ºC. Estudios futuros deben basarse en la posibilidad de diseñar los LIs para conseguir una mayor solubilización del aceite y las extremadamente bajas tensiones interfaciales necesarias en esta aplicación, al mismo tiempo que se busca un surfactante medioambientalmente respetuoso. Otra investigación necesaria consiste en el estudio de la influencia de la presión, de la adsorción de los LIs en las rocas, comportamiento con el crudo real…

En cuanto al pretratamiento de la biomasa con DEs, se concluye que es un proceso prometedor debido a la alta selectividad de los disolventes estudiados por la lignina en presencia de celulosa y hemicelulosa. Sin embargo, esta investigación está en sus comienzos y todavía se necesitan llevar a cabo numerosas optimizaciones del proceso para obtener resultados que sean la base de una implementación a mayor escala.